DESALINATION USING VAPOR-COMPRESSION DISTILLATION

A Thesis

by

MIRNA RAHMAH LUBIS

Submitted to the Office of Graduate Studies of
Texas A&M University
in partial fulfillment of the requirements for the degree of

MASTER OF SCIENCE

May 2009

Major Subject: Chemical Engineering

DESALINATION USING VAPOR-COMPRESSION DISTILLATION

A Thesis

by

MIRNA RAHMAH LUBIS

Submitted to the Office of Graduate Studies of
Texas A&M University
in partial fulfillment of the requirements for the degree of

MASTER OF SCIENCE

Approved by:

Chair of Committee,	Mark T. Holtzapple
Committee Members,	Maria A. Barrufet
	Mahmoud M. El-Halwagi
Head of Department,	Michael Pishko

May 2009

Major Subject: Chemical Engineering

ABSTRACT

Desalination Using Vapor-Compression Distillation. (May 2009)

Mirna Rahmah Lubis, B.E., Syiah Kuala University

Chair of Advisory Committee: Dr. Mark T. Holtzapple

The ability to produce potable water economically is the primary purpose of seawater desalination research. Reverse osmosis (RO) and multi-stage flash (MSF) cost more than potable water produced from fresh water resources. As an alternative to RO and MSF, this research investigates a high-efficiency mechanical vapor-compression distillation system that employs an improved water flow arrangement.

The incoming salt concentration was 0.15% salt for brackish water and 3.5% salt for seawater, whereas the outgoing salt concentration was 1.5% and 7%, respectively. Distillation was performed at 439 K (331^{o}F) and 722 kPa (105 psia) for both brackish water feed and seawater feed. Water costs of the various conditions were calculated for brackish water and seawater feeds using optimum conditions considered as 25 and 20 stages, respectively. For brackish water at a temperature difference of 0.96 K (1.73^{o}F), the energy requirement is 2.0 kWh/m^3 (7.53 kWh/kgal). At this condition, the estimated water cost is \$0.39/m^3 (\$1.48/kgal) achieved with 10,000,000 gal/day distillate, 30-year bond, 5% interest rate, and \$0.05/kWh electricity. For seawater at a temperature difference of 0.44 K (0.80^{o}F), the energy requirement is 3.97 kWh/m^3 (15.0 kWh/kgal) and the estimated water cost is \$0.61/m^3 (\$2.31/kgal).

Greater efficiency of the vapor compression system is achieved by connecting multiple evaporators in series, rather than the traditional parallel arrangement. The efficiency results from the gradual increase of salinity in each stage of the series arrangement in comparison to parallel. Calculations using various temperature differences between boiling brine and condensing steam show the series arrangement has the greatest improvement at lower temperature differences.

The following table shows the improvement of a series flow arrangement compared to parallel:

ΔT (K)	Improvement (%)*
1.111	15.21
2.222	10.80
3.333	8.37

* Incoming salt concentration: 3.5%
Outgoing salt concentration: 7%
Temperature: 450 K (350^{o}F)
Pressure: 928 kPa (120 psig)
Stages: 4

DEDICATION

To my parents

Drh. Hasanuddin Lubis, M.S.

and

Rosnia Siregar

My sisters and brothers

Ermila Hasti Lubis, S.H. and Muhibuddin, S.H.

Dr. Rina Hastuti Lubis and Dr. Syahroni

Drh. Triva Murtina Lubis, M.P.

Thanks for your love, pray, unconditional moral support, and sharing your life with me.

There are not enough words to express how very grateful I am

to have all of you in my life

I am in great debt to you...

ACKNOWLEDGEMENTS

I would like to express my sincere gratitude to my advisor Dr. Mark T. Holtzapple for all his encouraging, knowledgeable advice, patience, and unwavering belief in me. His very supportive enthusiasm to communicate his ideas has been inspirational.

I also would like to thank my committee members, Dr. Barrufet and Dr. El-Halwagi, for their guidance throughout the completion of this research. I am truly grateful to Dr. Jorge Lara, the faculty, and the staff of the Chemical Engineering Department of Texas A&M University for all their professionalism, indispensable advice, and encouragement. I also would like to thank my student colleagues for their support and invaluable advice.

However, most of all this work would not have been completed without the love, help, and facilities provided by my mother, father, sisters Emi, Uti, Iva, and my brothers Muhib and Roni.

Finally, I would like to thank my friends at Aceh Fulbright Association for your fellowship during our studies in the United States. Also, many thanks for The American Indonesia Exchange Foundation and everybody for giving me the wonderful opportunity of pursuing my studies in this reputable university. Peace of mind for you all.

TABLE OF CONTENTS

CHAPTER Page

LIST OF FIGURES

FIGURE Page

LIST OF TABLES

TABLE Page

CHAPTER I

INTRODUCTION

The shortage of fresh water is important because it continuously increases and adversely effects many countries. Water shortages involve more than 80 countries and 40% of the world population [1]. There are 1.1 billion people without adequate drinking water. Based on forecasts for 2020, over 60% of humanity will be exposed to water shortages. Currently, about 15,000 desalination units are operating worldwide [2]. To make desalination technology more attractive, there is a need to lower costs.

Previous Studies and Results

The desalination units that operate worldwide include distillation, membrane, ion exchange, and freeze desalination technologies [3].

Distillation. Distillation methods include multistage flash (MSF), multiple-effect distillation (MED), solar distillation, and vapor compression (VC) [4]. Multistage flash is the standard process for high-volume desalination [5] (Figure 1-1). In this process, seawater is heated and separated from dissolved salt by evaporation [6]. It occurs by heating saline water to high temperatures and passing it through vessels of decreasing pressures, which flashes off water vapor. The key to the process is the selection of equipment that can survive saline brine at elevated temperatures.

This thesis follows the style of Desalination.

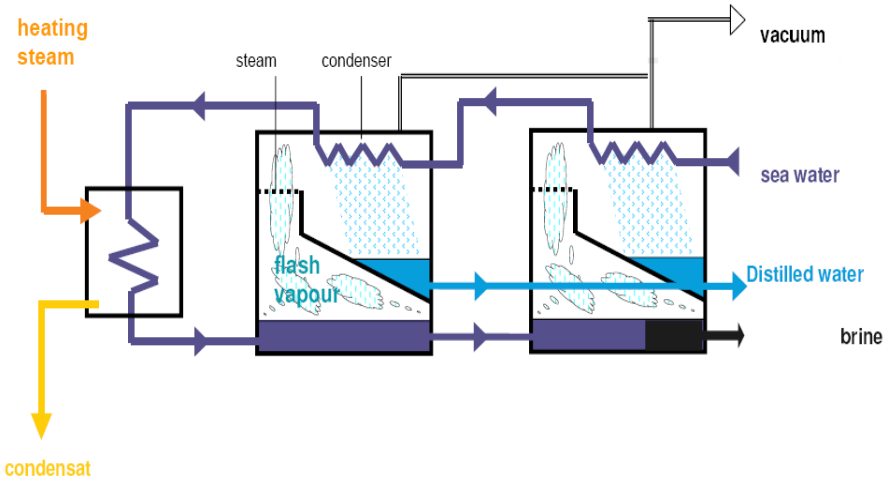

Figure 1-1. Multistage flash distillation unit [7].

In multiple-effect evaporators, high-pressure vapor from one heat exchanger in the series enters the next heat exchanger in the series to evaporate water at a lower temperature and pressure (Figure 1-2).

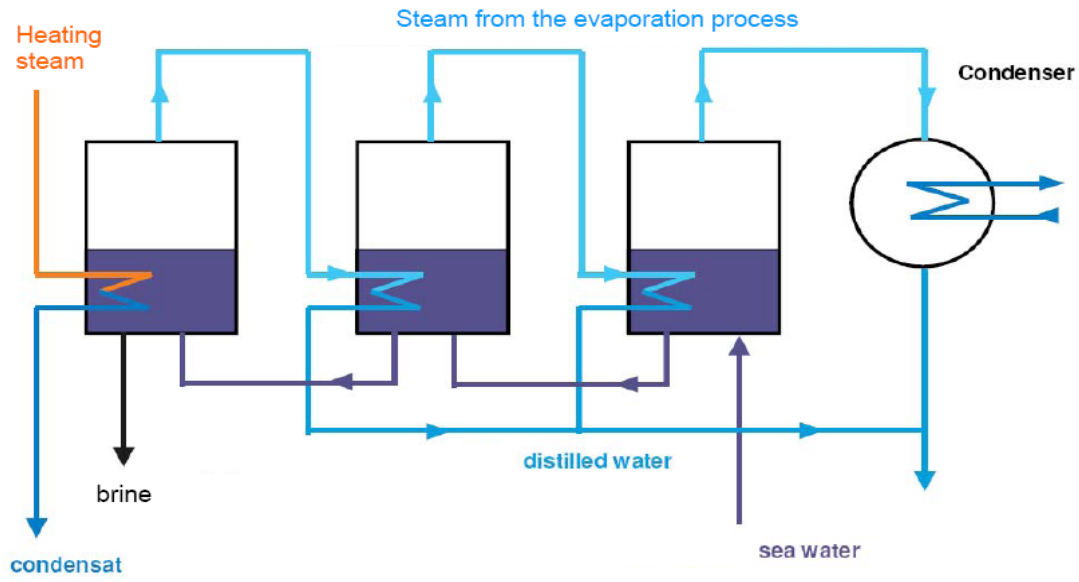

Figure 1-2. Schematic of conventional MED system [7].

Solar distillation is a low-cost system suitable only for small outputs. In this distillation, Clayton [4] states that the sun evaporates seawater in a glass-covered still (Figure 1-3). The vapor is condensed and collected on the cover; however, it requires good sealing to avoid vapor and heat loss.

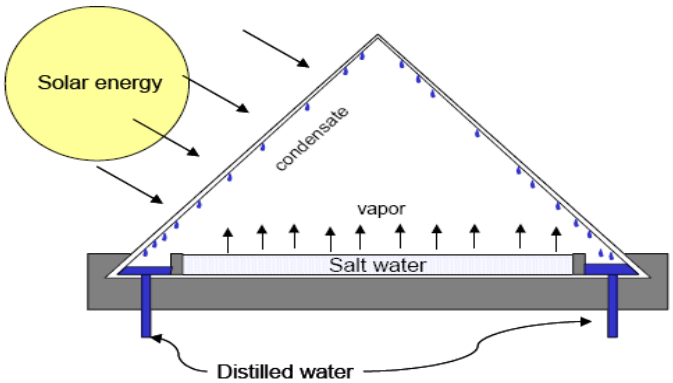

Figure 1-3. Diagram of a solar distillation system [3].

In vapor-compression distillation (Figure 1-4), the process occurs by evaporating seawater, compressing the vapor, and using the hot compressed vapor as a heat source to evaporate additional seawater. This process uses compressors as the energy input for evaporation. VC units are generally used where the requirement for desalinated water is relatively small, such as in holiday resorts or ships.

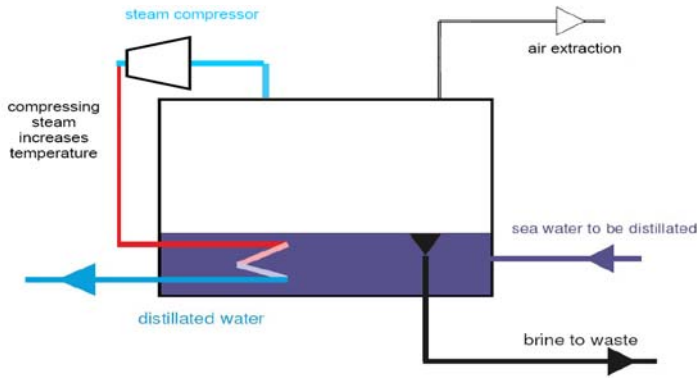

Figure 1-4. Vapor-compression distillation unit [7].

Membrane. Membrane processes includes reverse osmosis (RO) and electrodialysis (ED). In reverse osmosis, seawater is pumped across a membrane surface causing water to diffuse through the membrane and separate from the brine solution [8] (Figure 1-5). The brine concentration depends on the salinity of the feed water, pressure differential between feed water and the product water, and type of membrane. Because the process does not require heating and phase change, it is very energy efficient and is widely used for desalination. RO plants require pretreatment to remove suspended solids and to prevent membrane fouling by using acids, biocides, coagulants, antiscalants, and other compounds.

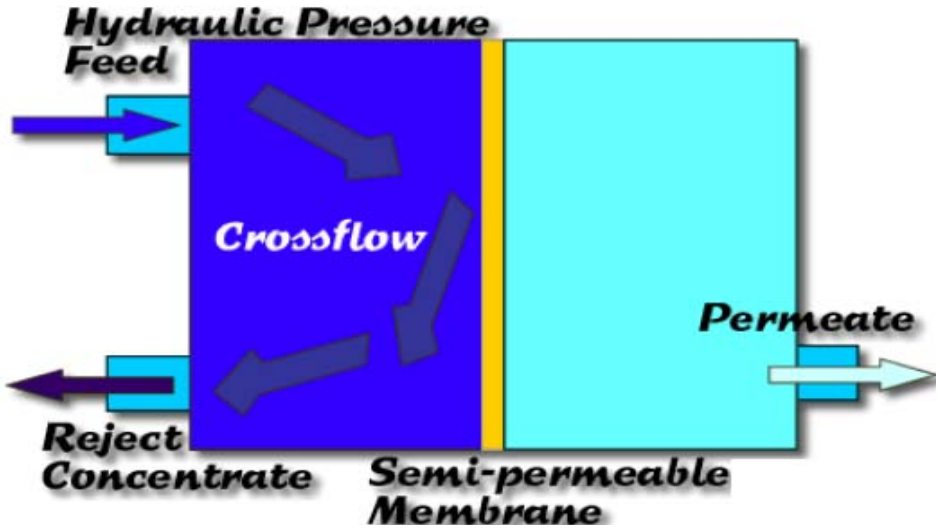

Figure 1-5. Elements of reverse osmosis system [8].

Electrodialysis (ED) is an electrochemical separation process that uses a stack of ion-exchange membranes [9]. Dissolved salt are ionic, which are separated by anion

exchange membranes and cation exchange membranes [10] (Figure 1-6). Cations are attracted to the cathode and pass through the cation-selective membrane. Similarly, anions are attracted to the anode and pass through the anion-selective membrane. All ions in brine such as sodium (+), calcium (++), and carbonate (--) are dispersed in the solution and move to the extent of their concentration and mobility. Periodically, the membranes must be cleaned by reversing the direction of the electric current, which is known as electrodialysis reversal (EDR). ED is still used today, but has been overtaken by reverse osmosis as the preferred process.

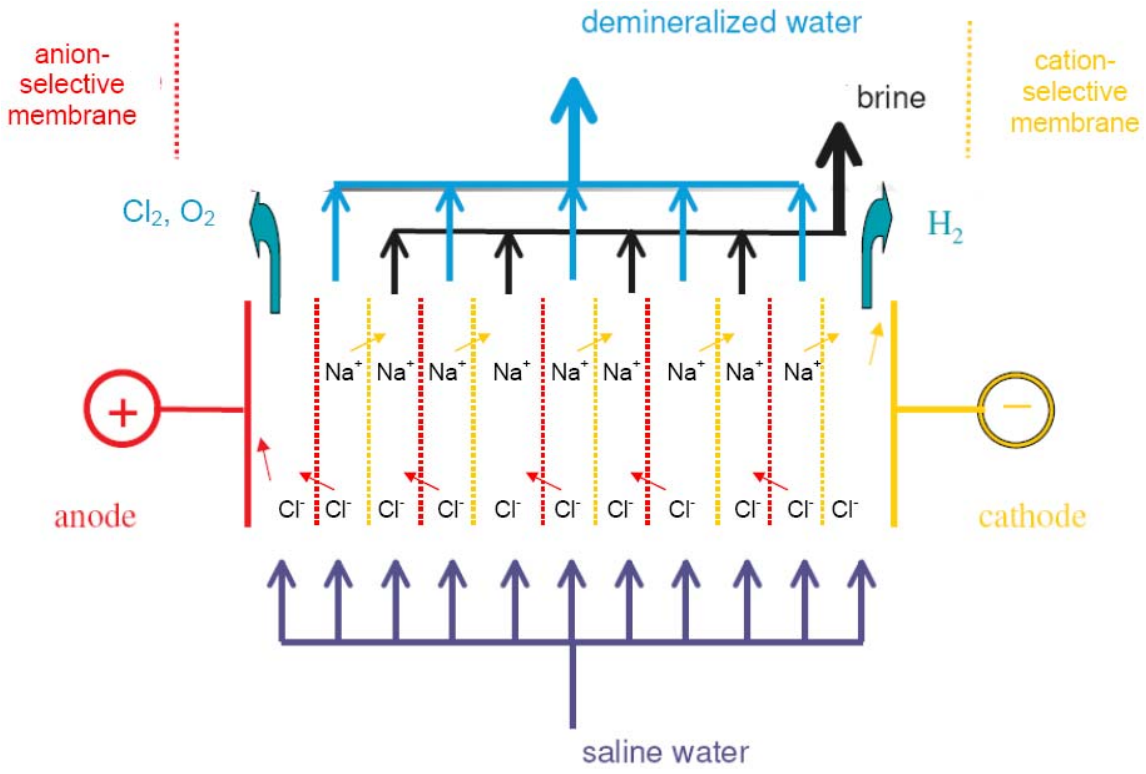

Figure 1-6. Electrodialysis desalination principle [10].

Ion exchange. Ion exchange is a reversible chemical reaction where an ion from the solution is exchanged for a similarly charged ion attached to small beads of zeolites or synthetic resin [11] (Figure 1-7). Ion exchange resins can be regenerated by using acids and bases and are used for 500 – 1,500 cycles [12].

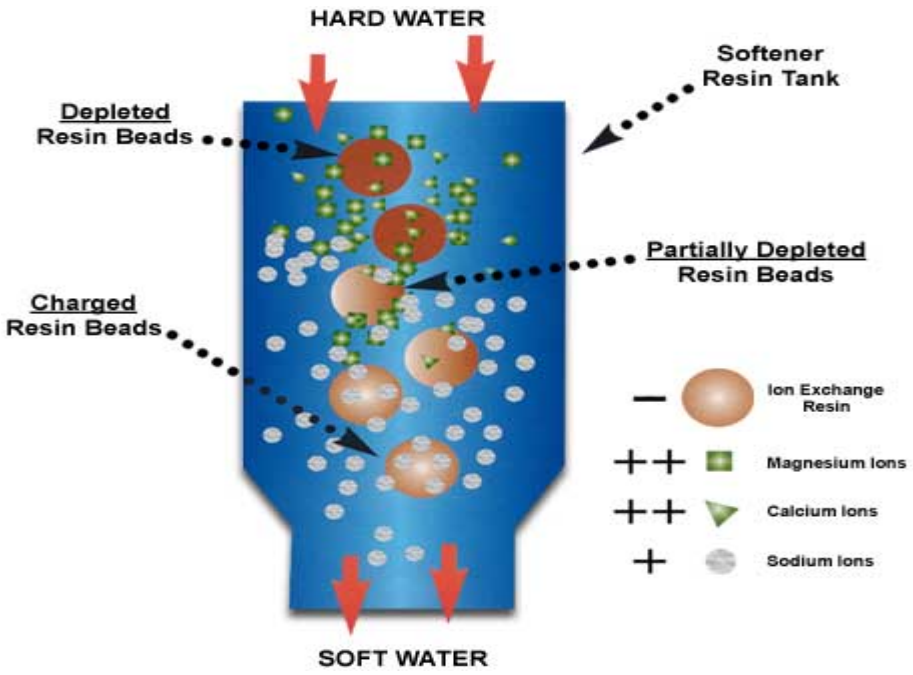

Figure 1-7. Ion exchange process [11].

An important application of ion exchange systems is softening (i.e., decalcification, demineralization/deionization). This application uses two-bed and mixed-bed deionizers [13]. As a water softener, ion exchange removes scale-forming calcium and magnesium ions from hard water. Soluble iron and organic acids can also be converted into their salts with softeners. Most industrial applications of ion exchange use a resin column, resin, a brine tank, piping, valves, and instruments.

Ion exchange deionizers use resins that are strong- or weak-acid-cation exchangers and strong- or weak-base-anion exchangers. Salt water passes through a bed of strong-acid resin to remove cations and then through strong-base resin to remove anions. Weak-acid and weak-base resins are strongly influenced by pH; therefore, each exhibits minimum exchange capacity below a pH of 7 and above a pH of 7, respectively.

Ion exchange processing can be performed by mixed-bed or two-bed deionizers. In the mixed-bed method, the cation and anion resins are mixed in a single tank through which the salt solution flows. In two-bed deionizers, the salt solution passes through two tanks in series, each containing a bed of different resins. When the resin cannot exchange further ions, the tanks are backwashed and the resin beds are contacted with hydrochloric acid and sodium hydroxide solutions, respectively.

Freeze desalination. In freeze desalination, cooled seawater is sprayed into a vacuum chamber where water evaporates. The resulting cooling causes ice crystals to form. During the formation of ice crystals, dissolved salts are naturally excluded [13]. Desalinated water is produced when ice crystals are separated from the brine. The frozen crystals float on the brine and are washed to remove salt that adheres to the crystals. Finally, the ice crystals are melted to produce pure water.

In theory, freezing has a lower energy requirement than other thermal process with minimal potential for corrosion and little scaling problems. However, it is difficult to handle and process ice/water mixtures. Although a number of plants have been built over the past 50 years, the process has never been commercially developed. This method is used commercially to treat industrial wastes rather than produce drinking water.

Mechanical Vapor Compression (MVC)

According to Aly and El-Fiqi [14], vapor-compression (VC) distillation is commonly used for small- and medium-scale desalination units. There are two methods to compress the vapor: mechanical compressors and steam jets. Lara [6] states that mechanical vapor compression is very efficient. Unlike other distillation systems, it does not require a large external heating source; however, it requires very skilled operators and has higher maintenance costs compared to thermal vapor compression [15].

Brackish water or seawater entering the evaporators is preheated using sensible heat exchangers that extract thermal energy from the exiting product water and brine. Steam from the saline solution is transferred from the evaporator to the compressor, which increases the steam pressure and temperature. The high-pressure steam condenses to form distilled water. The heat of condensation provides the heat of evaporation needed in the saline solution. The vapor-compression system is explained in Chapter II. This research focuses on optimizing the VC system so it can be more useful in future applications.

Project Description

The goal of this project is to estimate the capital and operating costs of vapor-compression seawater desalination system to determine the product cost. Evaporators are designed in series and parallel (Figures 1-8 and 1-9) to determine the energy savings from the series system.

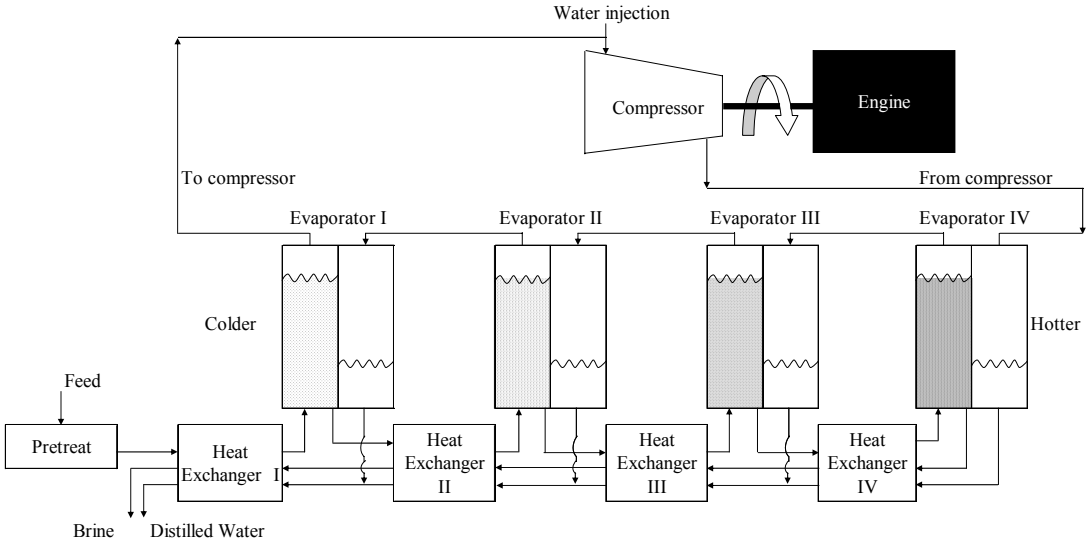

Figure 1-8. Series vapor-compression desalination.

Objectives

The specific objective for this project is to find the recommended operating conditions for the system and to find the optimal cost of potable water ($/thousand gallons).

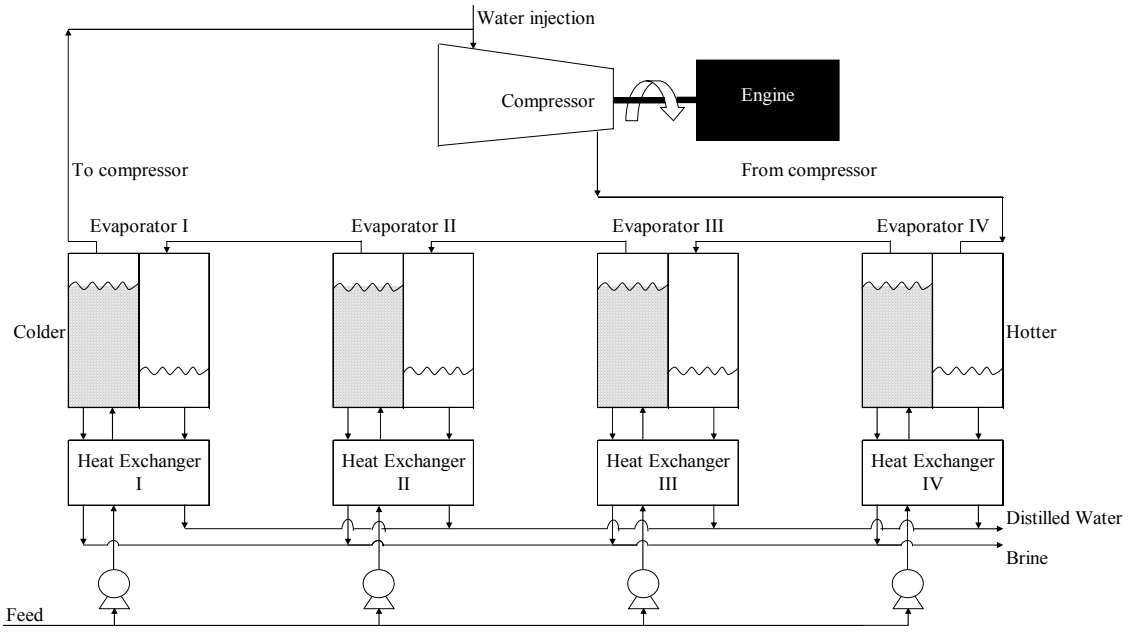

Figure 1-9. Parallel vapor-compression desalination.

CHAPTER II

MECHANICAL VAPOR COMPRESSION

According to Vishmanathappa [16], VC distillation was first used during World War II for shipboard use. Many vessels were propelled by diesel engines, which were better at furnishing mechanical energy than steam. Also, the VC distiller was extensively used in advance-base military operations, where the distiller with its internal-combustion-engine drive would be skid-mounted to be mobile. These units used the same quality of fuel as the accompanying automotive transport equipment, as well as being much easier to operate than equivalent thermal distillers.

Following World War II, many of these small units were used by oil producer in isolated areas. Many VC units were built for several U.S. Air Force installations, each producing approximately 200,000 gallons per day (gpd) [14]. Each of these installations, exemplified by the one at Kindley Air Force base in Bermuda, had four identical units operating in parallel. Each unit used a Roots blower-type VC, a single condenser-evaporator, and a three-fluid heat exchanger for preheating the incoming seawater by cooling the brine and condensate. These vapor compressors were very expensive and large. The positive-displacement Roots blower-type compressor was preferred because it overcame the problem of evaporator scaling. As scale accumulated, the compressor discharge pressure would increase to produce an increase steam temperature on the condensing side and thus maintain the rated output. Water produced by these units was expensive. Careful review of operating data indicated that reductions in water cost would

require preventing scale deposition, improving heat-transfer coefficients in the evaporator, and increasing compressor efficiency.

In MVC system (Figure 2-1), an electric motor or diesel engine compresses the water vapor thus raising its pressure and saturation temperature. This temperature difference is essential for the evaporation process. Capacities and pressure ratios of the vapor compressors play major roles in MVC systems. Small inter-effect temperature differences minimize the mechanical energy input required to drive the compressor. One design employed a centrifugal compressor that has a compression ratio of about 1.6 [17]. For smooth operation, compressor maintenance is essential. Carryover of salty liquid can cause difficulties and affect the unit performance. This can be reduced by using demister, but the pressure drop across the compressor will increase, giving a higher compression ratio. Operating at low temperatures increases the handled volume considerably and the compressor capital cost increases accordingly. In general practice, MVC uses a limited number of effects at temperatures close to ambient.

Societe Internationale de Desalement (SIDEM) has developed four adjacent effects using mechanical vapor compression. Lucas and Murat [18] state that the seawater desalination process has low energy consumption, an important characteristic, which can reach 9 kWh per m^3 of product water. It is located at nuclear power plant in Flamanville, France, and produces 1,500 m^3/day of high-quality product water.

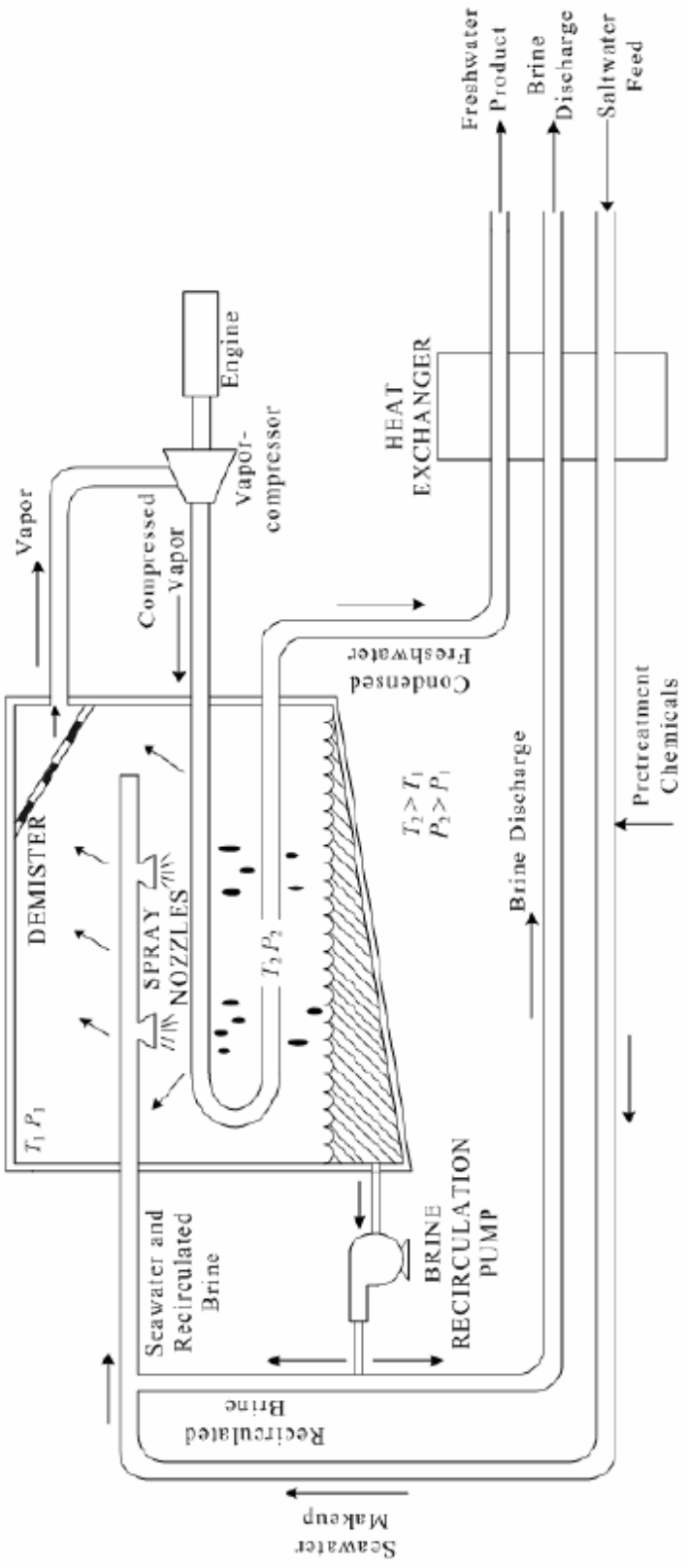

Figure 2-1. Diagram of vapor-compression plant [16].

Low energy consumption is a major advantage of mechanical vapor compression. These plants have many other attractive features such as the following:

- Packaged-type concept

  Packed systems minimize the installation work on site and obtain high standards of quality construction. The plant is entirely shop-fabricated before shipment. Civil works are limited to a single concrete slab. On-site works are limited to the seawater, brine, distillate, and power connections.

- Ease of operation and maintenance

  All plant auxiliaries (pumps, heat exchangers, etc.) are installed on the skid supporting the evaporator and therefore are readily accessible for maintenance.

  The selected operating temperature limits tube scaling to a minimum and allows the plant to meet its guaranteed performances without repeated acid cleanings of the heat exchangers.

- Reliability and resistance to corrosion

  Low operating temperatures combined with a careful selection of the materials in contact with seawater gives this plant excellent corrosion resistance.

- Economical operation

  The process offers both the advantage of low energy consumption (11 kWh/m^3) plus simple and economical pretreatment of the seawater.

The main factors evaluated in the economical optimization of VC units are the choice of the compression ratio (i.e., energy operating costs) versus the heat exchange surface of the evaporator (i.e., capital costs). In a rather complicated study, Lucas and

Tabourier [19] showed that this optimization is reached for a compression ratio that gives an overall temperature difference of 13^{o}C between the first and fourth effects. This agrees with the initial choice of the process factors, such as limited temperature differences between each cell or between the tube bundles and the evaporator cells.

Ettouney, El-Dessouky, and Al-Roumi [20] state that MVC can be driven by electricity; therefore, it is suitable for remote population areas with access to the power grid. Another advantage of VC systems is the absence of the bottoming condenser and its cooling water requirements. This is because the compressor operates entirely on vapor formed within the system. Other advantages of the system include:

(1) Moderate investment cost.

(2) Proven industrial reliability for long lifetime operation.

(3) Simple seawater intake and pretreatment.

(4) High heat transfer coefficient.

(5) Low-temperature operation allows for reduced scaling and heat loses.

(6) Modular system is simple to enlarge production volume by installing additional modules.

(7) High product purity.

(8) Simple system adjustment to load variations, by manipulating temperature.

Juwayhel, El-Dessouky, and Ettouney [15] state that energy conservation within the MVC system is maintained by recovering energy in the rejected brine and condensate steams. In conventional systems, the compressed vapor becomes superheated, which provides part of the thermal energy required for system operation.

Single-effect Evaporation with Mechanical Vapor Compression

The main characteristic of the stand-alone single-effect evaporation (SEE) system is that the amount of steam needed to evaporate the feedwater exceeds the amount of product water [21]. There are several types of VC heat pumps that may be used to address this situation. Mechanical vapor compression is the process most commonly applied on a commercial scale. The capacity of SEE-MVC systems has increased over the years from small production volumes 50 m^3/d to present values of around 5,000 m^3/d. Electricity can be the sole energy input so that it renders the technology suitable for locations removed from sources of process steam.

The SEE-MVC process has five major components:

a. A mechanical vapor compressor;

b. An evaporator/condenser heat exchanger;

c. Preheaters for the intake seawater;

d. Brine and product pumps;

e. A venting system.

Figure 2-2 describes a schema of the process, showing how the compressor and evaporator/condenser heat exchanger constitute a single unit. The evaporator/condenser heat exchanger has falling-film horizontal heat exchange tubes, spray nozzles, a vapor suction tube, and a wire-mesh mist eliminator. As is shown by Lucas and Murat [18], the compressor operates on the vapor formed in the evaporator, where it is superheated to a temperature higher than the temperature of the boiling brine.

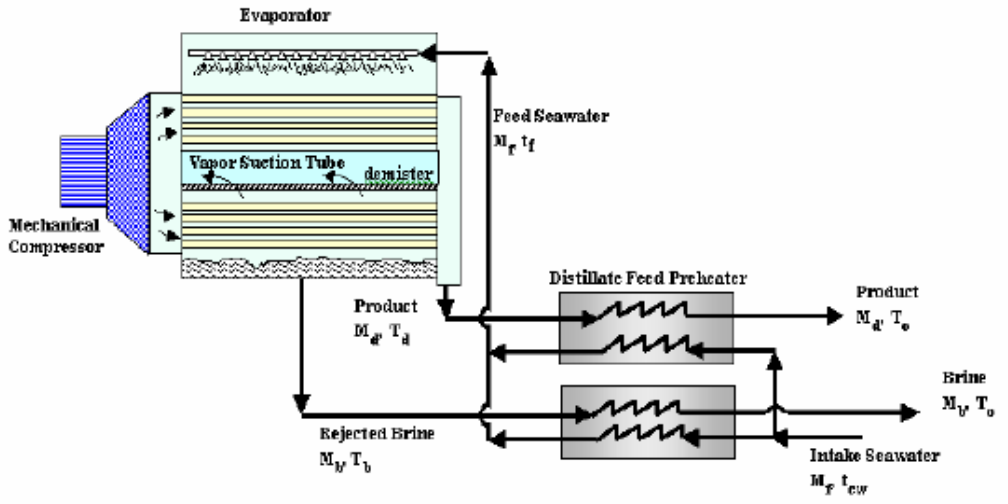

Figure 2-2. Single-effect evaporation with mechanical vapor compression [21].

According to Kronenberg and Lokiec [22], the heat necessary to boil feed water is provided by steam passing through the inside of a tube bundle. Spraying feed water on the outside of the heated tube bundle causes it to boil and partially evaporate. A compressor extracts vapor and pressurizes it so that it condenses within the tube bundle housed in the same vessel.

A vent or vacuum pump is used to withdraw non-condensable gases from the steam condensation space. An initial supply of steam is provided to induce the process. This is generally achieved using electrical heating, although other heat sources may be used as well.

The vapor compressor is the central unit in the vapor compression process. Generated vapor is compressed, which raises its temperature, thus allowing it to condense and transfer latent heat to the feed water, resulting in boiling. Thus, electrical

energy supplied to the compressor motor constitutes the major energy input for driving the process.

For steam-jet vapor compression units, also called thermo-compressors, a venturi orifice extracts water vapor from the main vessel and compresses it, thus serving the same role as a mechanical compressor.

Feed preheaters are plate-type heat exchangers that exchange heat between the intake seawater and the hot liquid streams leaving the evaporator. Hence, the feed temperature is increased from 25^{o}C to a higher value within 3 – 6^{o}C of the condensate and the rejected brine temperature [20]. The SEE-MVC process does not incorporate a bottoming condenser, because all vapor formed is routed to the mechanical compressor [21]. This eliminates the need for a cooling seawater stream and associated accessories, including pumping and treatment units.

Multiple-effect Distillation with Mechanical Vapor Compression

A schema of the MED-MVC process is presented in Figure 2-3. This system has a similar layout to that of MED units. The bottoming condenser is eliminated because the entire vapor formed in the last effect is routed to the mechanical vapor compressor, where it is compressed to the desired temperature and pressure. This results in an improved ability to recover sensible heat in rejected brine and distillate product streams, raising overall thermal efficiency.

The commercial availability of MED-MVC systems is limited. Existing units have no more than four effects and production capacities of less than 5,000 m^3/d. Unit

design limits the temperature drop per effect to 2°C. As a result, the temperature increase in the compressor is limited to 8 – 15°C.

Analyses of processes show that the thermodynamics and mass and energy balances of single- and multiple-effect MVC systems are identical. The main difference between the two configurations relates to production capacity. Assuming the same volumetric capacity at the compressor inlet, a four-effect system produces four times as much product water as a single-effect system.

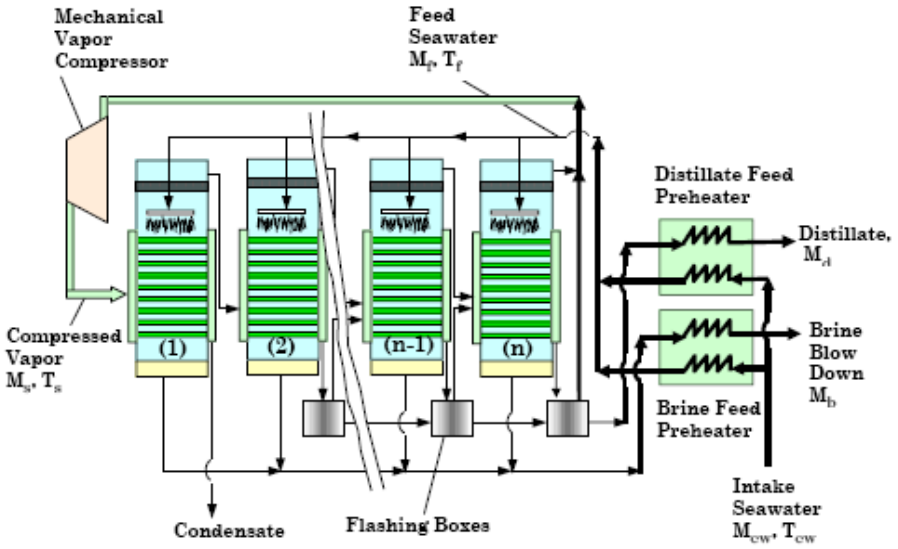

Figure 2-3. Multiple-effect distillation with mechanical vapor compression [21].

Comparison of Single- and Multiple-effect Distillation Process with Vapor Compression

In 1995, research conducted by B.W. Tleimat and M. C. Tleimat demonstrated that the use of MED-VC with series flow has greater energy savings than a SEE-VC [23]. In MED-VC unit, the work required to compress one kilogram of vapor is more

than that from a SEE-VC unit. However, for each kilogram of vapor compressed by a compressor in a MED-VC unit, the unit produces more kilograms of product, and thus the energy required per unit of product from the MED-VC unit becomes less. The research shows that higher recovery rates mean larger energy savings; actual savings in specific energy consumption may range from 20 to 50%, depending on the number of effects. Energy savings are attributed to the gradual increase in salinity in each MED-VC effect, a process unlike the conventional shell-and-tube SEE-VC systems.

Future Outlook for Vapor Compression Processes

Improvements in the design of mechanical vapor compression systems are required before it can compete with other desalination processes. Efficiency of the mechanical compressor must be enhanced and its design improved to simplify maintenance and reduce spare parts requirements.

Original MVC designs were limited to capacities of less than 500 m^3/d. Subsequent developments in compressor design increased single-effect capacities to 1,000 m^3/d. More recent advances in compressor design have allowed the construction and operation of single units with production capacities of 5,000 m^3/d, which gives a production capacity of 15,000 m^3/d for a three-effect unit.

Kronenberg and Lokiec [22] state that the main factor in increasing MVC capacity with series flow is to develop compressors with higher volumetric flow and head. The higher head enables the implementation of more effects in the unit, which yields more product for the same volumetric flow. The capacity of each individual effect

can be increased by using more efficient heat transfer surfaces, smaller diameter or grooved tubes, optimal wetting, and larger vessel diameters.

Increasing the latent heat exchanger area reduces the temperature driving force, which saves energy. For example, for seawater, reducing the temperature difference from 2.2^{o}C to 1.2^{o}C, reduces the specific energy consumption from 8 – 8.5 kWh/m^3 to 6 kWh/m^3. Reducing the temperature difference in the latent heat exchanger also reduces the approach temperature in the sensible heat exchanger, which can make it uneconomically large. In some cases, this problem is partially solved by introducing waste heat into the system when it is available. Table 2-1 shows typical values of the evaporator section and describes the number of effects, total heat transfer area, and the seawater salt concentration.

Al-Juwayhel, El-Dessouky, and Ettouney [15] state that the VC system can be driven by electric power and does not require an external heating source. As a result, they can be used in remote areas with access to power lines. MVC does have a number of operational drawbacks; however, including the need for high-quality electric power, limitations imposed by the capacity of the compressor, and maintenance.

Table 2-1. Developments in vapor compression [24-26]

Year	Unit Size (m^3/d)	Number of Effects	Heat Transfer Area (m^2)	Feed Salt Concentration (g/kg)
1981	500	1	1000	35
2004	1200	2	2261	42
2007	1500	2	3709	42

Since the development of MVC in the late 1960s, process improvements have been made in system design and operation. Energy requirements of seawater MVC plants have been reduced (from 20 kWh/m^3) and currently range from 8 to 12 kWh/m^3, with potential for further reductions. According to Aly and El-Fiqi [14], medium- to large-scale units with a low energy consumption of about 6 kWh/m^3 are being developed. Product costs are now below \$0.46/m^3. Based on literature collected by Ettouney, El-Dessouky, and Gowing, unit product costs for MVC desalination process are given in Table 2-2.

Table 2-2. Unit product costs for MVC process using seawater feed [27]

Unit size	Product Cost (\$/m^3)	Reference
100 m^3/d	5.0	28
500 m^3/d	3.22	29
750 m^3/d	0.89	30
1,000 m^3/d	1.51	31
4,000 m^3/d	2.48	32
4,546 m^3/d	2.43	33
20,000 m^3/d	0.46	34

For comparison, Zimerman [34] has reviewed two technologies using electricity from the grid: (1) MVC and (2) seawater reverse osmosis (SWRO) with energy recovery as shown in Table 2-3.

Gsell [35] states that energy costs vary in the vapor-compression process, depending if the water is produced at hot or at ambient temperatures. If large amounts of water are produced, the difference in energy costs can be significant. If ambient-temperature water is produced, heat is recovered, and the energy cost of the VC process is cut dramatically.

Table 2-3. Operating costs comparison [34]

Plant operation cost	MVC*		SWRO	
	$/m^3	$/kgal	$/m^3	$/kgal
Electricity	0.41	1.56	0.30	1.14
Maintenance	0.03	0.11	0.04	0.15
Chemical	0.05	0.19	0.07	0.26
Operators	0.05	0.19	0.05	0.19
Membrane	–	–	0.12	0.45
Total operation	0.54	2.05	0.58	2.19
Credit for blending	-0.08	-0.30	–	–
Net operating costs	0.46	1.75	0.58	2.19

*Water impurity less than 5 ppm total dissolved solids (TDS).

According to Bahar, Hawlader, and Woei [36], the system performs better when fed with lower concentration brine. Increasing rotary-lobe compressor speed produces more high-temperature steam, but also increases compressor power consumption. In their case, it was not possible to raise the rotary-lobe compressor speed above 2400 rpm. Their MVC unit produced high-quality distillate with unmeasurably low salt concentration.

Matz and Zimerman (1985) reported economic data for single- and two-effect vapor compression systems [16]. A decade later, Zimerman (1994) reported expansion of the MVC industry to more than 200 units operating in single- or multi-effect modes. As systems grow larger, Darwish [30] states that advantages of operating VC become more apparent. VC plants with proper preventive maintenance operate very reliably without unscheduled downtime. The entire water treatment system should be evaluated to get a comprehensive view of maintenance and reliability.

Minton [37] reported that improvements have been made in evaporator technology in the last half-century. The improvements take many forms and affect the following:

- Greater evaporation capacity through understanding of heat transfer mechanisms.
- Better economy by using more efficient evaporator types.
- Longer cycles between cleaning because of understanding of salting, scaling, and fouling.
- Less expensive unit costs from using modern fabrication techniques and larger unit size.
- Lower maintenance costs and improved product quality by using better materials of construction and better understanding of corrosion.
- More logical application of evaporator types to specific operation.
- Better understanding and application of control techniques and instrumentation improves product quality and reduces energy consumption.
- Greater efficiency resulting from enhanced heat transfer surfaces and energy economy.
- Compressor technology and availability permit the application of mechanical vapor compression.

The following trends in evaporator design can be expected:

- Evaporation that used single-effect designs because of low capacity or expensive materials will increasingly use vapor compression to improve efficiency. As a minimum, thermal compression will be used.
- An increased number of effects is economical for multi-effect evaporators. Each evaporator system design will be analyzed more closely to define the most economical number of effects.
- Extensive heat exchange between outgoing streams and the incoming feed will be used. Gasketed plate heat exchangers will be used increasingly for this application.
- Evaporators will be equipped with instrumentation and devices necessary to monitor the performance of operating evaporators.
- Increased automated and computerized control will be used to maintain optimum operation.
- There will be less use of evaporation schemes that inhibit the recovery of the latent heat energy of the vaporized water. For example, submerged combustion evaporation will be used only when absolutely necessary.
- Mechanical compression, often combined with multi-effects, will gain increasing application for solutions with low boiling point rises.
- Each evaporator system will be designed to reduce energy loss.
- More attention will be given to the effects of time/temperature on product quality.

Al-Juwayhel, El-Dessouky, and Ettouney [15] state that a combination of MEE and MVC system has many advantages over conventional MSF or RO systems. Some of these advantages follow:

- Moderate investment cost.
- Flexible operation and maintenance, i.e., load adjustment through temperature variations.
- Simplicity of seawater pretreatment.
- Good product quality.
- High reliability and long lifetime.

Many advantages of MEE-MVC are gained at low top brine temperatures (50 – 70°C). This increases the plant factor, which is defined as follows:

$$\text{plant factor} = \frac{\text{actual monthly production}}{\frac{\text{days}}{\text{month}} \times \text{daily production}} \tag{2.1}$$

However, most MVC plants operate in the single-effect mode.

Table 2-4 qualitatively compares the main advantages between MSF and VC distillation processes.

In the early 1960s, Aqua-Chem was the first to apply spray-film design to vapor compression distillation [38]. The combined design minimized scaling and enhanced heat transfer coefficients. Most modern vapor compression distillers use horizontal spray-film evaporators.

Table 2-4. Comparative advantages of different distillation processes [19]

	Vapor compression at low temperature		MSF
	Thermal compression	Mechanical compression	
Compactness	***	***	*
Civil works and erection	***	***	*
Seawater pumping	**	***	*
Seawater treatment	***	***	**
Reliability and resistance to corrosion	***	***	***
Purity of distillate	***	***	***
Ease of operation and maintenance	***	**	**
Energy consumption	**	***	**
Investment	***	**	**
Annual cost per m^3 produced	**	***	**

*** excellent, ** good, * fair.

Vapor compression units are designed and built so they have the following characteristics.

- More efficient than other desalination methods.
- Product water is not affected by feedwater characteristics.
- Maintain adequate wetting rates.
- A completely packaged system designed for easy, low-cost installation.
- They are upgraded to meet required electrical codes and operating conditions.
- The most reliable tubing materials.
- To ensure trouble-free operation, the units were checked.

Finally, such units may be used to produce drinking water to communities or high-purity process water to power, petrochemical and fertilizer plant, or other industrial needs. Zimerman [34] reported that the experience accumulated with commercial MVC

plants shows that such plants have superior technological characteristics compared with other systems for seawater applications. These characteristics, resulting from the low-temperature design, provide long-term operation under remarkably stable conditions. Scale formation and corrosion are minimal or absent and these factors lead to exceptional high plant availabilities of 94% to 96%.

All this reflects in the economics of these plants, which have lower production costs and overall economics than other seawater desalination processes.

Minton [37] reported that large centrifugal compressors have proven to be highly reliable in evaporator systems. Most operational problems are caused by improper matching of the compressor to the evaporator, and excessive entrainment.

Desalination systems employing distillation depend on plate heat exchangers. They consist of many corrugated titanium or naval brass plates, which have been specially developed for desalination. One set of plates forms the evaporator plate channels and another forms the condensing channels. The brine is introduced into the plate pack and evenly distributed to the evaporator channel. On the condensing side, the steam flows into the condensing channels of the plate pack. The plate concept is designed specially for multi-effect, thermo-vapor compression and mechanical vapor compression plants.

Holtzapple *et al.* [39, 40] conceived of the "sheet shell" heat exchangers depicted in Figures 2-4, 2-5, and 2-6. Figure 2-4 shows a sectional view of the assembled heat exchangers with pump present. Figure 2-5 shows a top view of the heat exchanger cassettes with steam flowing through the sides of the heat exchanger plates.

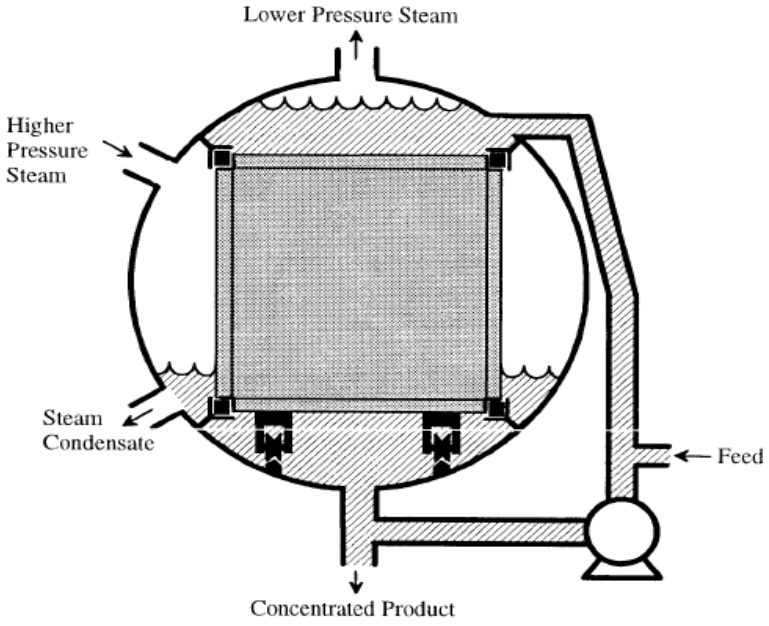

Figure 2-4. Sectional view of heat exchanger [39].

Baffles ensure that the steam velocity is nearly constant for optimal performance (about 5 ft/s). The side view shows the circulation pattern in the salt water. A pump pressurizes motive fluid sent to ejector nozzles, which induces forced convection on the liquid side.

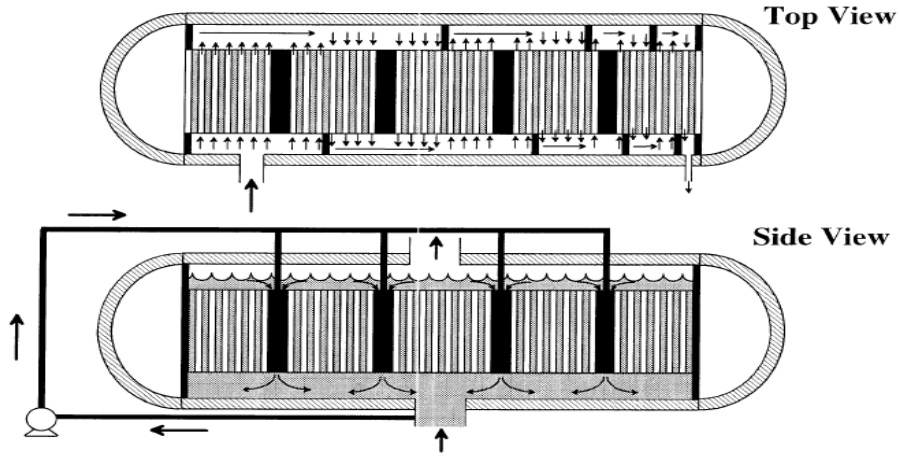

Figure 2-5. Plate arrangement of heat exchanger assembly [39].

Figure 2-6 shows the heat exchanger plate design. The goal for the high-pressure side of the sheet-shell heat exchanger is to produce dropwise condensation. This is promoted with a hydrophobic surface (e.g., gold, chrome, silver, titanium nitride, Teflon) [39].

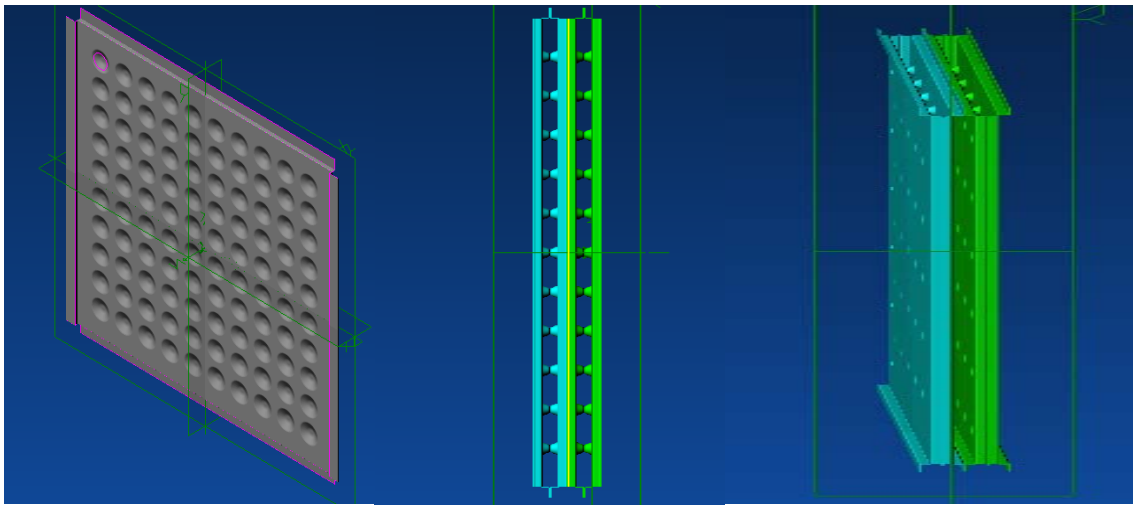

Figure 2-6. Plate design of heat exchanger [40].

Holtzapple and Noyes [41] assumed ΔT = 6°C as the temperature difference across each evaporator heat exchanger. A review on the subject [39] indicates that small temperature difference driving forces for condensation (0.02 to 6°C) were accurately maintained. Further, one benefit of operating at higher temperatures is that the pressure increases, which raises the density of the vapors entering the compressor.

Experiments performed by Lara show that as the temperature difference in latent heat exchanger increases, the heat transfer coefficient decreases significantly. He shows that heat transfer coefficients have the highest value at ΔT= 0.34°F (Figure 2-7).

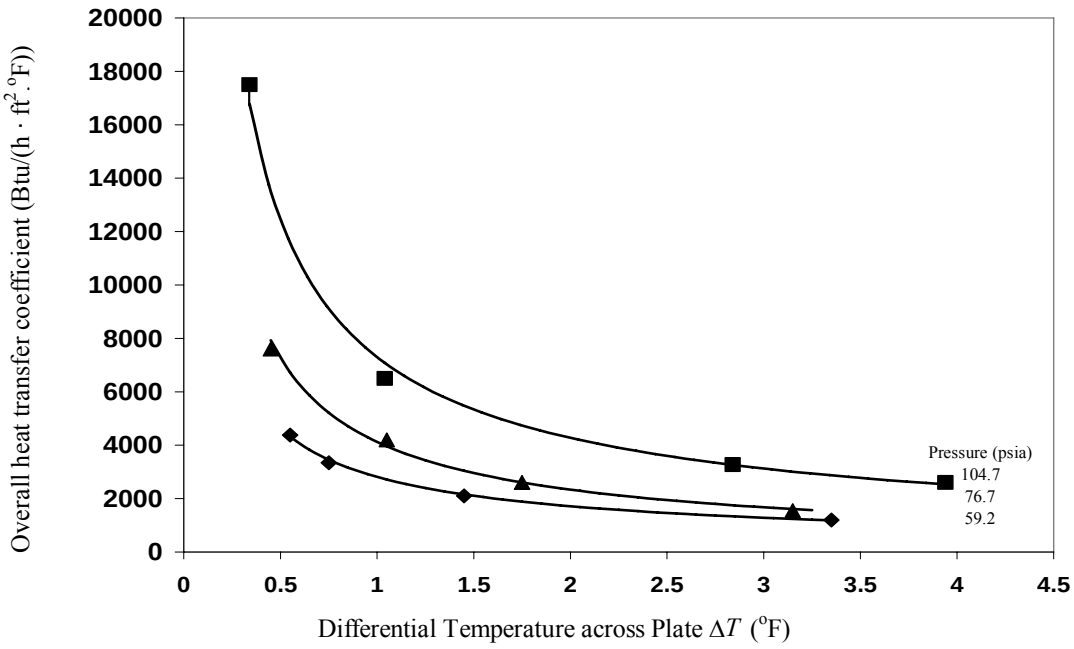

Figure 2-7. Measured heat transfer coefficients for dropwise condensation of pressurized steam (unpublished data by Jorge Lara).

Figure 2-7 shows at a ΔT of 0.34°F, the heat transfer coefficient increases to 17,500 Btu/(h·ft^2·°F) at 104.7 psia. As pressure increases, the heat transfer coefficient increases significantly. However, the coefficient rapidly decreases and then gradually decreases as the temperature difference increases. The above measurements correspond to the best observed performance as of January 2009.

Heat transfer coefficients at the pressures for each temperature difference also can be determined by rearranging Figure 2-7 as shown in Figure 2-8. It shows the projected heat transfer coefficient for a pressure of 120 psia, which the literature suggests is the maximum pressure where dropwise condensation occurs [6].

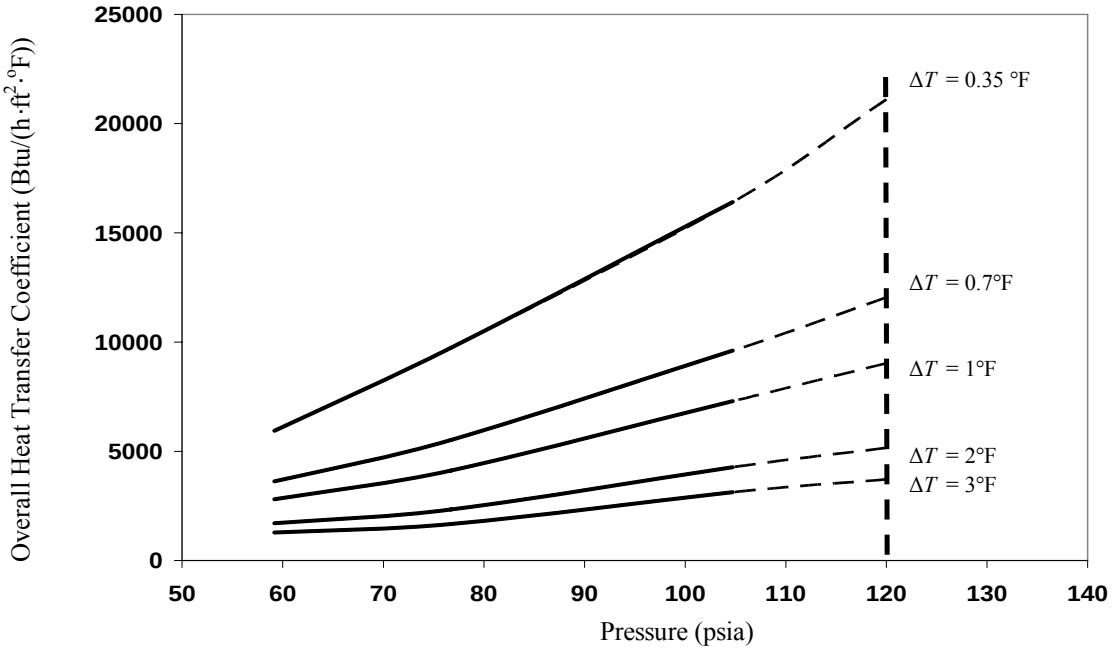

Figure 2-8. Effect of pressure on heat transfer coefficient of latent heat exchanger.

Figure 2-9 shows heat flux calculation based on experiments performed by Lara. At 104.7 psia, he shows it is possible to have a flux of up to 8,909 Btu/(h·ft^2) when the temperature difference is 3.98^{o}F. The flux drops sharply below 1^{o}F. Above $\Delta T \approx 0.3^o$F, the heat flux is virtually independent of temperature difference; therefore, it does not make sense to operate with very large temperature differences. On the other hand, sensible heat exchangers get large with very small temperature differences, so it is necessary to make appropriate economic tradeoffs. High heat fluxes result in smaller and less costly latent heat exchangers. However, higher heat flux is achieved at higher temperature differences, which require more compressor energy. Therefore, to determine the optimum condition, economic calculations must be done at a pressure of 104.7 psia and in the range 0.34 – 3.98^{o}F.

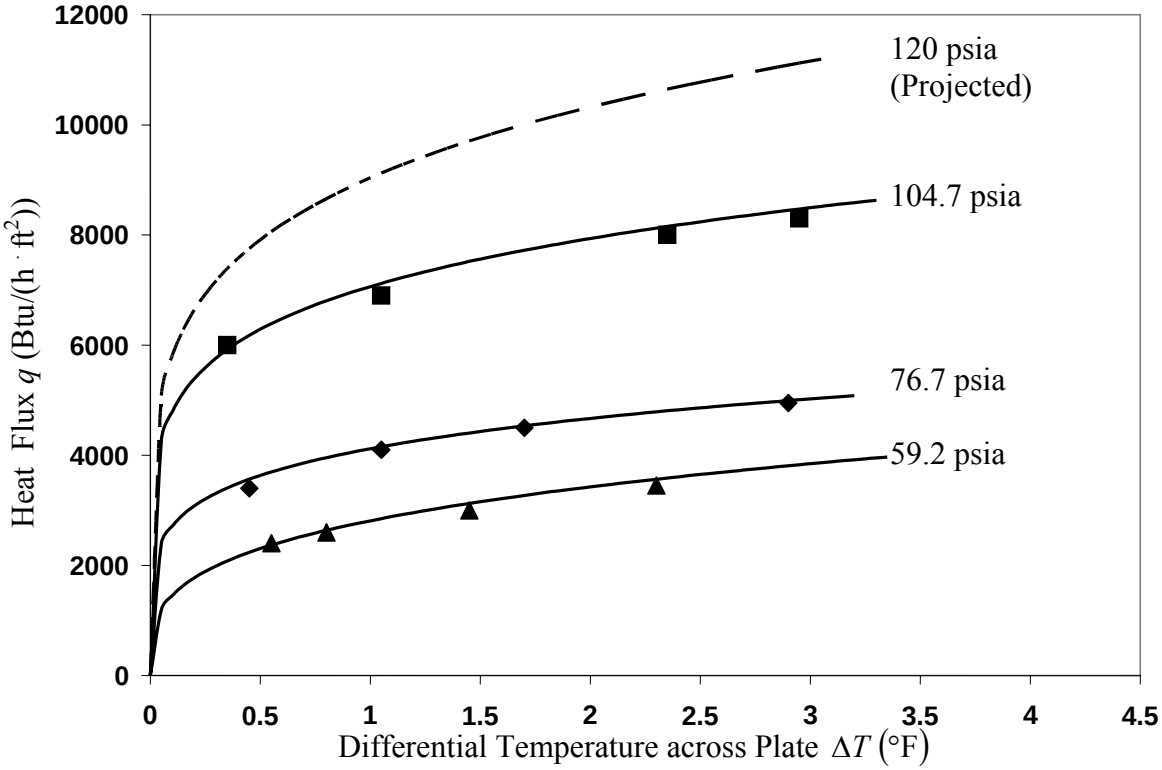

Figure 2-9. Effect of temperature difference on latent heat exchanger heat flux (unpublished data by Jorge Lara).

Overall heat transfer coefficient could be calculated by adjusting specific conditions, for example:

- steam temperature, T_s (^{o}F)
- liquid temperature, T_b (^{o}F)
- steam pressure, P_s (psia)
- heat transfer surface thermal conductivity, k (Btu/(h·ft·^{o}F))
- steam-side heat transfer coefficient, h_{cond} (Btu/(h·ft^2·^{o}F))
- liquid-side heat transfer coefficient, $h_{boiling}$ (Btu/(h·ft^2·^{o}F))
- plate thickness, Δx (ft)

Caillaud *et al.* [42] state that evaporators can operate above 120^{o}C with addition of crystalline nuclei into the heated seawater to reduce scaling problems. Scaling salts include sodium carbonate, sodium sulfate, calcium carbonate, calcium sulfate, calcium phosphate, calcium fluoride, magnesium carbonate, and magnesium sulfate. Each of these becomes less soluble in higher temperature. Sulfate removal is not necessary below 120^{o}C with concentration factor below 2, which are currently employed in MSF desalination plants.

The main technique currently employed in thermal seawater desalination plants to control alkaline scales, such as calcium carbonates, is the addition of antiscalants [43]. In general, techniques used to remove Ca^{2+} or SO_4^{2-} are lime-magnesium carbonate, nanofiltration (NF), and ion exchange (IX) using cationic or anionic resins [44]. Sulfate can be removed from seawater acidified at pH 4–5 by using weak-base anion exchange resin. The free-base form of weak base anion exchange resin performs sulfate removal by dissociating weak "hydroxide" form in equilibrium with water. Resin Relite MG1/P can be an ideal choice because of its high selectivity towards SO_4^{2-} at seawater concentration and preference for Cl^- at higher solution concentrations.

Anion exchange units can remove sulfate and other negatively charged anions. Figure 2-10 shows an ion exchange system that removes sulfate ions from the fresh feed [39]. The feed is acidified to remove carbonate as CO_2 in the vacuum stripper.

Sulfuric acid is usually used to lower the pH to about 3 to 6. The feed passes through the exhaustion ion exchange bed to remove sulfate ions from feed and to release chloride ions from the bed. Approximately 95% of sulfate ions can be removed when the

exit pH during the removal is between 5 and 5.2. The desulfonated product is fed to a vacuum stripper to remove dissolved carbon dioxide; other degassing means (e.g., sparging, heating, and vacuum) can be used. The liquid exiting the vacuum stripper has a pH of about 7 to 7.2 and contains a low level of carbonates and sulfate ions. The degassed feed is fed into the vapor-compression evaporator. The exiting brine is used to regenerate the ion exchange bed and typically, it will have a concentration of about 2.5 to 4 times larger than the feed.

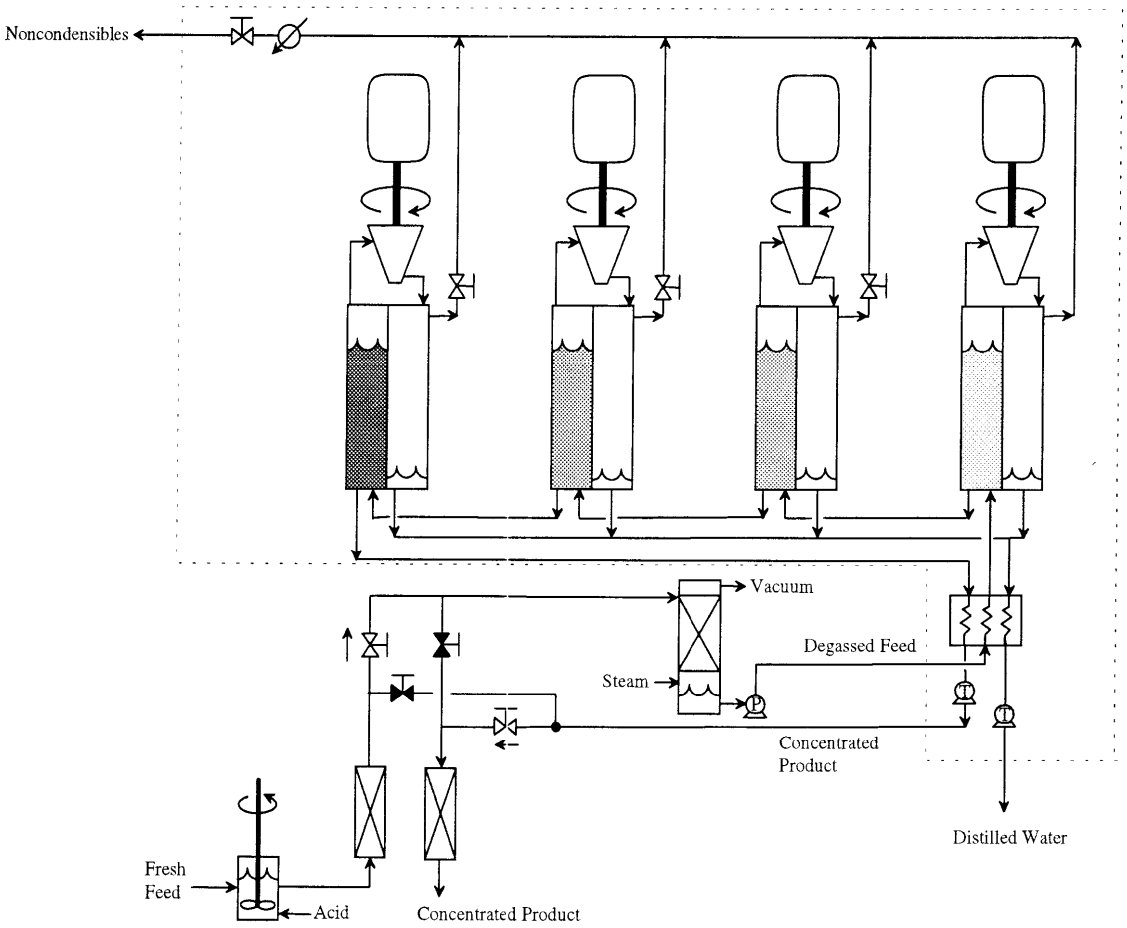

Figure 2-10. Ion exchange system [39].

Zhu, Granda, and Holtzapple [45] reported that high brine temperature requires greater sulfate removal by reducing seawater feed rate to the ion exchange bed or increasing the brine: feed concentration ratio. For a fixed quantity of produced water, the amount of treated seawater depends only on the adopted value of the ratio.

Holtzapple *et al.* [39] stated that at temperatures over 120^{o}C (248^{o}F), seawater tends to deposit scale, which interferes with heat exchanger operation. Heat exchanger surfaces made from titanium are particularly useful in instances when magnesium, calcium, carbonate, and sulfate ions are present in the water. Non-stick surfaces include the following:

a. Teflon used with metal kitchen tools and with temperature up to 290^{o}C.
b. Vacuum aluminization modified by barrier anodizing and polytetrafluoroethylene (PTFE) inclusion.
c. Aluminium anodized, followed by PTFE inclusion.
d. TiC, TiN, or TiB developed by physical vapor deposition.
e. Impact coating obtained aluminium with polyphenylene sulfide (PPS).

CHAPTER III

METHODS

An evaporator separates feed water into two streams: (1) fresh water and (2) concentrated brine (high salts). For this study, the feeds are brackish water (1.5 g/kg) and seawater (35 g/kg). The brine products are 15 g/kg and 70 g/kg, respectively. ΔT is the temperature rise of the distillate and brine compared to the feed water and is proportional to compressor work per distillate mass (W/m_s). Lara [6] states that increasing the seawater concentration elevates its boiling temperature and reduces its vapor pressure. His evaporator uses a mechanical vapor compression technology for the separation. This section briefly elaborates on two factors used in this research that affect evaporator performance.

Seawater Vapor Pressure

The water vapor pressure of seawater and its concentrates has been measured from 100°C to 180°C by Emerson and Jamieson [46]. The results of their measures are close to the analytical method described by The National Engineering Laboratory of England. The vapor pressure p_o of pure water at a measured temperature can be obtained from steam tables or it can be calculated as follows:

$$\log_{10} p_o = a + \frac{b}{z} + \frac{cx}{z}\left(10^{dx^2} - 1\right) + e10^{fy^{1.25}} \tag{3.1}$$

where

p_o = pure water vapor pressure (10^5 N/m^2)

$x = z^2 - g$

$y = 344.11 - t$

$z = t + 273.16$

t = measured temperature ^oC

$a = 5.432368$

$b = -2.0051 \times 10^3$

$c = 1.3869 \times 10^{-4}$

$d = 1.1965 \times 10^{-11}$

$e = -4.4000 \times 10^{-3}$

$f = -5.7148 \times 10^{-3}$

$g = 2.9370 \times 10^5$

The activity p / p_o fits an equation of the form

$$\log_{10}(p / p_o) = hS + jS^2 \qquad (3.2)$$

where

p = vapor pressure of salt water at the same temperature (10^5 N/m^2)

$h = -2.1609 \times 10^{-4}$

$j = -3.5012 \times 10^{-7}$

S = salinity (g salt/kg seawater)

Compressor

For a wet compressor, the isentropic compressor work is evaluated by Lara [3] as

$$W = \frac{(1 + x)\hat{H}_2^{vap} - (\hat{H}_1^{vap} + x\hat{H}_1^{liq})}{\eta_c} \tag{3.3}$$

where

$\hat{H}_2^{vap}$ = vapor enthalpy at compressor exit (2) (J/kg)

$\hat{H}_1^{vap}$ = vapor enthalpy at compressor inlet (1) (J/kg)

$\hat{H}_1^{liq}$ = liquid enthalpy at compressor inlet (J/kg)

η_c = compressor efficiency = 0.85 (assumed)

x = the amount of injection water that evaporates in the compressor

$$= \frac{S_1^{vap} - S_2^{vap}}{S_2^{vap} - S_1^{liq}} \tag{3.4}$$

where

S_1^{liq} = entropy of liquid water at compressor inlet (J/(kg·K))

S_1^{vap} = entropy of steam at compressor inlet (J/(kg·K))

S_2^{vap} = entropy of steam at compressor exit (J/(kg·K))

Lara stated that in all cases, the wet compressor had significantly less work requirements [3], so only wet compressors were evaluated here.

Boiling Point Elevation

The boiling point elevation corresponding to each measured value of vapor temperature is plotted against the salinity in Figure 3-1.

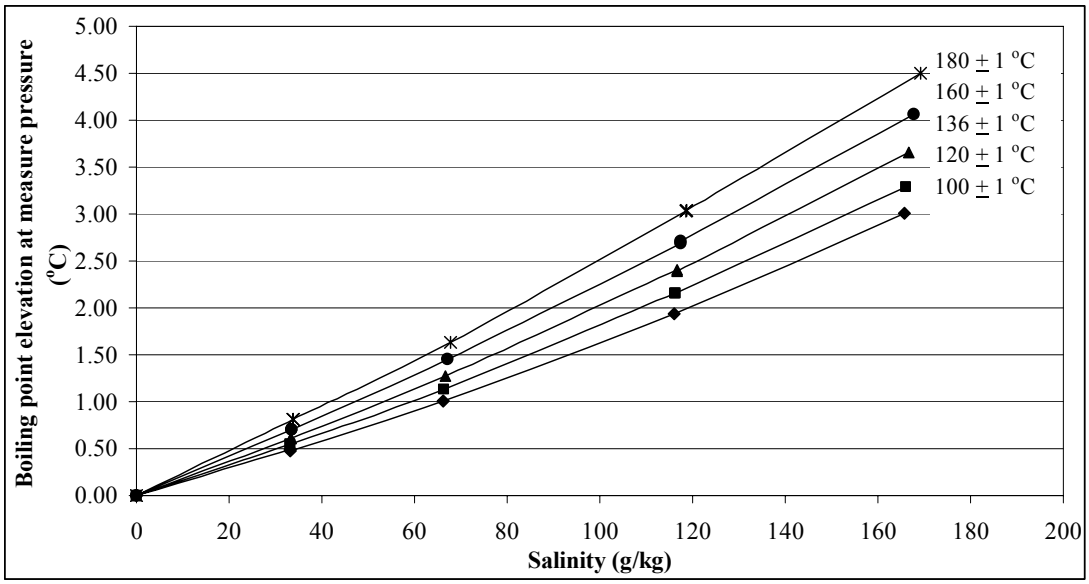

Figure 3-1. Boiling point elevation and salinity at various temperatures. Data from Table A-7.

Research Procedure

The research is performed in two stages: (1) comparison of series and parallel flow arrangements and (2) economic analysis.

Energy comparison of series and parallel flow arrangements. Degassed seawater supplied to the evaporator trains is passed through the sensible heat exchanger shown in Figures 1-8 and 1-9. The seawater salinity is 35 g/kg. Then the seawater is fed upflow into the latent heat exchangers. Saturated steam is supplied at the trains at various temperature differences. Three trade-off cases will be studied with ΔT 3.333 K (6°F), 2.222 K (4°F), and 1.111 K (2°F). Appendix B provides a detailed thermodynamic evaluation of each case. Table B-1 summarizes the results. In all cases, the brine salt

concentration is 70 g/kg brine. Lara [6] states that the maximum pressure on the steam side is limited to 120 psig to ensure dropwise condensation.

The design is performed with series and parallel evaporators to determine the effect on energy efficiency, as summarized in Table 3-1. The results obtained are useful to design systems and to evaluate the economic perspectives of this technology.

Table 3-1. Preliminary design parameters of the series and parallel MVC distillation

Design parameters	Unit	Value
Feed water salinity	g/kg	35
Brine salinity	g/kg	70
Temperature difference in latent heat exchanger	K	1.111; 2.222; 3.333

Economic analysis. To begin the economic analysis, a hypothetical base system is developed that employs MVC to desalt feed water (see Table 3-2). The feed waters are brackish and seawater, with salinities 1.5 g/kg and 35 g/kg, respectively. Based on the salinities, a recovery rate of the MVC unit can be determined. The recovery rate (*RR*) is determined by

$$RR = \frac{f_P}{f_f} \times 100\% \tag{3-5}$$

where,

f_P = the product water flow rate (m^3/s)

f_f = the feed water flow rate (m^3/s).

The distillate production capacity in the economic analysis is 10,000,000 gallons/day (0.4381 m^3/s). Figure 3-2 shows the single-stage vapor-compression desalination system

used in the economic evaluation. For simplicity, heat exchanger operational conditions applied in the calculations are for the last-stage latent heat exchanger and the first-stage sensible heat exchanger.

Table 3-2. MVC base system

Design parameters	Unit	Value	
Feed water salinity	g/kg	1.5	35
Brine salinity	g/kg	15	70
Plant capacity	m^3/s	0.4381	
Feed water temperature	K	294	
Steam pressure	kPa	418; 427; 722	
ΔT in latent heat exchanger	K	0.19; 0.39; 0.56; 1.11; 1.67; 2.21	
Interest rate	%	5; 10; 15; 20	
Electricity	$/kWh	0.05; 0.10; 0.15	
Plant lifetime	year	30	
Number of stages used will be determined based on the data.			

The amount of brackish water feed required to supply the distillate flow rate is calculated by the corresponding mass balance. The brackish water temperature is assumed 294 K (70^{o}F). The evaporator is constructed with naval brass with a coating that promotes dropwise condensation. Heat transfer coefficients of the evaporator for each condition come from Ruiz's measurements (Figure 2-7). The heat flux is calculated by multiplying the heat transfer coefficient by the temperature difference. Lara shows that above $\Delta T \approx 0.3^o$F, the heat flux is virtually independent of temperature difference (Figure 2-9). Nonetheless, to find the economic optimum, the explored ΔT will range from 0.34 to 3.98^{o}F (0.19 to 2.21 K). Figure 2-9 shows a strong benefit from operating at higher pressures, so economic calculations will focus on a selected pressure of 104.7 psia (722 kPa).

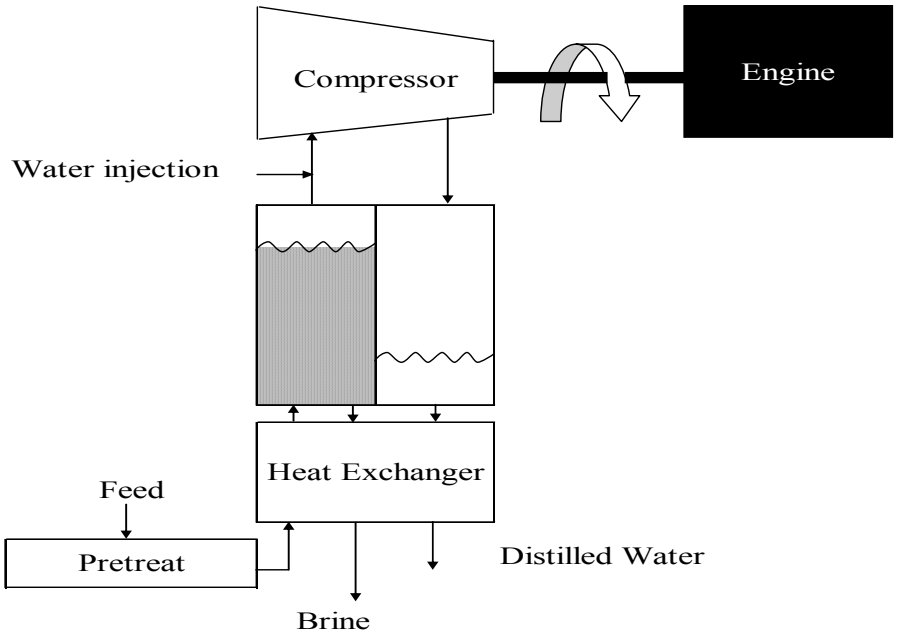

Figure 3-2. Single-stage vapor-compression desalination.

The heat duty for the latent heat exchanger is calculated by

$$Q = mL \tag{3-6}$$

where,

Q = the amount of energy required to change the water phase (J/s)

m = the mass of the distillate (kg/s)

L = the specific latent heat for distillate (J/kg)

The heat exchanger area is given by [47]

$$A = \frac{Q}{U\Delta T} \tag{3-7}$$

where,

A = area of heat transfer surface (m^2)

Q = amount of heat transferred to distillate from evaporator (J/s)

U = overall heat transfer coefficient (J/(s·m^2·K))

ΔT = temperature difference in latent heat exchanger (K)

Equation 3-7 is used to calculate the area of heat exchanger surface for each temperature difference used.

The total capital investment is calculated by selecting the overall temperature difference (Appendix C). The cost model for the VC desalination system consists of both operating costs and capital costs associated with purchased equipment and installation. The basis for all capital and operating costs is 2008 U.S. dollars. Costs found in previous years are recalculated in year 2008 dollars by applying the *Engineering News Record Construction Cost Index*. The cost for a past year is multiplied by the ratio of the *Engineering News Record Construction Cost Index* for 2008 over the *Engineering News Record Construction Cost Index* for that given year. These costs are combined to form the total capital investment [48].

Purchased equipment sizes are determined from the requirements of each configuration and the costs are derived from several sources. The compressor and pump costs come from the Matches Web site (www.matche.com), which is known in the chemical process industry as a source for up-to-date costs. Electric motor costs are determined from correlation tables and calculation. The latent and sensible heat exchangers are predicted directly as \$10.02/ft^2 and \$20.08/ft^2, respectively (see Appendix D). The cost of injecting brine is from recent deep-well injection system [49].

The final cost is estimated by multiplying the purchased equipment cost by a Lang factor. A Lang factor of 3.68 is used for skid-mounted equipment rather than a Lang factor of 5.04, which is typical of a field-erected plant. Table 3-3 shows the Lang factor for these costs as a percentage of the equipment total.

Table 3-3. Lang factor for field-erected and installed skid-mounted fluid-processing plants

Item	Field-erected*	N^{th} skid-mounted	Comment
Equipment purchase	1.00	1.00	
Purchased equipment installation	0.47	0.38	Shop efficiency.
Instrumentation and controls (installed)	0.36	0.30	Shop efficiency.
Piping (installed)	0.68	0.54	Shop efficiency.
Electrical systems (installed)	0.11	0.08	Shop efficiency.
Buildings	0.18	0.10	Few buildings needed.
Yard improvements	0.10	0.05	Few improvements needed.
Service facilities (installed)	0.70	0.35	Few service facilities needed.
Engineering and supervision	0.33	0.17	Previous plants built.
Construction expenses	0.41	0.21	Shop efficiency.
Legal expenses	0.04	0.04	
Contractor's fee	0.22	0.15	Easy to install at site.
Contingency	0.44	0.31	Previous experience, less risk.
Total	5.04	3.68	

* Source: Peters, Timmerhaus, and West, 5th ed.

Operating costs include fixed costs (bond interest, maintenance, and insurance) and variable costs (labor, electricity, and brine injection well) as shown in Table 3-4.

Table 3-4. Variable costs of MVC system

Variable expenditure	Value
Labor for plant of 10,000,000 gallon/day ($/year)	500,000[a]
Electricity ($/kWh)	0.05; 0.10; 0.15
Brine injection well handling 500,000 gallon/day - Capital cost ($) - Operating cost ($/month)	 2,000,000[b] 10,000[b]

[a] Source: RosTek Associates, Inc., *Desalting Handbook for Planners*, 3rd ed.
[b] Source: http://www.waterandwastewater.com/blog/archives/2007/08/class_i_deep_in.shtml.

Interest payments for capital are based on the total capital investment and the interest rate using an amortization factor, a, shown in Equation 3-8 [20]. The interest rate i, is taken as 5 – 20%, which is average for this type of cost estimation, and the plant lifetime n is taken as 30 years.

$$a = \frac{i(1+i)^n}{(1+i)^n - 1} \tag{3-8}$$

Maintenance and insurance are taken respectively as 4% and 0.5% [50] of fixed capital investment. Summing interest, maintenance, and insurance costs yield the total fixed cost for annual operation, which are independent of the VC production level.

Variable costs depend on the level of plant production. These include the costs of labor, brine disposal, and utilities. The total production is calculated by the number of operating hours in a year. The amount of water is the steady-state production basis for the cost model. Labor costs were determined from available desalination industry estimates of water.

Brine disposal costs vary from site to site. In some sites, discharge of brine may be feasible (surface or well); in others it may not be required. Based on calculations in

Appendix C, if a brine injection well is built, an average of $1.38/kgal of brine is used to estimate these costs.

The only utility that is used is grid electricity. To account for energy operating expenses, the costs of electricity are varied as $0.05/kWh, $0.10/kWh, and $0.15/kWh.

Adding the fixed and variable costs gives the total cost per unit of distilled water product (U.S. $/kgal). From these values, the optimum cost of water is determined for different salinities. Water cost is a function of many variables, like latent and sensible heat exchanger costs. Tables C-3 – C-5 show example capital and water cost calculations for brackish water feedstock. Tables C-6 to C-8 show examples for seawater feedstock. Tables C-9 to C-11 show calculated water costs at various pressure and interest rates.

CHAPTER IV

RESULTS AND DISCUSSION

Energy Comparison of Serial and Parallel Flow Arrangements

Degassed seawater with 3.5% salt supplied to the evaporator train is connected in series and parallel to satisfy individual evaporator temperature needs. The feed flow rate is 295 kg/s for series and parallel flows. Four evaporator stages are assumed, each unit with ΔT = 3.333 K (6^{o}F), 2.222 K (4^{o}F), 1.111 K (2^{o}F), and 7% brine. At lower ΔT, the compressor shaft work requirements are lower. The work requirements of series and parallel mechanical vapor-compression desalination were compared to determine the relative efficiency.

The seawater passed through the evaporator trains is shown in Figure 1-8. The flow diagram is shown more clearly in Figure 4-1. The temperature and pressure were calculated at the inlet and outlet of each evaporator (Appendix B). From these state values, enthalpy and entropy of water were determined (Table B-1) using steam tables. The compressor work was calculated for each ΔT.

The seawater entering the evaporators is also connected in parallel (Figure 4-2). The energy analysis was repeated for parallel desalination (Table B-1). Details of the calculations are shown in Appendix B.

The results in Table 4-1 show that the series configuration is more efficient than the parallel configuration. The efficiency improvement is larger for small ΔT because the boiling point elevation of the salt water is a larger portion of the overall ΔT.

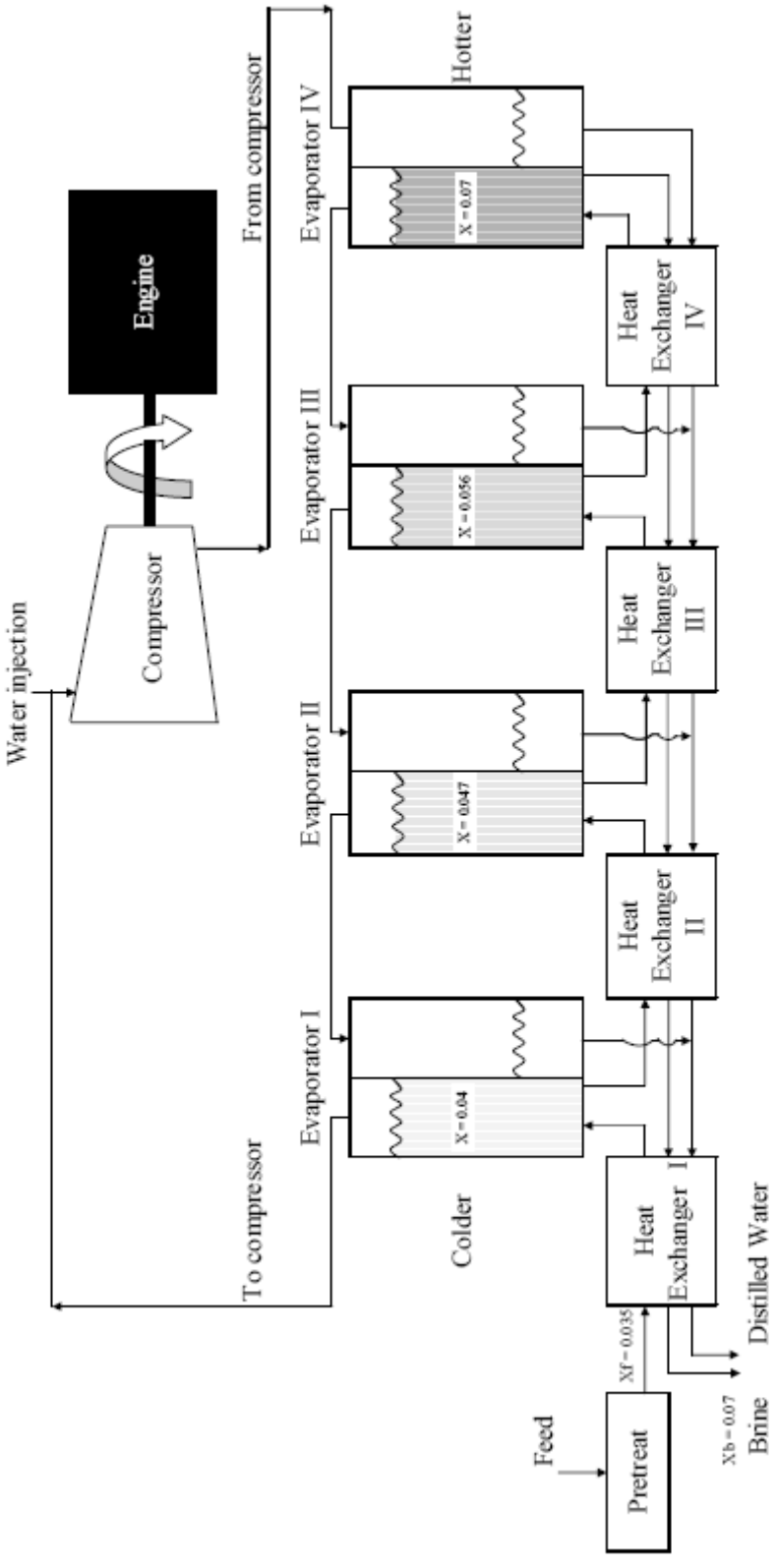

Figure 4-1. Series vapor-compression desalination.

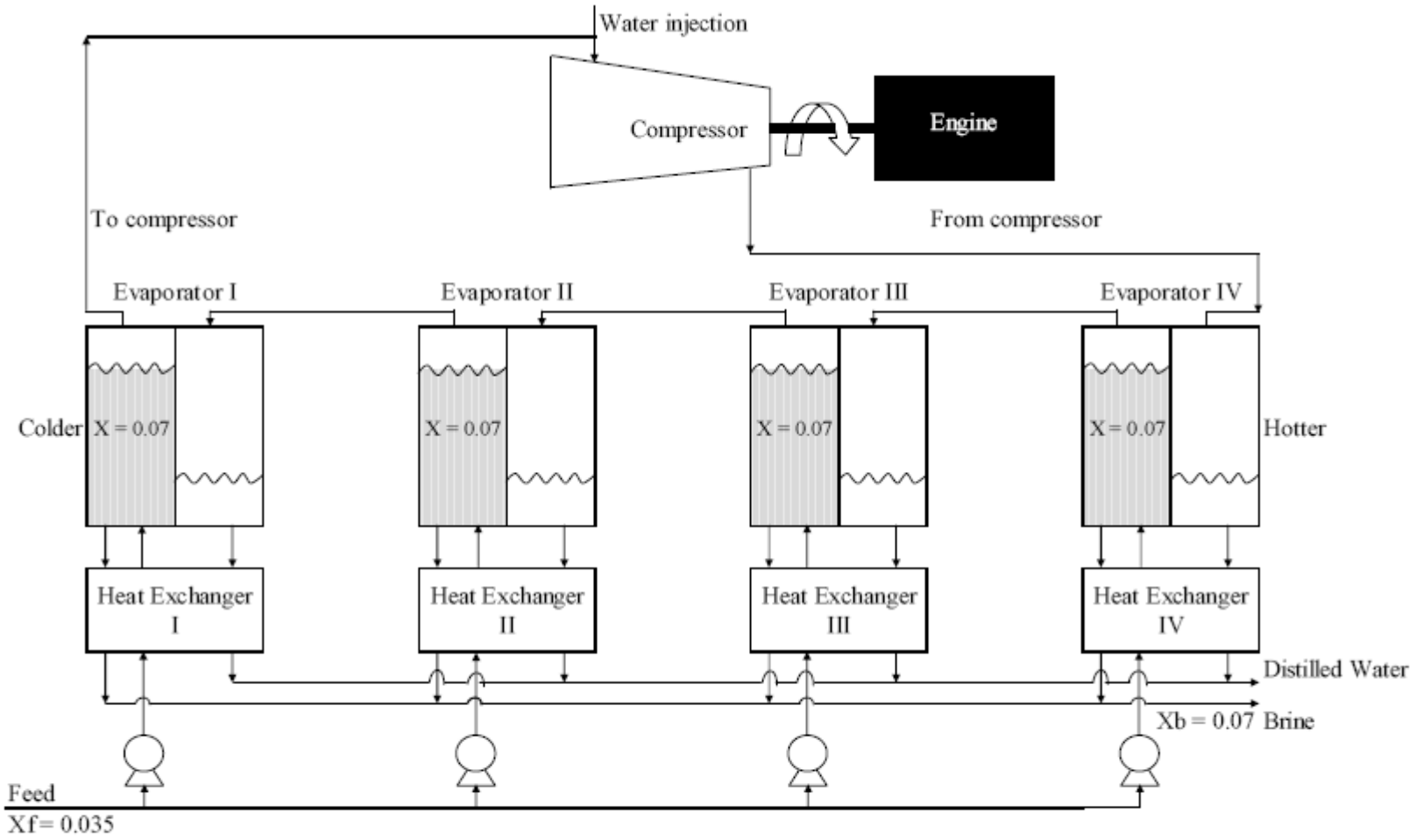

Figure 4-2. Parallel vapor-compression desalination.

Table 4-1. Percent reduction in compressor power consumption for series desalination compared to parallel desalination

ΔT (K)	Reduction in Power Consumption (%)
1.111	15.21
2.222	10.80
3.333	8.37

Based on these results, only the series configuration will be used to calculate the cost of water produced from brackish and seawater. These values show that pressure differences of compressor for series desalination are lower than those of parallel desalination. Vapor formed in the first latent heat exchanger goes to the compressor where its pressure and saturation temperature are raised. The vapor pressure of series desalination is higher than that of parallel desalination because of its lower salinity. The higher vapor pressure in the first latent heat exchanger results in the lower pressure difference of the compressor. Power consumption of the compressor, and therefore the efficiency of the process, is proportional to this pressure difference. By lowering the pressure difference, it is possible to decrease the energy consumption of the process.

Both the values reported in Table 4-1 and values from the study by Tleimat [23] show energy savings from the series arrangement. However, the two studies cannot be compared because the equipment was different. The study by Tleimat compared actual energy consumption of series multi-effect vapor compression distillation to that of single-effect distillation. Based on Tleimat's study, actual savings in the energy consumption are higher than the values in Table 4-1 and depend on the number of effects. In contrast, the research done here compares series to parallel multi-effect vapor-compression distillations using calculations, rather than actual performance.

Economic Analysis

Lara shows that the economic latent heat exchanger ΔT recommended for the United States and the Middle East are 1.111 K and 3.333 K, respectively [6]. The ΔT has a large effect on the compressor work. At lower ΔT, the compressor work needed to increase the temperature is lower. However, if the ΔT is too low, a larger heat exchanger is needed, which is not economical. All water cost are calculated at various temperature differences based on the heat flux shown in Figure 2-9. Based on the temperature differences and pressures used, the areas of both latent and sensible heat exchangers can be calculated.

The sensible heat exchanger is a key component of the desalination system. To improve heat transfer, a microchannel design is employed. It consists of three plates. Figure 4-3 shows a schematic of the three unit plates with the microchannels in a horizontal orientation. The distillate from the latent heat exchanger enters into the first plate. The feed water or brine from previous latent heat exchanger enters into the second plate. The brine from the last latent heat exchanger enters into the third plate. Inlet distillate velocity was determined based on the same pressure drop (<25 psi/ft or <52.5 kPa/m) for each microchannel heat exchanger. Table 4-2 shows the effect of operating pressure on total heat exchanger area (latent plus sensible heat exchangers). The total area strongly depends on the latent heat exchanger area. All calculation results showed that the higher the pressure in the latent heat exchanger, the smaller the total areas; therefore, to minimize cost, the water cost calculation only focuses on the highest pressure (104.7 psia, 722 kPa).

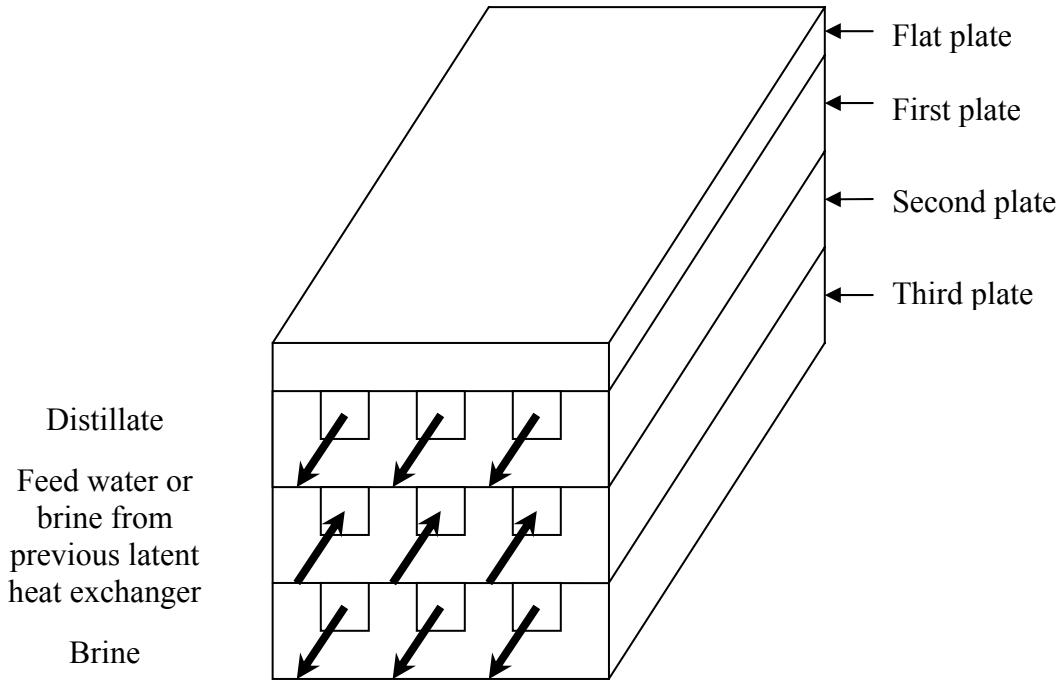

Figure 4-3. Schematic of microchannel heat exchanger.

The sensible heat exchanger can be produced using titanium-coated naval brass. The titanium coat provides a tough surface that resists abrasion and reduces fouling whereas the naval brass core provides good heat transfer. With a wall thickness of 1.5 mm (0.059 inches) as a standard sold in the market, the prototype is counter-current microchannel heat exchanger with single-passage microchannels. All the channels have the same length, making it possible to minimize the variance of the residence time distribution. The costs of sensible and latent heat exchangers are $\$20.55/ft^2$ and $\$8.48/ft^2$, respectively (see Appendix D). With low-cost manufacturing as investigated by Ruiz, it appears that less expensive heat exchanger can be made using naval brass 464.

Table 4-2. Required areas of heat exchangers at various pressures

Description	Brackish water feed	Seawater feed
Latent heat exchanger temperature difference (K)	1.111	0.389
Number of stages	25	20
Inlet distillate velocity in sensible heat exchanger (m/s)	14	14
Distillate pressure drop in sensible heat exchanger (kPa/m)	576	561
Heat transfer areas at 104.7 psia (722 kPa)		
- Latent heat exchanger (m^2)	36,100	54,000
- Sensible heat exchanger (m^2)	13,300	20,500
- Total areas (m^2)	49,400	63,500
Heat transfer areas at 76.7 psia (528.8 kPa)		
- Latent heat exchanger (m^2)	62,500	75,500
- Sensible heat exchanger (m^2)	11,400	18,700
- Total areas (m^2)	73,900	94,200
Heat transfer areas at 59.2 psia (408.2 kPa)		
- Latent heat exchanger (m^2)	86,400	117,000
- Sensible heat exchanger (m^2)	9,900	17,000
- Total areas (m^2)	96,300	134,000

Appendix C shows that when brackish water is used, the minimum water cost can be achieved by using 25 stages. If seawater is used, the system requires 20 stages. Based on the various stages, the cost of water is calculated.

For brackish and seawater feeds, respectively, Tables 4-3 and 4-4 show the cost of desalinated water at three electricity costs: \$0.05/kWh, \$0.1/kWh, and \$0.015/kWh. In these tables, very small temperature differences (0.34 – 2^{o}F, 0.189 K – 1.111 K) were employed. For all electricity costs, potable water from brackish water feed is less expensive (\$0.41/m^3, \$1.54/kgal) than seawater feed (\$0.61/m^3, \$2.31/kgal) (see Appendix C). The water costs are achieved at 5% interest rate and 722 kPa (104.7 psia).

Table 4-3. Water cost for brackish water feed at three electricity costs

Cost for brackish water feed	Electricity cost[a] $0.05/kWh		Electricity cost[b] $0.1/kWh		Electricity cost[b] $0.15/kWh	
	$/m^3	$/yr	$/m^3	$/yr	$/m^3	$/yr
Electricity	0.110	1,532,969	0.135	2,094,736	0.202	2,803,334
Labor[c]	0.036	500,000	0.036	500,000	0.036	500,000
Bond (5%, 30 years)	0.131	1,810,891	0.170	2,320,413	0.170	2,353,734
Maintenance (0.04 x FCI)	0.081	1,113,514	0.105	1,426,818	0.105	1,447,307
Insurance (0.005 x FCI)	0.010	139,189	0.013	178,352	0.013	180,913
Total	0.368	5,096,563	0.459	6,520,319	0.526	7,285,289
Brine injection well	0.041	559,488	0.041	559,488	0.041	559,488
Total	0.409	5,656,051	0.500	7,079,807	0.567	7,844,777

[a]Latent heat exchanger temperature difference is 2°F (1.111 K)
[b]Latent heat exchanger temperature difference is 1°F (0.556 K)
[c]Source: RosTek Associates, Inc., *Desalting Handbook for Planners*, 3rd ed.

Table 4-4. Water cost for seawater feed at three electricity costs

Cost for seawater feed	Electricity cost[a] $0.05/kWh		Electricity cost[a] $0.1/kWh		Electricity cost[b] $0.15/kWh	
	$/m^3	$/yr	$/m^3	$/yr	$/m^3	$/yr
Electricity	0.194	2,684,199	0.389	5,368,399	0.536	7,411,639
Labor[c]	0.036	500,000	0.036	500,000	0.036	500,000
Bond (5%, 30 years)	0.193	2,672,029	0.193	2,672,029	0.215	2,964,897
Maintenance (0.04 x FCI)	0.119	1,643,025	0.119	1,643,025	0.132	1,823,110
Insurance (0.005 x FCI)	0.015	205,378	0.015	205,378	0.017	227,889
Total	0.557	7,704,631	0.752	10,388,831	0.936	12,927,535
Ion Exchange Unit	0.055	760,072	0.055	760,072	0.055	760,072
Total	0.612	8,464,704	0.807	11,148,903	0.991	13,687,607

[a]Latent heat exchanger temperature difference is 0.7°F (0.389 K)
[b]Latent heat exchanger temperature difference is 0.34°F (0.189 K)
[c]Source: RosTek Associates, Inc., *Desalting Handbook for Planners*, 3rd ed.

Figures 4-4, 4-5, and 4-6 summarize the water cost for a variety of interest rates at each electricity cost and brackish water feed. Each figure shows that lower interest rates reduce the water cost. Based on the figures, it is clearer that at low interest rates (5%) typical of municipalities, water is estimated to cost \$0.39/m^3 (\$1.47/kgal) at \$0.05/kWh and ΔT = 1.73^{o}F (0.96 K). For \$0.15/kWh, 5% interest rate, the cost of water is \$0.56/m^3 (\$2.15/kgal) and ΔT = 1.24^{o}F (0.69 K). At high interest rates (20%) typical of industry, water is estimated to cost \$0.70/m^3 (\$2.66/kgal) at \$0.05/kWh (ΔT = 2.11^{o}F or 1.17^{o}K) and \$0.91/m^3 (\$3.45/kgal) at \$0.15/kWh.

Figures 4-7, 4-8, and 4-9 show the water cost for seawater using a variety of interest rates and electricity costs. These figures show similar trends as those for brackish water feed. For \$0.05/kWh electricity, the product water selling price is estimated to be \$0.61/m^3 (\$2.31/kgal) at 5% interest and ΔT = 0.80^{o}F (0.44^{o}K).

Similarly, the price is estimated to be \$0.96/m^3 (\$3.70/kgal) at 20% interest and ΔT = 2.54^{o}F (1.41 K). For \$0.15/kWh, the product water selling price is estimated to be \$0.99/m^3 (\$3.75/kgal) at 5% interest (ΔT = 0.34^{o}F or 0.19^{o}K) and \$1.44/m^3 (\$5.48/kgal) at 20% interest. In this system (see Table C-9), the estimated prices are relatively attractive compared to conventional desalination methods.

The costs of water from brackish water feed are significantly less than that from seawater feed; therefore, brackish water should be selected when available. The saving results primarily from the lower salt concentration.

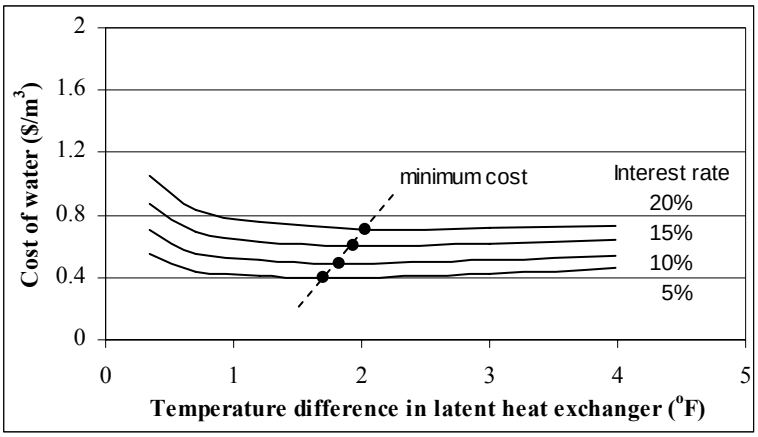

Figure 4-4. Cost of water for a variety of interest rates at energy cost $0.05/kWh, 722 kPa, and brackish water feed.

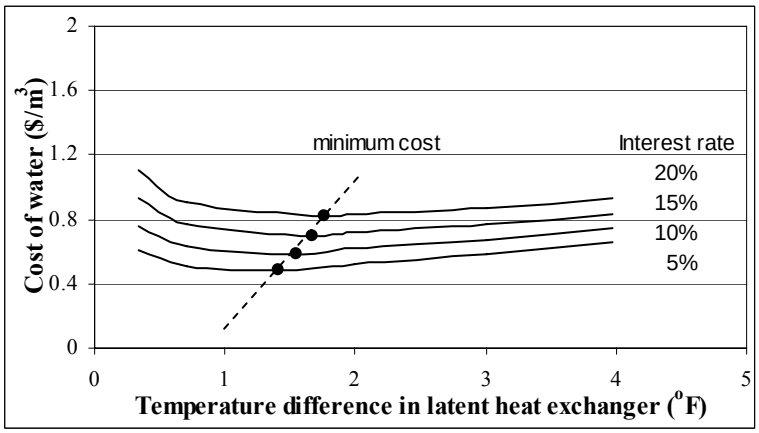

Figure 4-5. Cost of water for a variety of interest rates at energy cost $0.1/kWh, 722 kPa, and brackish water feed.

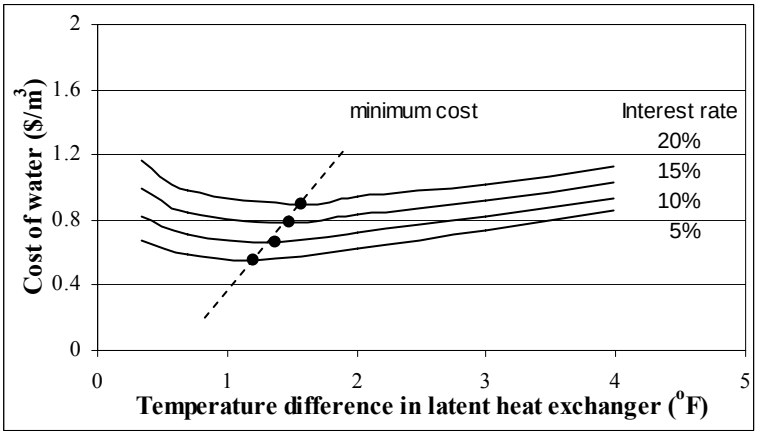

Figure 4-6. Cost of water for a variety of interest rates at energy cost $0.15/kWh, 722 kPa, and brackish water feed.

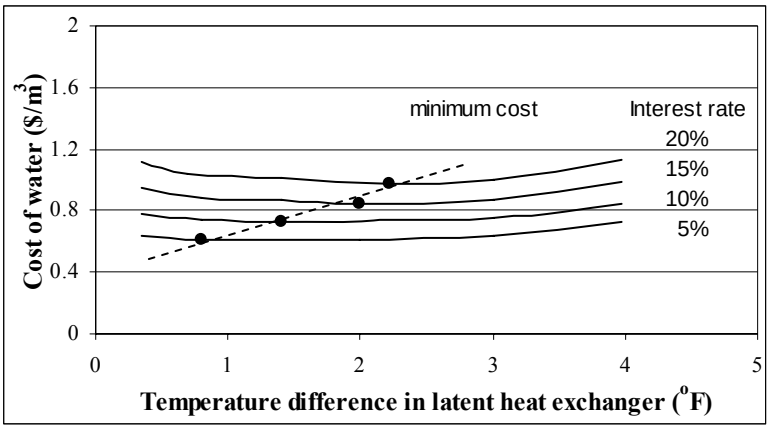

Figure 4-7. Cost of water for a variety of interest rates at energy cost $0.05/kWh, 722 kPa, and seawater feed.

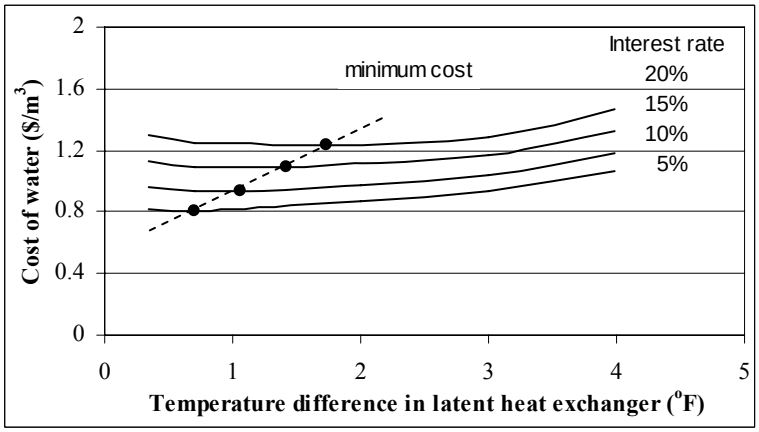

Figure 4-8. Cost of water for a variety of interest rates at energy cost $0.1/kWh, 722 kPa, and seawater feed.

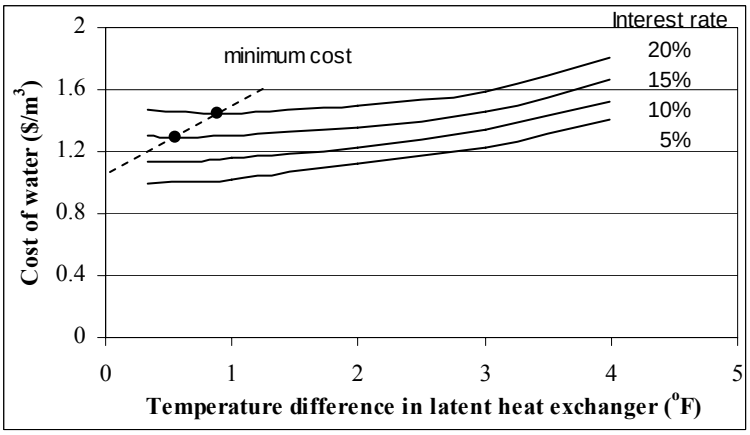

Figure 4-9. Cost of water for a variety of interest rates at energy cost $0.15/kWh, 722 kPa, and seawater feed.

When brackish water feed is used, the brine salt concentration is 15 g/kg and feed recovery is 90%, whereas when seawater is used, the brine salt concentration is 70 g/kg and the recovery is 50%. The lower salt concentration contributes to the higher vapor pressure of salt water and therefore reduces the compression energy requirement.

These results show the optimum cost of water occurs with small different temperature difference (ΔT) in the latent heat exchanger. These curves show that optimal ΔT giving the minimum cost of water is equal to 1.73^{o}F (0.96 K) when brackish water is used at \$0.05/kWh electricity cost. The results represented by Figures 4-7 and 4-8 reveal that the optimal ΔT in the exchanger is 1.57^{o}F (0.87 K) when seawater feed is used.

In temperature difference 0.34 – 2.27^{o}F (0.19 – 1.26 K), the optimum water costs are achieved at heat transfer coefficients (U) from 3,570 to 17,300 Btu/(h·ft^{2}·^{o}F) (20,300 to 98,400 W/(m^{2}·K)). The value is approximately three times higher than the measurement conducted by Tleimat [23]. He showed that at temperature 140^{o}F (333.2 K), the value of U was about 2500 Btu/(h·ft^{2}·^{o}F) (14,200 W/(m^{2}·K))) at temperature difference 0.63 – 2.25^{o}F (0.35 – 1.25K). The result showed that the presence of dissolved salts influenced the value of U in the last effect evaporator because of lower thermal conductivity and higher brine viscosity. The trend reflects the dependence of U on temperature.

Table 4-5 shows that a temperature difference less than 0.389 K needs to be reconsidered because the surface area of latent heat exchanger becomes larger. The temperature difference in the sensible heat exchanger for brackish water feed is much lower than for seawater feed because of the higher percent recovery.

Table 4-5. Summary of operational data and the results of calculations

Description	Brackish water feed	Seawater feed
Pressure (kPa)	722	722
Recovery (%)	90	50
Latent heat exchanger temperature difference 0.189 K		
Heat transfer coefficient (W/(m^2·K))	98,400	98,400
Area of latent heat exchanger surface (m^2)	48,600	48,600
Sensible heat exchanger I surface area (m^2)	23,200	28,800
Temperature difference (K) in Sensible HX I	0.57	1.11
Output distillate temperature (K)	295	295
Number of stages	54	20
Latent heat exchanger temperature difference 0.389 K		
Heat transfer coefficient (W/(m^2·K))	54,000	54,000
Area of latent heat exchanger surface (m^2)	43,000	43,000
Sensible heat exchanger I surface area (m^2)	22,300	24,900
Temperature difference (K) in Sensible HX I	0.80	1.24
Output distillate temperature (K)	295	296
Number of stages	50	20
Latent heat exchanger temperature difference 0.556 K		
Heat transfer coefficient (W/(m^2·K))	40,100	40,100
Area of latent heat exchanger surface (m^2)	40,500	40,500
Sensible heat exchanger I surface area (m^2)	14,700	24,000
Temperature difference (K) in Sensible HX I	0.68	1.35
Output distillate temperature (K)	295	296
Number of stages	40	15

To preheat the incoming feed, the MVC system requires a large sensible heat exchanger prior to the first evaporator stage. Small sensible heat exchangers are located between the remaining evaporator stages. The evaporators operate at high temperatures because of the following benefits: higher heat transfer coefficient, smaller compressor, and less compressor work (lower enthalpy difference of vaporization). However, higher temperatures require larger sensible heat exchangers, expensive pressure vessels, and removal of scaling ions.

Table 4-6 compares the cost of desalinated water produced at the optimum conditions determined in this research to other desalination methods. The costs are based on electricity cost of $0.05/kWh, a value that can be attained in the Gulf States and the United States [27]. Table 4.6 shows that for both brackish and seawater feeds, vapor compression desalination designed in this research is relatively less expensive than most of the alternatives.

Table 4-6. Comparison of various desalination processes at large scale [a]

Process	Water cost ($/m^3)	Capital cost ($/(m^3/day))	Electrical power consumption (MJ/m^3)	Heat (MJ/m^3)
Multi-stage flash desalination[b]	0.77 – 1.84	1,598 – 2,269	14.4	240-290
Reverse osmosis[b]	0.58 – 1.98	1,035 – 1,666	21.6 – 36.0	-
Conventional MVC[b]	0.46 – 2.48	894 – 1,322	21.6 – 36.0	-
Proposed MVC:				
Brackish water feed	0.39	892	7.2[c]	-
Seawater feed	0.61	1,143	14.3[d]	-

[a] Interest rate = 5%, plant life = 30 year, and electric cost = $0.05/kWh
[b] Source: Evaluating the Economics of Desalination, www.cepmagazine.org, 12, 2002
[c] Includes power to drive compressor, pump, and degassing unit.
[d] Includes power to drive compressor, pump, degassing unit, and ion exchange unit.

CHAPTER V

CONCLUSION

Series desalination requires less work than parallel desalination. As shown in Table 4-1, the percent reduction in power consumption increases with decreasing temperature difference in the evaporator. Compared to parallel desalination, series vapor-compression desalination reduces power consumption by 8.37 – 15.21%. This savings is achieved because much of the water is removed at a lower salt concentration, which has a higher vapor pressure and requires less compression ratio. The improvement is more pronounced with small temperature differences in the evaporator (1.111 to 2.222 K, 2 to 4^{o}F).

Optimum conditions for mechanical vapor-compression desalination were determined. The latent heat exchanger employs dropwise condensation, which allows economical operation with very low temperature difference in the evaporator, which makes the system more efficient.

For brackish water feed at 722 kPa, ΔT = 0.96 K, and \$0.05/kWh, the water cost is \$0.39/m^3. These optimal conditions have the following properties:

- heat transfer coefficient = 25,400 W/(m^2·K)
- electricity consumption = 2.0 kWh/m^3
- latent heat exchanger area = 37,000 m^2
- sensible heat exchanger area = 15,800 m^2
- $\Delta T_{\text{sensible}}$ = 1.15 K

- Number of stages = 25

For seawater feed at 722 kPa, ΔT = 0.44 K, and \$0.05/kWh, the water cost is \$0.61/m^3. The optimal conditions have the following properties:

- heat transfer coefficient = 48,300 W/(m^2·K)
- electricity consumption = 3.97 kWh/m^3
- latent heat exchanger area = 42,100 m^2
- sensible heat exchanger area = 23,900 m^2
- $\Delta T_{sensible}$ = 1.27 K
- Number of stages = 20

CHAPTER VI

FUTURE WORK

The following are recommendations for future study:

- Improve heat transfer surfaces

  A recent review [3] recommends that improved heat transfer surfaces be used to facilitate mechanical vapor-compression desalination and reduce cost. The review suggests that additional research is required to optimize both the surface area and cost of water by using polymeric heat-transfer materials.

- Distillate recovery

  Further study should focus on analyzing the effect of varying distillate recovery percentages.

- Higher operating pressure

  Figure 2-9 shows improved heat transfer at higher operating pressures. The effect of higher operating pressures on heat transfer coefficients should be determined experimentally.

When performing these studies, evaluation should be done by designing a 30-year plant and determining the effect on the cost of produced water. Finally, the results obtained in this study should be experimentally tested in the mechanical vapor-compression desalination system.

REFERENCES

[1] V. K. Sharma, G. Fiorenza, and G. Braccio, Seawater Desalination, Presented at NATO Advanced Research Workshop, Hammamet, Tunisia, 2006.

[2] C. Riverol and M. V. Pilipovik, Assessing the seasonal influence on the quality of seawater using fuzzy linear programming, Desalination, 230 (2008) 175-182.

[3] Desalination, with a Grain of Salt – A California Perspective, June 2006, http://www.pacinst.org/reports/desalination/appendix_A.pdf.

[4] R. Clayton, Desalination for Water Supply, Foundation for Water Research, United Kingdom, Foundation for water Research, United Kingdom, 2006.

[5] Flowserve Corporation, Desalination, http://www.flowserve.com/vgnfiles/Files/ Literature/Products/ Pumps/fpd-10-e.pdf. (Accessed on May 8, 2006)

[6] J. H. H. Lara Ruiz, An Advanced Vapor-Compression Desalination System, Ph.D. Dissertation, Texas A&M University, 2005.

[7] S. Nisan, Sea Water Desalination with Innovative Nuclear Reactors and Other Energy Sources: The Eurodesal Project, Commissariat a l'Energie Atomique, Cadarache, France, 2002.

[8] Desalination by Reverse Osmosis, http://www.oas.org/dsd/publications/Unit/oea59e/ch20.htm. (Accessed on May 8, 2006).

[9] Electrodialysis (ED), http://www.ionics.com/technologies/ed/. (Accessed on May 8, 2006).

[10] Electrodialysis, http://www.serve.com/damien/home/solarweb/desal/electrodialysis.htmls. (Accessed on May 8, 2006).

[11] Canadian Salt Company Limited, The Principle of Ion Exchange, 2002, http://www.systemsaver.com/windsor-website/education/how-softeners-work.html.

[12] Groupe Novasep, Novasep Technologies: Ion Exchange, 2008, http://www.novasep.com/Technologies/Ion-exchange.asp.

[13] Filters, Water & Instrumentation, Inc., Ion Exchange System, http://www.filterswater.com/water-purification/ionexch.htm. (Accessed on June 8, 2006).

[14] N. H. Aly and A. K. El-Fiqi, Mechanical vapor compression desalination systems-A case study, Desalination, 158 (2003) 143-150.

[15] F. Al-Juwayhel, H. El-Dessouky, and H. Ettouney, Analysis of single-effect evaporator desalination systems combined with vapor compression heat pumps, Desalination, 114 (1997) 253-275.

[16] M. D. Vishwanathappa, Desalination of Seawater Using a High Efficiency Jet Ejector, M.S. Thesis, Texas A&M University, 2005.

[17] S. J. Senatore, Vapor compression distillation with maximum use of waste heat, Desalination, 38 (1981) 3-12.

[18] M. Lucas and F. Murat, Desalination by mechanical vapor compression operational results after one year operation of the Flamanville unit comparison with other desalination processes by evaporation, Desalination, 55 (1985) 33-42.

[19] M. Lucas and B. Tabourier, The mechanical vapour compression process applied to seawater desalination: A 1,500 ton/day unit installed in the nuclear power plant of Flamanville, France, Desalination, 52 (1985) 123-133.

[20] H. Ettouney, H. El-Dessouky, and Y. Al-Roumi, Analysis of mechanical vapour compression desalination process, Int. J. Energy Res., 23 (1999) 431-451.

[21] Economic and Social Commission for Western Asia, Water Desalination Technologies in the ESCWA Member Countries, http://www.escwa.un.org/information/publications/edit/upload/tech-01-3-e.pdf. (Accessed on August 6, 2006).

[22] G. Kronenberg and F. Lokiec, Low-temperature distillation processes in single- and dual-purpose plants, Desalination, 136 (2001) 189-197.

[23] B.W. Tleimat and M. C. Tleimat, Reduced Energy Consumption Evaporator for Use in Desalting Impaired Waters, Water Treatment Technology Report No. 11, United States Department of the Interior, Bureau of Reclamation, Denver Office, 1995.

[24] R. Rautenbach and B. Arzt, Large scale diesel driven vapor compression units, Desalination, 38 (1981) 75-84.

[25] A. S. Nafey, H. E. S. Fath, and A. A. Mabrouk, A new visual package for design and simulation of desalination processes, Desalination, 194 (2006) 281-296.

[26] A. S. Nafey, H. E. S. Fath, and A. A. Mabrouk, Thermoeconomic design of a multi-effect evaporation mechanical vapor compression (MEE-MVC) desalination process, Desalination, 230 (2008) 1-15.

[27] H. M. Ettouney, H. T. El-Dessouky and P. J. Gowing, Evaluating the economics of desalination, CEP Magazine, December 2002, http://cepmagazine.org.

[28] M. A. Darwish, M. A. Jawad, and G. S. Aly, Comparison between small mechanical vapor compression (MVC) and reverse osmosis (RO) desalting plants, Desalination, 78 (1990) 313-326.

[29] J. M. Veza, Mechanical vapour compression desalination plant: A case study, Desalination, 101 (1995) 1-10.

[30] M. A. Darwish and N. M Al Najem, Energy consumptions and costs of different desalting systems, Desalination, 64 (1987) 83-96.

[31] R. Matz and U. Fisher, A comparison of the relative economics of sea water desalination by vapour compression and reverse osmosis for small to medium capacity plants, Desalination, 36 (1981) 137-151.

[32] G. Leitner, Water desalination: What are today's costs, Desalination and Water Reuse, 2 (1992) 39-43.

[33] O. J. Morin, Desalting plant cost update: 2000, in Proc. IDA World Congress on Desalination and Water Reuse, California, III (1999) 341-359.

[34] Z. Zimerman, Development of large capacity high efficiency mechanical vapor compression (MVC) units, Desalination, 96 (1994) 51-58.

[35] G. Gsell, Water systems utilizing multiple effect and vapor compression technologies compared, ISPE, 24 (2004) 48-72.

[36] R. Bahar, M. N. A. Hawlader, L. S. Woei, Performance evaluation of a mechanical vapor compression desalination system, Desalination, 166 (2004) 123-127.

[37] P. E. Minton, Handbook of Evaporation Technology, Noyes Publications, Union Carbide, VA , 1986.

[38] Aqua-Chem Inc., Vapor Compression, 2007, http://www.aqua-chem.com/ index.php?page=57.

[39] M. Holtzapplze, A. Rabroker, L. Zhu, J. Lara, and S. Watanawanafet, Updated vapor-compression evaporator and heat exchanger systems, Disclosure of invention, Department of Chemical Engineering, Texas A&M University, June 2006.

[40] M. Holtzapple, Advanced vapor compression desalination, Slide presentation, Department of Chemical Engineering, Texas A&M University, 2007.

[41] M. T. Holtzapple and G. P. Noyes, Vapor-Compression Evaporation System and Method, United States Patent 7251944, August 7, 2007.

[42] A. Caillaud, P. Charuit, C. Duffau, and J. Ravoire, Apparatus for the Prevention of Scaling in Desalination Apparatus, United States Patent 3963619, June 15, 1976.

[43] S. A. Al-Saleh and A. R. Khan, Comparative study of two anti-scale agents Belgard EVN and Belgard EV 2000 in multi-stage flash distillation plants in Kuwait, Desalination, 97 (1994) 97-107.

[44] D. Barba, G. D. Giacomo, F. Evangelista, and G. Tagliaferri, High temperature distillation process with seawater feed decalcification pretreatment, Desalination, 40 (1982) 347-355.

[45] L. Zhu, C. B. Granda, and M. T. Holtzapple, Prevention of calcium sulfate formation in seawater desalination by ion exchange, Texas A&M University.

[46] W. H. Emerson and D. T. Jamieson, Some physical of sea water in various concentration, Desalination, 3 (1967) 213.

[47] U. S. Environmental Protection Agency, Evaporation Process, Office of Research and Development, Washington, DC, 1996.

[48] M. S. Peters and K. D. Timmerhaus, Plant Design and Economics for Chemical Engineers, 4th Ed., McGraw-Hill, New York, 1991.

[49] D. Howard, Water and Waste Water Blog, 2007, http://www.waterandwastewater.com/blog/archives/2007/08/class_i_deep_in.shtml .

[50] Rostek Associates and US Department of the Interior, Bureau of Reclamation, Desalting Handbook for Planners, 3rd ed., Denver Federal Center, Colorado, 2003.

[51] G. F. Hewitt, Ed., Handbook of Heat Exchanger Design, Beggel House Inc., New York, 1992.

[52] Matches, Compressor Costs, August 2007, http://matche.com/EquipCost/Compressor.htm.

[53] Siemens, Pricing Guide for Horizontal above NEMA Motors ANSP-6000-0508, May 2008, http://www2.sea.siemens.com/NR/rdonlyres/AF22CB1C-9C9C-4234-8AD5-0B48654872F7/0/Siemens_Pricing_Guide_Horizontal_ANEMA_ANSP600000508_R0.pdf.

[54] H. P. Loh and J. Lyons, Process Equipment Cost Estimation, Technical Report, National Energy Technology Center, Pittsburgh, PA, 2002.

[55] Online Metals Company, Online Metals, http://www.onlinemetals.com. (Accessed on December 27, 2008)

[56] Alloy Calculator, http://metalprices.com/FreeSite/alloycalc/AlloyCalc.aspx. (Accessed on December 30, 2008)

[57] Davis Industrial Coatings, Figuring Cost, http://www.davispaint.com/figure.htm. (Accessed on February 15, 2009)

[58] Pacific Northwest Pollution Prevention Resource Center, Evaluating Less Toxic Paints and Coatings?, http://www.pprc.org/pubs/factsheets/coatcost.html. (Accessed on February 15, 2009)

[59] Tiax Llc, Energy Efficient Rooftop Air-Conditioner, Tiax Llc, Cambridge, MA, 2003.

Supplemental Sources Consulted

Alpha Knife Supply, Titanium Sheets, August 2007, http://www.alphaknifesupply.com/ti-small.htm.

Matches, Pump Pos Displ Cost, August 2007, http://matche.com/EquipCost/PumpPositive.htm.

Perry, J. H. Chemical Engineers' Handbook, 5th ed., McGraw-Hill, New York, 1973.

Siemens, Pricing Guide for Horizontal above NEMA Motors ANSP-60000-1205, June 2008, http://www.sea.siemens.com/motorsbu/product/Pricing%20Guides/Siemens_Pricing_Guide_Horizontal_ANEMA_ANSP-60000-1205pv.pdf.

WebDopc, Boiling Point problem Solution, August 2007, http://dbhs.wvusd.k12.ca.us/webdocs/Solutions/BP-Elev-Probs.html.

APPENDIX A

SALT WATER PROPERTIES

Table A-1 shows the typical composition of seawater. "Average" seawater [51] contains about 35 g/kg dissolved solid. Table A-2 shows that density of seawater depends on the temperature as well as the solute concentration. The dynamic viscosity of seawater is 1.877×10^{-3} N/(m^2·s) at 0^{o}C and 0.163×10^{-3} N/(m^2·s) at 180^{o}C (Table A-3). Tables A-4 to A-7 show other properties at selected levels of salinity in seawater used in the economic analysis.

Table A-1. Composition of seawater [51]

Ion	Concentration in seawater (g/kg)
Chloride	19.344
Sodium	10.773
Sulfate	2.712
Magnesium	1.294
Calcium	0.412
Potassium	0.399
Bicarbonate	1.142
Bromide	0.067
Strontium	0.008
Boron	0.004
Fluoride	0.0013
Total	35.00

Table A-2. Density of seawater and its concentrates (kg/m^3) [51]

Salinity (g/kg)																
t (°C)	0[a]	10	20	30	40	50	60	70	80	90	100	110	120	130	140	150
0	999.8	1008.1	1016.2	1024.2	1032.0	1039.8	1047.6	1055.5	1063.5	1071.6	1079.7	1088.0	1096.2	1104.4	1112.5	1120.4
10	999.7	1007.7	1015.5	1023.2	1.030.2	1038.4	1046.0	1053.8	1061.6	1669.6	1077.6	1085.7	1093.9	1102.0	1110.1	1118.0
20	998.4	1005.8	1013.3	1020.8	1028.3	1035.9	1043.5	1051.2	1058.9	1066.7	1074.5	1082.4	1090.3	1098.2	1106.2	1114.2
30	995.4	1002.8	1010.2	1017.6	1025.1	1032.6	1040.2	1047.8	1055.4	1063.1	1070.8	1078.5	1086.3	1094.1	1102.0	1109.9
40	991.9	999.2	1006.6	1013.9	1021.4	1028.8	1036.3	1043.8	1051.4	1059.0	1066.6	1074.2	1081.9	1089.6	1091.4	1105.2
50	987.7	995.0	1002.3	1009.7	1017.1	1024.5	1031.9	1039.4	1046.9	1054.4	1062.0	1069.5	1077.1	1084.8	1092.4	1100.1
60	982.9	990.2	997.5	1004.9	1012.2	1019.6	1027.0	1034.5	1041.9	1049.4	1056.9	1064.4	1072.0	1079.5	1087.1	1094.8
70	977.6	984.9	992.2	999.5	1006.9	1014.3	1021.7	1029.1	1036.5	1043.9	1051.4	1058.9	1066.4	1074.0	1081.5	1089.1
80	971.7	979.0	986.4	993.7	1001.1	1008.4	1015.8	1023.2	1030.6	1038.1	1045.5	1053.0	1060.5	1068.0	1075.6	1083.1
90	965.3	972.7	980.0	987.4	994.7	1002.1	1009.5	1017.0	1024.4	1031.8	1039.3	1046.8	1054.3	1061.8	1069.3	1076.8
100	958.4	965.8	973.2	980.6	988.0	995.4	1002.8	1010.3	1017.7	1025.2	1032.7	1040.2	1047.7	1055.2	1062.7	1070.3
110	951.0	958.5	965.9	973.3	980.8	988.3	995.7	1003.2	1010.7	1018.2	1025.7	1033.2	1040.8	1048.3	1055.9	1063.4
120	943.2	950.7	958.2	965.7	973.2	980.7	988.2	995.8	1003.3	1010.9	1018.4	1026.0	1033.6	1041.2	1048.7	1056.3
130	934.8	942.4	950.0	957.6	965.2	972.8	980.4	988.0	995.6	1003.2	1010.8	1018.5	1026.1	1033.7	1041.3	1049.0
140	926.1	933.8	941.4	949.1	956.8	964.5	972.2	979.9	987.6	995.2	1002.9	1010.6	1018.3	1026.0	1033.7	1041.4
150	916.9	924.7	932.5	940.3	948.1	955.9	963.7	971.4	979.2	987.0	994.8	1002.5	1010.3	1018.0	1025.8	1033.6
160	907.3	915.2	923.2	931.1	939.0	946.9	954.8	962.7	970.6	978.5	986.3	994.2	1002.0	1009.9	1017.7	1025.5
170	897.3	905.4	913.5	921.6	929.6	937.7	945.7	953.7	961.7	969.7	977.6	985.6	993.5	1001.4	1009.3	1017.2
180	887.0	895.3	903.5	911.7	919.9	928.1	936.3	944.4	952.6	960.7	968.7	976.8	984.8	992.8	1000.8	1008.7

Table A-2. Continued

Salinity (g/kg)											
t (°C)	30	31	32	33	34	35	36	37	38	39	40
0	1024.2	1024.9	1025.7	1026.5	1027.3	1028.1	1028.9	1029.6	1030.4	1031.2	1032.0
10	1023.2	1023.9	1024.7	1025.4	1026.2	1027.0	1027.7	1028.5	1029.3	1030.0	1030.8
20	1020.8	1021.5	1022.3	1023.0	1023.8	1024.5	1025.3	1026.0	1026.8	1027.5	1028.3
30	1017.6	1018.4	1019.1	1019.9	1020.6	1021.4	1022.1	1022.9	1023.6	1024.4	1025.1
40	1013.9	1014.7	1015.4	1016.2	1016.9	1017.7	1018.4	1019.1	1019.9	1020.6	1021.4
50	1009.7	1010.4	1011.2	1011.9	1012.6	1013.4	1014.1	1014.8	1015.6	1016.3	1017.1
60	1004.9	1005.6	1006.3	1007.1	1007.8	1008.6	1009.3	1010.0	1010.8	1011.5	1012.2
70	999.5	1000.3	1001.0	1001.7	1002.5	1003.2	1003.9	1004.7	1005.4	1006.2	1006.9
80	993.7	994.4	995.2	995.9	996.6	997.4	998.1	998.8	999.6	1000.3	1001.1
90	987.4	988.1	988.8	989.6	990.3	991.1	991.8	992.5	993.3	994.0	994.7
100	980.6	981.3	982.1	982.8	983.5	984.3	985.0	985.8	986.5	987.2	988.0
110	973.3	974.1	974.8	975.6	976.3	977.1	997.8	978.6	979.3	980.0	980.8
120	965.7	966.4	967.2	967.9	968.7	969.4	970.2	970.9	971.7	972.4	973.2
130	957.6	958.4	959.1	959.9	960.6	961.4	962.1	962.9	963.7	964.4	965.2
140	949.1	949.9	950.7	951.4	952.2	953.0	953.7	954.5	955.3	956.0	956.8
150	940.3	941.1	941.8	942.6	943.4	944.2	945.0	945.7	946.5	947.3	948.1
160	931.1	931.9	932.7	933.5	934.4	935.1	935.8	936.6	937.4	938.2	939.0
170	921.6	922.4	923.7	924.0	924.8	925.6	926.4	927.2	928.0	928.8	929.6
180	911.7	912.6	913.4	914.2	915.0	915.8	916.7	917.5	918.3	919.1	919.9

[a] While these values for pure water are within the claimed accuracy, more accurate values are available in the appropriate ESDU Data Item

Table A-3. Dynamic viscosity of seawater and concentrates (10^{-3} Ns/m^2) [51]

	Salinity (g/kg)															
t (°C)	0[a]	10	20	30	40	50	60	70	80	90	100	110	120	130	140	150
0	1.775	1.802	1.831	1.861	1.893	1.928	1.965	2.005	2.049	2.096	2.147	2.202	2.261	2.326	2.395	2.470
10	1.304	1.327	1.350	1.375	1.401	1.429	1.459	1.491	1.526	1.563	1.603	1.646	1.693	1.743	1.797	1.855
20	1.002	1.021	1.041	1.061	1.083	1.106	1.131	1.157	1.185	1.216	1.248	1.283	1.321	1.361	1.404	1.451
30	0.797	0.814	0.830	0.848	0.866	0.886	0.906	0.929	0.952	0.977	1.004	1.033	1.064	1.098	1.133	1.171
40	0.653	0.667	0.681	0.696	0.712	0.729	0.747	0.765	0.786	0.807	0.830	0.845	0.880	0.908	0.938	0.970
50	0.546	0.559	0.571	0.585	0.599	0.613	0.629	0.645	0.662	0.681	0.700	0.721	0.744	0.768	0.793	0.821
60	0.466	0.477	0.488	0.500	0.512	0.525	0.539	0.533	0.568	0.584	0.602	0.620	0.639	0.660	0.682	0.706
70	0.404	0.414	0.424	0.434	0.445	0.457	0.469	0.481	0.495	0.509	0.524	0.540	0.558	0.576	0595	0.616
80	0.355	0.364	0.373	0.382	0.392	0.402	0.413	0.424	0.436	0.449	0.463	0.477	0.492	0.508	0.525	0.544
90	0.315	0.323	0.331	0.340	0.349	0.358	0.368	0.378	0.389	0.400	0.412	0.425	0.439	0.453	0.469	0.485
100	0.282	0.290	0.397	0.305	0.313	0.322	0.331	0.340	0.350	0.360	0.371	0.383	0.395	0.408	0.422	0.436
110	0.255	0.262	0.269	0.276	0.284	0.291	0.300	0.308	0.317	0.326	0.336	0.347	0.358	0.370	0.382	0.395
120	0.232	0.239	0.245	0.252	0.259	0.266	0.273	0.281	0.289	0.298	0.307	0.317	0.327	0.337	0.349	0.361
130	0.213	0.219	0.225	0.231	0.237	0.244	0.251	0.258	0.266	0.273	0.282	0.291	0.300	0.310	0.320	0.331
140	0.196	0.201	0.207	0.213	0.219	0.225	0.231	0.238	0.245	0.252	0.260	0.268	0.277	0.286	0.295	0.305
150	0.181	0.187	0.192	0.197	0.203	0.208	0.214	0.221	0.227	0.234	0.241	0.249	0.256	0.265	0.273	0.283
160	0.169	0.173	0.178	0.183	0.189	0.194	0.200	0.205	0.211	0.218	0.224	0.231	0.239	0.246	0.254	0.263
170	0.157	0.162	0.167	0.171	0.176	0.181	0.186	0.192	0.198	0.203	0.210	0.216	0.223	0.230	0.237	0.245
180	0.147	0.152	0.156	0.161	0.165	0.170	0.175	0.180	0.185	0.191	0.196	0.202	0.209	0.215	0.222	0.230

Table A-3. Continued

Salinity (g/kg)											
t (°C)	30	31	32	33	34	35	36	37	38	39	40
0	1.861	1.864	1.867	1.871	1.874	1.877	1.880	1.883	1.887	1.890	1.893
10	1.375	1.377	1.380	1.382	1.385	1.388	1.390	1.393	1.396	1.398	1.401
20	1.061	1.063	1.065	1.068	1.070	1.072	1.074	1.076	1.078	1.081	1.083
30	0.848	0.850	0.851	0.853	0.855	0.857	0.859	0.861	0.862	0.864	0.866
40	0.696	0.698	0.699	0.701	0.702	0.704	0.706	0.707	0.709	0.710	0.712
50	0.585	0.586	0.587	0.589	0.590	0.592	0.593	0.594	0.596	0.597	0.599
60	0.500	0.501	0.503	0.504	0.505	0.506	0.507	0.509	0.510	0.511	0.512
70	0.434	0.435	0.437	0.438	0.439	0.440	0.441	0.442	0.443	0.444	0.445
80	0.382	0.383	0.384	0.385	0.386	0.387	0.388	0.389	0.390	0.391	0.392
90	0.340	0.341	0.342	0.343	0.343	0.344	0.345	0.349	0.347	0.348	0.349
100	0.305	0.306	0.307	0.308	0.308	0.309	0.310	0.311	0.312	0.312	0.313
110	0.276	0.277	0.278	0.278	0.279	0.280	0.281	0.281	0.282	0.283	0.284
120	0.252	0.252	0.253	0.254	0.254	0.255	0.256	0.257	0.257	0.258	0.259
130	0.231	0.231	0.232	0.233	0.233	0.234	0.235	0.235	0.236	0.237	0.237
140	0.213	0.213	0.214	0.215	0.215	0.216	0.216	0.217	0.218	0.218	0.219
150	0.197	0.198	0.198	0.199	0.199	0.200	0.200	0.201	0.202	0.202	0.203
160	0.183	0.184	0.184	0.185	0.186	0.186	0.187	0.187	0.188	0.188	0.189
170	0.171	0.172	0.172	0.173	0.173	0.174	0.174	0.175	0.175	0.176	0.176
180	0.161	0.161	0.161	0.162	0.162	0.163	0.163	0.164	0.164	0.165	0.165

[a]While these values for pure water are within the claimed accuracy, more accurate values are available in the appropriate ESDU Data Item

Table A-4. Heat capacity of seawater and its concentrates (kJ/(kg·K)) [51]

Salinity (g/kg)																
t (°C)	0[a]	10	20	30	40	50	60	70	80	90	100	110	120	130	140	150
0	4.209	4.143	4.081	4.021	3.964	3.910	3.858	3.809	3.763	3.720	3.679	3.641	3.606	3.573	3.543	3.516
10	4.198	4.136	4.077	4.020	3.965	3.913	3.863	3.815	3.770	3.727	3.686	3.648	3.612	3.579	3.547	3.518
20	4.189	4.131	4.074	4.020	3.967	3.917	3.868	3.822	3.777	3.735	3.649	3.656	3.619	3.584	3.552	3.521
30	4.184	4.128	4.074	4.021	3.971	3.922	3.874	3.829	3.785	3.743	3.702	3.663	3.626	3.591	3.557	3.525
40	4.180	4.127	4.075	4.024	3.975	3.927	3.881	3.836	3.793	3.751	3.710	3.671	3.633	3.597	3.562	3.529
50	4.180	4.128	4.078	4.029	3.981	3.934	3.888	3.844	3.801	3.759	3.719	3.679	3.641	3.604	3.568	3.533
60	4.181	4.131	4.082	4.034	3.987	3.941	3.896	3.853	3.810	3.768	3.727	3.687	3.649	3.611	3.574	3.538
70	4.186	4.137	4.088	4.041	3.995	3.950	3.905	3.861	3.819	3.777	3.736	3.696	3.657	3.618	3.581	3.544
80	4.192	4.144	4.096	4.050	4.004	3.959	3.914	3.871	3.828	3.786	3.745	3.704	3.665	3.626	3.588	3.551
90	4.202	4.154	4.106	4.059	4.014	3.968	3.924	3.880	3.837	3.795	3.754	3.713	3.673	3.634	3.595	3.558
100	4.213	4.165	4.118	4.071	4.025	3.979	3.934	3.891	3.847	3.805	3.763	3.722	3.82	3.642	3.603	3.565
110	4.228	4.179	4.131	4.083	4.037	3.991	3.946	3.901	3.857	3.815	3.772	3.731	3.690	3.651	3.612	3.573
120	4.245	4.195	4.146	4.097	4.050	4.003	3.957	3.912	3.868	3.825	3.782	3.740	3.700	3.659	3.620	3.582
130	4.264	4.213	4.162	4.113	4.064	4.016	3.970	3.924	3.879	3.835	3.792	3.750	3.709	3.669	3.629	3.591
140	4.286	4.233	4.181	4.129	4.079	4.030	3.982	3.936	3.890	3.845	3.802	3.760	3.718	3.678	3.639	3.601
150	4.311	4.255	4.201	4.148	4.096	4.045	3.996	3.948	3.902	3.856	3.812	3.769	3.728	3.688	3.649	3.611
160	4.338	4.279	4.222	4.167	4.113	4.061	4.010	3.961	3.913	3.867	3.823	3.780	3.738	3.698	3.659	3.622
170	4.367	4.306	4.246	4.188	4.132	4.078	4.025	3.974	3.926	3.878	3.833	3.790	3.748	3.708	3.670	3.634
180	4.399	4.334	4.271	4.210	4.152	4.095	4.041	3.988	3.938	3.890	3.844	3.800	3.758	3.719	3.681	3.646

Table A-4. Continued

Salinity (g/kg)											
t (°C)	30	31	32	33	34	35	36	37	38	39	40
0	4.021	4.015	4.010	4.004	3.998	3.992	3.987	3.981	3.975	3.970	3.964
10	4.020	4.014	4.009	4.003	3.998	3.992	3.987	3.981	3.976	3.971	3.965
20	4.020	4.015	4.009	4.004	3.999	3.993	3.988	3.983	3.978	3.973	3.967
30	4.021	4.016	4.011	4.006	4.001	3.996	3.991	3.986	3.981	3.976	3.971
40	4.024	4.019	4.014	4.009	4.004	4.000	3.995	3.990	3.985	3.980	3.975
50	4.029	4.024	4.019	4.014	4.009	4.004	4.000	3.995	3.990	3.985	3.981
60	4.034	4.029	4.025	4.020	4.015	4.011	4.006	4.001	3.997	3.992	3.987
70	4.041	4.037	4.032	4.027	4.023	4.018	4.013	4.009	4.004	4.000	3.995
80	4.050	4.045	4.040	4.036	4.031	4.027	4.022	4.017	4.013	4.008	4.004
90	4.059	4.055	4.050	4.046	4.041	4.036	4.032	4.027	4.023	4.018	4.014
100	4.071	4.066	4.061	4.057	4.052	4.048	4.043	4.038	4.034	4.029	4.025
110	4.083	4.079	4.074	4.069	4.065	4.060	4.055	4.051	4.046	4.041	4.037
120	4.097	4.092	4.088	4.083	4.078	4.073	4.069	4.064	4.059	4.054	4.050
130	4.113	4.108	4.103	4.098	4.093	4.088	4.083	4.078	4.074	4.069	4.064
140	4.129	4.124	4.119	4.114	4.109	4.104	4.099	4.094	4.089	4.084	4.079
150	4.148	4.142	4.137	4.132	4.127	4.121	4.116	4.111	4.106	4.101	4.096
160	4.167	4.162	4.156	4.151	4.145	4.140	4.135	4.129	4.124	4.119	4.113
170	4.188	4.182	4.177	4.171	4.165	4.160	4.154	4.149	4.143	4.137	4.132
180	4.120	4.204	4.198	4.192	4.187	4.181	4.175	4.169	4.163	4.157	4.152

[a]While these values for pure water are within the claimed accuracy, more accurate values are available in the appropriate ESDU Data Item

Table A-5. Thermal conductivity of seawater and its concentrates (mW/(m·K)) [51]

	Salinity (g/kg)																
t (°C)	0[a]	10	20	30	35[b]	40	50	60	70	80	90	100	110	120	130	140	150
0	572	570	569	567	566	565	563	562	560	558	556	554	552	550	548	546	544
10	589	587	586	584	584	583	581	580	578	577	575	573	571	570	568	566	564
20	604	603	602	600	600	599	598	597	595	594	592	591	589	588	586	585	583
30	618	617	616	615	614	614	613	612	611	609	608	607	606	604	603	602	600
40	630	629	629	628	628	627	626	626	625	624	623	622	621	620	618	617	616
50	641	641	640	640	639	639	639	638	637	637	636	635	634	633	632	631	630
60	651	651	650	650	650	650	649	649	649	648	648	647	646	646	645	644	644
70	659	659	659	659	659	659	659	659	658	658	658	658	657	657	656	656	655
80	666	666	667	667	667	667	667	667	667	667	667	667	667	666	666	666	666
90	672	672	673	673	673	674	674	674	674	675	675	675	675	675	675	675	675
100	676	677	678	678	679	679	680	680	681	681	681	682	682	682	682	682	683
110	680	681	682	683	683	683	684	685	685	686	687	687	688	688	688	689	689
120	682	683	684	685	686	686	687	688	689	690	691	691	692	693	693	694	694
130	683	685	686	687	688	688	690	691	692	693	694	695	695	696	697	698	699
140	684	685	687	688	689	689	691	692	693	694	696	697	698	699	700	701	702
150	683	684	686	688	688	689	691	692	694	695	696	698	699	700	701	702	703
160	681	683	684	686	687	688	690	691	693	694	696	697	699	700	701	703	704
170	678	680	682	684	685	686	687	689	691	693	694	696	698	699	701	702	704
180	674	676	678	680	681	682	684	686	686	690	692	694	695	697	699	700	702

[a] While these values for pure water are within the claimed accuracy, more accurate values are available in the appropriate ESDU Data Item.
[b] "Normal" seawater

Table A-6. Prandtl number of seawater and its concentrates [51]

	Salinity (g/kg)																
t (°C)	0[a]	10	20	30	35[b]	40	50	60	70	80	90	100	110	120	130	140	150
0	13.1	13.1	13.1	13.2	13.2	13.3	13.4	13.5	13.6	13.8	14.0	14.3	14.5	14.8	15.2	15.5	16.0
10	9.29	9.35	9.39	9.46	9.49	9.53	9.62	9.72	9.84	9.97	10.1	10.3	10.5	10.7	11.0	11.2	11.6
20	6.95	6.99	7.04	7.11	7.13	7.17	7.24	7.33	7.43	7.53	7.67	7.80	7.96	8.13	8.32	8.52	8.76
30	5.40	5.45	5.49	5.54	5.58	5.60	5.67	5.74	5.82	5.92	6.01	6.12	6.24	6.39	6.54	6.69	6.88
40	4.33	4.38	4.41	4.46	4.48	4.51	4.57	4.63	4.70	4.78	4.86	4.95	5.05	5.16	5.28	5.42	5.56
50	3.56	3.60	3.64	3.68	3.71	3.73	3.77	3.83	3.89	3.95	4.02	4.10	4.18	4.28	4.38	4.48	4.60
60	2.99	3.03	3.06	3.10	3.12	3.14	3.19	3.24	3.28	3.34	3.40	3.47	3.54	3.61	3.69	3.78	3.88
70	2.57	2.60	2.63	2.66	2.68	2.70	2.74	2.78	2.82	2.87	2.92	2.98	3.04	3.11	3.18	3.25	3.33
80	2.23	2.26	2.29	2.32	2.34	2.35	2.39	2.42	2.46	2.50	2.55	2.60	2.65	2.71	2.77	2.83	2.90
90	1.97	2.00	2.02	2.05	2.06	2.08	2.11	2.14	2.18	2.21	2.25	2.29	2.34	2.39	2.44	2.50	2.56
100	1.75	1.78	1.80	1.83	1.84	1.86	1.88	1.92	1.94	1.98	2.01	2.05	2.09	2.13	2.18	2.23	2.28
110	1.59	1.61	1.63	1.65	1.66	1.68	1.70	1.73	1.75	1.78	1.81	1.84	1.88	1.92	1.96	2.00	2.05
120	1.44	1.47	1.49	1.51	1.51	1.53	1.55	1.57	1.60	1.62	1.65	1.68	1.71	1.75	1.78	1.82	1.86
130	1.33	1.35	1.37	1.38	1.39	1.40	1.42	1.44	1.46	1.49	1.51	1.54	1.57	1.60	1.63	1.66	1.70
140	1.23	1.24	1.26	1.28	1.29	1.30	1.31	1.33	1.35	1.37	1.39	1.42	1.44	1.47	1.50	1.53	1.56
150	1.14	1.16	1.18	1.19	1.20	1.21	1.22	1.24	1.26	1.27	1.30	1.32	1.34	1.36	1.39	1.42	1.45
160	1.08	1.08	1.10	1.11	1.12	1.13	1.14	1.16	1.17	1.19	1.21	1.23	1.25	1.28	1.30	1.32	1.35
170	1.01	1.03	1.04	1.05	1.06	1.06	1.07	1.09	1.10	1.12	1.132\	1.16	1.17	1.20	1.22	1.24	1.26
180	0.959	0.975	0.983	0.997	1.00	1.00	1.02	1.03	1.04	1.06	1.07	1.09	1.10	1.13	1.14	1.17	1.19

[a] While these values for pure water are within the claimed accuracy, more accurate values are available in the appropriate ESDU Data Item
[b] "Normal" seawater

Table A-7 shows the boiling point elevation increases with salinity and temperature. The values in the table are used to determine compressor inlet temperature.

Table A-7. Measured boiling point elevation at the solution temperature [46]

Sample No.	Salinity (g/kg)	Temperature (^{o}C)	Measured pressure (P) (10^5 N/m^2)	Boiling point elevation at measured pressure (^{o}C)
1	33.13	100.392	1.0098	0.49
	33.21	119.686	1.9317	0.55
	33.32	136.705	3.2318	0.61
	33.56	159.998	6.0698	0.70
	33.88	180.315	9.9134	0.81
2	33.13	99.887	0.9922	0.48
	33.21	120.155	1.9608	0.55
	33.32	136.542	3.2162	0.61
	33.54	159.808	6.0410	0.70
	33.84	177.948	9.3850	0.81
3	66.26	101.970	1.0484	1.01
	66.41	119.422	1.8806	1.13
	66.66	137.635	3.2570	1.27
	67.09	158.705	5.7608	1.45
	67.72	179.031	9.4414	1.63
4	115.97	101.776	1.0074	1.94
	116.24	119.748	1.8385	2.16
	116.66	138.059	3.1907	2.41
	117.44	159.583	5.7069	2.69
	118.61	180.531	9.4616	3.03
5	116.27	121.250	1.9289	2.16
	116.67	138.354	3.2181	2.39
	117.49	160.463	5.8357	2.71
	118.69	181.240	9.6170	3.04
6	165.68	102.800	1.0059	3.01
	166.03	119.030	1.7322	3.29
	166.68	137.520	3.0285	3.66
	167.70	158.330	5.3304	4.06
	169.27	178.760	8.7678	4.50

APPENDIX B

VAPOR COMPRESSION TRADE-OFFS

The following basic process-design variables are used to determine the work requirements of series and parallel mechanical vapor-compression desalination. The seawater feed is assumed to be 295 kg/s, which is based on previous research [6]. The feed is 35 g salt/kg seawater ($x_f = 0.035$). In this analysis, four evaporators stages will be used because the optimum number of stages has not been determined yet. In steady-state flow, the seawater concentration on the liquid side is specified to be 70 g salt/kg seawater. Figure B-1 shows the system boundary for an overall mass balance.

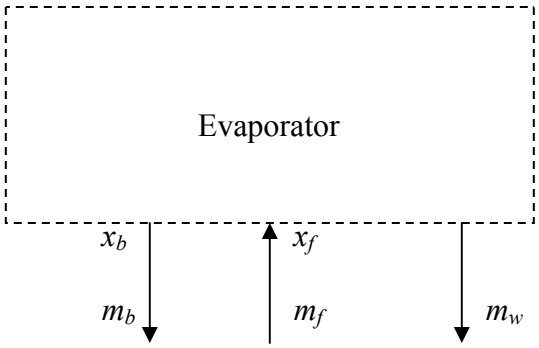

Figure B-1. Overall mass-balance.

The mass balance is: $m_{w\,tot} + m_{b\,tot} = m_{f\,tot}$

Salt mass balance: $m_{f\,tot} \cdot x_f = m_{b\,tot} \cdot x_b$

$$295 \text{ kg/s} \cdot 0.035 = m_{b\,tot} \cdot 0.07$$

$$m_{b\,tot} = 147.5 \text{ kg/s}$$

$m_{w\,tot} + m_{b\,tot} = m_{f\,tot}$

$$m_{w\,tot} + 147.5 \text{ kg/s} = 295 \text{ kg/s}$$

$$m_{w\,tot} = 147.5 \text{ kg/s}$$

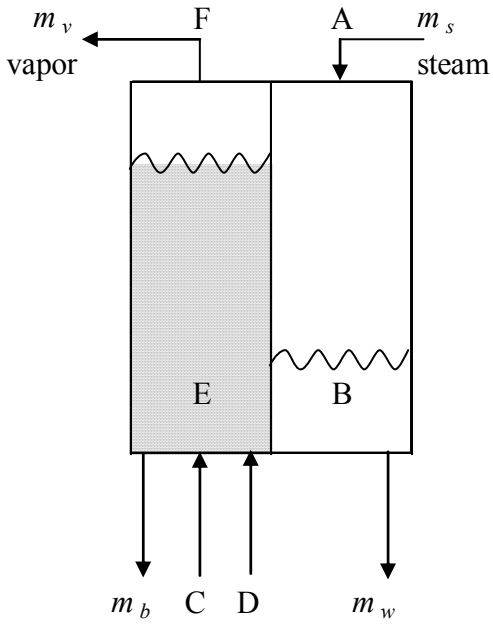

Figure B-2. Evaporator mass balance diagram.

Figure B-2 shows the nomenclature used to identify each stage of the evaporator.

Based on Figure B-2, the mass flow in each stage of the evaporator follows:

$$m_s = m_w = m_v = m_{w\,tot} / 4$$

$$= 147.5 / 4$$

$$= 36.9 \text{ kg/s}$$

Salt mass flow $= 0.035 \times 295$ kg/s

$= 10.3$ kg/s

In the first step, it is assumed there are four evaporator stages because the optimum number of stage has not been known yet, the last one with concentration 70 g/kg seawater.

Evaporator I

Mass balance: $m_s + m_f = m_w + m_v + m_b$

$$36.9 \text{ kg/s} + 295 \text{ kg/s} = 36.9 \text{ kg/s} + 36.9 \text{ kg/s} + m_b$$

$$m_b = 258.1 \text{ kg/s}$$

The brine concentration (x_b) in Evaporator I:

$$x_b = \frac{\text{salt mass}}{\text{brine mass}}$$

$$x_b = \frac{10.3 \text{ kg}}{258.1 \text{ kg}}$$

$$x_b = 0.040$$

Evaporator II

Mass balance:

$$36.9 \text{ kg/s} + 258.1 \text{ kg/s} = 36.9 \text{ kg/s} + 36.9 \text{ kg/s} + m_b$$

$$m_b = 221.3 \text{ kg/s}$$

The brine concentration (x_b) in Evaporator II:

$$x_b = \frac{10.3 \text{ kg}}{221.3 \text{ kg}}$$

$$x_b = 0.047$$

Evaporator III

$$36.9\ \text{kg/s} + 221.3\ \text{kg/s} = 36.9\ \text{kg/s} + 36.9\ \text{kg/s} + m_b$$

$$m_b = 184.4\ \text{kg/s}$$

The brine concentration (x_b) in Evaporator III:

$$x_b = \frac{10.3\ \text{kg}}{184.4\ \text{kg}}$$

$$x_b = 0.056$$

Evaporator IV

$$36.9\ \text{kg/s} + 184.4\ \text{kg/s} = 36.9\ \text{kg/s} + 36.9\ \text{kg/s} + m_b$$

$$m_b = 147.5\ \text{kg/s}$$

The brine concentration (x_b) in Evaporator IV:

$$x_b = \frac{10.3\ \text{kg}}{147.5\ \text{kg}}$$

$$x_b = 0.070$$

THERMODYNAMICS CALCULATIONS FOR WET COMPRESSOR

Case I. ΔT_{cond} **= 1.111 K (2°F)**

7% Salt Activity Calculation

For S = 70 g/kg, substitute in the activity formula as follows:

$\log_{10}(P/P_o) = hS + jS^2$

where P = vapor pressure of salt water at the same temperature (10^5 N/m^2)

$h = -2.1609 \cdot 10^{-4}$

$j = -3.5012 \cdot 10^{-7}$

S = salinity (g salt/kg seawater)

$$\log_{10}(P/P_o) = (-2.1609 \cdot 10^{-4})(70) + (-3.5012 \cdot 10^{-7})(70)^2$$

$$= -0.016842$$

$$P/P_o = 10^{-0.016842}$$

$$= 0.961962$$

The nomenclature follows Figure B-2.

Stage 4

Point A P = 9.16 atm (maximum pressure for dropwise condensation, 120 psig)

T = 449.84 K (saturated steam table)

Point B P = 9.16 atm

T = 449.846 K

Point F T = 449.846 K – 1.111 K

= 448.735 K

P_o = 8.92447 atm (Saturated steam table)

P = 0.961962 (8.92447 atm)

= 8.58500 atm

5.6% Salt Activity Calculation

For S = 56 g/kg, substitute in the activity formula as follows:

$\log_{10}(P/P_o) = hS + jS^2$

$\log_{10}(P/P_o) = (-2.1609 \cdot 10^{-4})(56) + (-3.5012 \cdot 10^{-7})(56)^2$

= –0.013199

$P/P_o = 10^{-0.013199}$

= 0.970065

Stage 3

Point A P = 8.58500 atm

T = 448.735 K

Point B P = 8.58500 atm

T = 447.092 K

Point F T = 447.092 K – 1.111 K

= 445.981 K

P_o = 8.36126 atm

P = 0.970065 (8.36126 atm)

= 8.11097 atm

4.7% Salt Activity Calculation

For $S = 47$ g/kg, substitute in the activity formula as follows:

$$\log_{10}(P/P_o) = (-2.1609 \cdot 10^{-4})(47) + (-3.5012 \cdot 10^{-7})(47)^2$$

$$= -0.010930$$

$$P/P_o = 10^{-0.010930}$$

$$= 0.975148$$

Stage 2

Point A $P = 8.11097$ atm

$T = 445.981$ K

Point B $P = 8.11097$ atm

$T = 444.71$ K

Point F $T = 444.71 \text{ K} - 1.111 \text{ K}$

$= 443.599$ K

$P_o = 7.89714$ atm

$P = 0.975148 \ (7.89714 \text{ atm})$

$= 7.70088$ atm

4% Salt Activity Calculation

For $S = 40$ g/kg, substitute in the activity formula as follows:

$$\log_{10}(P/P_o) = (-2.1609 \cdot 10^{-4})(40) + (-3.5012 \cdot 10^{-7})(40)^2$$

$$= -0.009204$$

$$P/P_o = 10^{-0.009204} = 0.979030$$

Stage 1

Point A P = 7.70088 atm

T = 443.599 K

Point B P = 7.70088 atm

T = 442.558 K

Point F T = 442.558 K – 1.111 K

= 441.447 K

P_o = 7.4956 atm

P = 0.979030 (7.4956 atm)

= 7.33842 atm

Parallel flow

In the second step, the seawater concentration on the liquid side of each evaporator is considered to be 7%.

7% Salt Activity Calculation, ΔT_{cond} = 1.111 K (2°F)

Stage 4

Point A P = 9.16 atm (maximum pressure for dropwise condensation, 120 psig)

T = 449.846 K (saturated steam table)

Point B P = 9.16 atm

T = 449.846 K

Point F T = 449.846 K – 1.111 K

= 448.735 K

P_o = 8.92447 atm (saturated steam table)

P = 0.961962 (8.92447 atm)

= 8.58500 atm

Stage 3

Point A P = 8.58500 atm

T = 448.735 K

Point B P = 8.58500 atm

T = 447.092 K

Point F T = 447.092 K – 1.111 K

= 445.981 K

P_o = 8.36126 atm

P = 0.961962 (8.36126 atm)

= 8.04322 atm

Stage 2

Point A P = 8.04322 atm

T = 445.981 K

Point B P = 8.04322 atm

T = 444.360 K

Point F T = 444.360 K – 1.111 K

= 443.249 K

P_o = 7.83070 atm

P = 0.961962 (7.83070 atm) = 7.53284 atm

Stage 1

Point A P = 7.53284 atm

T = 443.249 K

Point B P = 7.53284 atm

T = 441.650 K

Point F T = 441.650 K – 1.111 K

= 440.539 K

P_o = 7.33111 atm

P = 0.961962 (7.33111 atm)

= 7.05225 atm

Case II. ΔT_{cond} = 2.222 K (4°F)

Series flow

7% Salt Activity Calculation

The nomenclature follows Figure B-2.

Stage 4

Point A P = 9.16 atm (maximum pressure for dropwise condensation, 120 psig)

T = 449.846 K (saturated steam table)

Point B P = 9.16 atm

T = 449.846 K

Point F T = 449.846 K – 2.222 K

= 447.624 K

P_o = 8.69377 atm (saturated steam table)

P = 0.961962 (8.69377 atm)

= 8.36308 atm

5.6% Salt Activity Calculation

Stage 3

Point A P = 8.36308 atm

T = 447.624 K

Point B P = 8.36308 atm

T = 445.99 K

Point *E* T = 445.99 K – 2.222 K

= 443.768 K

P_o = 7.92938 atm

P = 0.970065 (7.92938 atm)

= 7.69202 atm

4.7% Salt Activity Calculation

Stage 2

Point A P = 7.69202 atm

T = 443.768 K

Point B P = 7.69202 atm

T = 442.511 K

Point F T = 442.511 K – 2.222 atm

= 440.289 K

P_o = 7.28632 atm

P = 0.975148 (7.28632 atm)

= 7.10524 atm

4% Salt Activity Calculation

Stage 1

Point A P = 7.10524 atm

T = 440.289 K

Point B P = 7.10524 atm

T = 439.265 K

Point F T = 439.265 K – 2.222 K

= 437.043 K

P_o = 6.72432 atm

P = 0.979030 (6.72432 atm)

= 6.58331 atm

Parallel flow

7% Salt Activity Calculation, ΔT_{cond} = 2.222 K (2^{o}F)

Stage 4

Point A P = 9.16 atm (maximum pressure for dropwise condensation, 120 psig)

T = 449.846 K (saturated steam table)

Point B P = 9.16 atm

T = 449.846 K

Point F T = 449.846 K – 2.222 K

= 447.624 K

P_o = 8.69377 atm (saturated steam table)

P = 0.961962 (8.69377 atm)

= 8.36308 atm

Stage 3

Point A P = 8.36308 atm

T = 447.624 K

Point B P = 8.36308 atm

T = 445.99 K

Point F T = 445.99 K – 2.222 K

= 443.768 K

P_o = 7.92938 atm

P = 0.961962 (7.92938 atm)

= 7.62777 atm

Stage 2

Point A P = 7.62777 atm

T = 443.768 K

Point B P = 7.62777 atm

T = 442.165 K

Point F T = 442.165 K – 2.222 K

= 439.943 K

P_o = 7.22470 atm

P = 0.961962 (7.22470 atm)

= 6.94989 atm

Stage 1

Point A P = 6.94989 atm

T = 439.943 K

Point B P = 6.94989 atm

T = 438.371 K

Point F T = 438.371 K – 2.222 K

= 436.149 K

P_o = 6.57575 atm

P = 0.961962 (6.57575 atm)

= 6.32562 atm

Case III. ΔT_{cond} = 3.333 K (6^{o}F)

Series flow

7% Salt Activity Calculation

Stage 4

Point A P = 9.16 atm (maximum pressure for dropwise condensation, 120 psig)

T = 449.846 K (saturated steam table)

Point B P = 9.16 atm

T = 449.846 K

Point F T = 449.846 K – 3.333 K

= 446.513 K

P_o = 8.46781 atm (saturated steam table)

P = 0.961962 (8.46781 atm)

= 8.14572 atm

5.6% Salt Activity Calculation

Stage 3

Point A P = 8.14572 atm

T = 446.513 K

Point B P = 8.14572 atm

T = 444.888 K

Point F T = 444.888 K – 3.333 K

= 441.555 K

P_o = 7.51535 atm

P = 0.970065 (7.51535 atm)

= 7.29038 atm

4.7% Salt Activity Calculation

Stage 2

Point A P = 7.29038 atm

T = 441.555 K

Point B P = 7.29038 atm

T = 440.312 K

Point F T = 440.312 K – 3.333 K

= 436.979 K

P_o = 6.71360 atm

P = 0.975148 (6.71360 atm)

= 6.54675 atm

4% Salt Activity Calculation

Stage 1

Point A P = 6.54675 atm

T = 436.979 K

Point B P = 6.54675 atm

T = 435.973 K

Point F T = 435.973 K – 3.333 K

= 432.640 K

P_o = 6.01765 atm

P = 0.979030 (6.01765 atm)

= 5.89146 atm

Parallel flow

7% Salt Activity Calculation, ΔT_{cond} = 3.333 K (6^{o}F)

Stage 4

Point A P = 9.16 atm (max. pressure for dropwise condensation, 120 psig)

T = 449.846 K (saturated steam table)

Point B P = 9.16 atm

T = 449.846 K

Point F T = 449.846 K – 3.333 K

= 446.513 K

P_o = 8.46781 atm (saturated steam table)

P = 0.961962 (8.46781 atm)

= 8.14572 atm

Stage 3

Point A P = 8.14572 atm

T = 446.513 K

Point B P = 8.14572 atm

T = 444.888 K

Point F T = 444.888 K – 3.333 K

= 441.555 K

P_o = 7.51535 atm

P = 0.961962 (7.51535 atm)

= 7.22948 atm

Stage 2

Point A P = 7.22948 atm

T = 441.555 K

Point B P = 7.22948 atm

T = 439.970 K

Point F T = 439.970 K – 3.333 K

= 436.637 K

P_o = 6.65653 atm

P = 0.961962 (6.65653 atm)

= 6.40333 atm

Stage 1

Point A P = 6.40333 atm

T = 436.637 K

Point B P = 6.40333 atm

T = 435.091 K

Point F T = 435.091 K – 3.333 K

= 431.758 K

P_o = 5.88349 atm

P = 0.961962 (5.88349 atm)

= 5.65970 atm

The wet compressor work is calculated by Equation 3-3 and it is shown in Table B-1.

Table B-1. Thermodynamic calculations for wet compressor, Cases I to III

T_1^{liq} = 300 K	H_1^{liq} = 111.826 kJ/kg	S_1^{liq} = 0.390384 kJ/(kg·K)				
P_2 = 9.16 atm	T_2^{sat} = 449.846 K	H_2^{vap} = 2773.58 kJ/kg				
S_2^{vap} = 6.60784 kJ/(kg·K)	η = 0.85					
ΔT_{cond} (K)	Flow	P_1 (atm)	T_1 (K)	H_1^{vap} (kJ/kg)	S_1^{vap} (kJ/(kg.K))	x	W/4 (kJ/kg)
1.111	Series	7.33842	441.447	2766.86	6.68871	0.01301	12.16
	Parallel	7.05225	440.539	2766.96	6.70626	0.01583	14.34
2.222	Series	6.58331	437.043	2762.21	6.72546	0.01892	18.15
	Parallel	6.32562	436.149	2762.20	6.74290	0.02172	20.35
3.333	Series	5.89146	432.640	2757.36	6.76291	0.02494	24.30
	Parallel	5.65970	431.758	2757.24	6.78026	0.02773	26.52

For ΔT = 1.111 K, compared to the parallel flow, the series flow desalination has reduced power consumption:

$$\eta = \frac{14.34 - 12.16}{14.34} \times 100\%$$

$$= 15.21\ \%$$

For ΔT = 2.222 K, compared to the parallel flow, the series flow desalination has reduced power consumption:

$$\eta = \frac{20.35 - 18.15}{20.35} \times 100\%$$

$$= 10.80\ \%$$

For ΔT = 3.333 K, compared to the parallel flow, the series flow desalination has reduced power consumption:

$$\eta = \frac{26.52 - 24.30}{26.52} \times 100\%$$

$$= 8.37\ \%$$

The series vapor-compression desalination with ΔT_{cond} = 1.111 K requires less energy than the others.

APPENDIX C

ECONOMICS OF VAPOR-COMPRESSION DESALINATION

All calculations in this section are based on 104.7 psia (722 kPa) and ΔT = 2°F (1.111 K) in evaporators. Using equations in Chapter III and the following calculations, estimate the cost of water for 10 million gallons per day (MGD) (0.4381 m^3/s) MVC plant. The compressor work requirements are calculated similar to the calculations shown in Appendix B. The results are summarized in Table C-1.

Table C-1. Summary of calculation example used to determine economics of MVC

Plant specifications	Brackish water	Seawater
Plant capacity (m^3/s)	0.4381	0.4381
Actual production (m^3/s)	0.4381	0.4381
Feed water salinity (g/kg)	1.5	35
Brine salinity (g/kg)	15	70
Recovery rate (%)	90	50
Feed water capacity (kg/s)	486.8	876.3
Brine capacity (kg/s)	48.7	438.1
Total number of stages	25	20
Intake feed water temperature (K)	294	294
Temperature of the last stage (K) - Point A - Point B - Point F	 439.4 439.4 438.3	 439.4 439.4 439.0
ΔT, approach for latent heat exchanger (K)	1.111	0.389
Pressure in latent heat exchanger (kPa)	722	722
Compressor compression ratio	2.48	2.07
Compressor work (kWh/m^3 distillate)	2.11	2.87
Plant life time (years)	30	30
Heat transfer coefficient in latent heat exchanger ($W/(m^2 \cdot K)$)	22,532	54,000
Heat transfer area in latent heat exchanger (m^2)	36,065	43,000

Latent Heat Exchanger

The produced rate of water is 10,000,000 gal/d, then

$$m = \frac{10{,}000{,}000\ \text{gal}}{\text{d}} \times \frac{\text{d}}{24\ \text{h}} \times \frac{8.337\ \text{lb}}{\text{gal}} = 3{,}473{,}750\ \text{lb/h}$$

$$Q = 3{,}473{,}750\ \text{lb/h} \times 886.894\ \text{Btu/lb} = 3.08 \times 10^9\ \text{Btu/h}$$

$$A = \frac{Q}{U\Delta T} = \frac{3.08 \times 10^9\ \text{Btu/h}}{\left(3968 \frac{\text{Btu}}{\text{h} \cdot \text{ft}^2 \cdot {}^\circ\text{F}}\right)\left(2^\circ\text{F}\right)} = 388{,}198\ \text{ft}^2$$

Latent heat exchanger price is \$8.57/ft^2 (Appendix D)

Cost = 388,198 ft^2 × \$8.57/ft^2 = \$3,326,852

Compressor

Assumptions:

ΔT = 2^{o}F = 0.556 K

Typical boiling point elevation = 0.53^{o}F (0.3 K) based on interpolation from Table A-7 or Figure 3-1 (see Table C-2).

Table C-2. Typical boiling point elevation at 104.7 psia (722 kPa)

No.	Pressure (10^5 N/m^2)	Salinity (g/kg)	Boiling-point elevation (K)
1	6.0698	33.56	0.70
2	9.9134	33.88	0.81
3	7.2188	33.65	0.73[a]
4	5.7608	67.09	1.45
5	9.4414	67.72	1.63
6	7.2188	67.34	1.52[b]
7	7.2188	15.00	0.30[c]

[a] Based on interpolation from number 1 and 2
[b] Based on interpolation from number 4 and 5
[c] Based on interpolation from number 3 and 6

Feed = brackish water with salinity 1.5 g/kg

Discharge = 15 g/kg

Maximum temperature = 439.4 K = 331.205^{o}F

Average compressor work = 2.11 kWh/m^3 = 8.0 kWh/kgal based on calculation similar to that shown by Appendix B

The water produced in the desalination plant is 10,000,000 gallons/day

$$\text{Compressor shaft power} = \frac{10{,}000{,}000\ \text{gal}}{\text{d}} \times \frac{8.0\ \text{kWh}}{\text{thous gal}} \times \frac{\text{day}}{24\ \text{h}} = 3{,}332\ \text{kW}$$

Let the number of stages for MVC unit designed are as follows.

20 stages

These stages are the amount of stages (evaporators) for MVC unit. Therefore,

$$m = \frac{1}{20} \times \frac{10{,}000{,}000\ \text{gal}}{\text{d}} \times \frac{\text{d}}{24\ \text{h}} \times \frac{8.337\ \text{lb}}{\text{gal}} = 173{,}688\ \text{lb/h}$$

Compressor inlet temperature = 331.205 – 20(2^{o}F) – 20(0.53^{o}F) = 281^{o}F

$$V = \frac{173{,}688\ \text{lb}}{\text{h}} \times \frac{\text{h}}{60\ \text{min}} \times \frac{\text{ft}^3}{0.117\ \text{lb}} = 24{,}841\ \text{ft}^3/\text{min}$$

25 stages

$$m = \frac{1}{25} \times \frac{10{,}000{,}000\ \text{gal}}{\text{d}} \times \frac{\text{d}}{24\ \text{h}} \times \frac{8.337\ \text{lb}}{\text{gal}} = 138{,}950\ \text{lb/h}$$

Compressor inlet temperature = 331.205 – 25(2^{o}F) – 25(0.53^{o}F) = 268^{o}F

$$V = \frac{138{,}950\ \text{lb}}{\text{h}} \times \frac{\text{h}}{60\ \text{min}} \times \frac{\text{ft}^3}{0.096\ \text{lb}} = 24{,}093\ \text{ft}^3/\text{min}$$

30 stages

$$m = \frac{1}{30} \times \frac{10{,}000{,}000\ \text{gal}}{\text{d}} \times \frac{\text{d}}{24\ \text{h}} \times \frac{8.337\ \text{lb}}{\text{gal}} = 115{,}792\ \text{lb/h}$$

Compressor inlet temperature = 331.205 – 30(2°F) – 30(0.53°F) = 255°F

$$V = \frac{115{,}792\ \text{lb}}{\text{h}} \times \frac{\text{h}}{60\ \text{min}} \times \frac{\text{ft}^3}{0.079\ \text{lb}} = 24{,}524\ \text{ft}^3/\text{min}$$

The optimum number of stages which has the lowest flow rate is 25 stages.

The typical compression ratio per stage is 1.037. The compression ratio for 40 stages is as follows: Compression Ratio = $(1.037)^{25} = 2.48$

Cost = $1,043,000 [52]

Electric Motor

The distillate flow rate in the desalination plant is 10,000,000 gal/d.

$$\text{Motor shaft power} = \frac{10{,}000{,}000\ \text{gal}}{\text{d}} \times \frac{8\ \text{kWh}}{\text{kgal}} \times \frac{\text{day}}{24\ \text{h}} = 3332\ \text{kW}$$

$$\text{Motor electrical power} = \frac{3332\ \text{kW}}{0.96} = 3470\ \text{kW}$$

$$\text{Energy} = 3470\ \text{kW} \times \frac{\text{d}}{10{,}000{,}000\ \text{gal}} \times \frac{24\ \text{h}}{\text{d}} = 8.33\ \text{kWh/kgal}$$

Cost = $179,857 [53]

Sensible Heat Exchanger

Figures C-1 and C-2 depict the microchannel heat exchanger corresponding to the individual sensible heat exchanger and its temperatures for first stage. Energy balance is performed for the sensible heat exchanger to compute the sensible heat exchanger area.

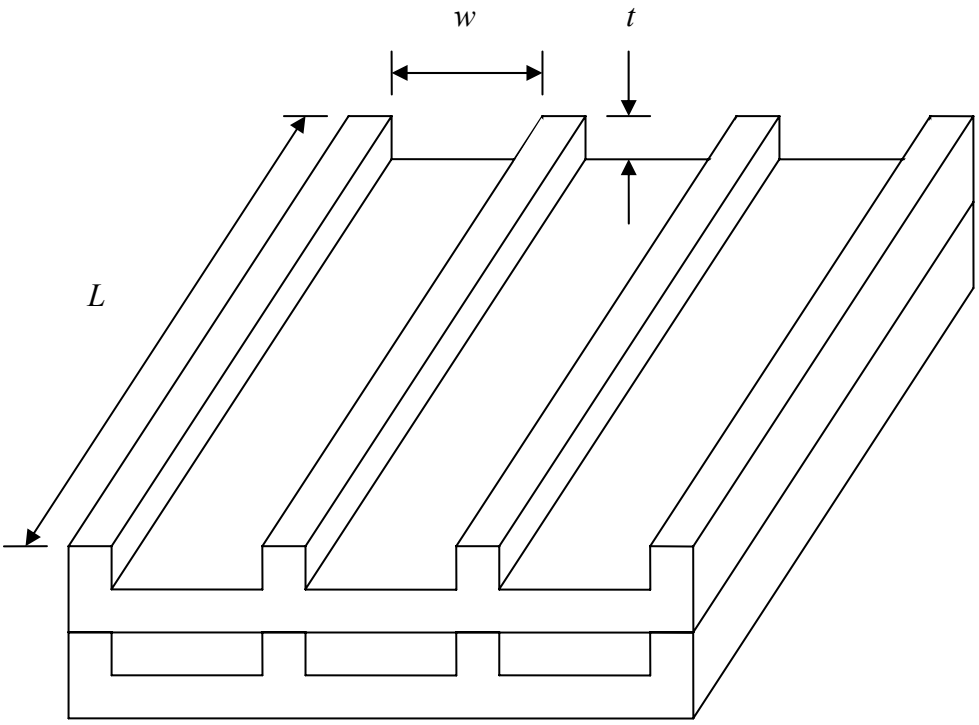

Figure C-1. Microchannel heat exchanger.

Input and output temperatures are based on an iterative process. The distillate flow rate produced in the desalination system is 10,000,000 gal/d and recovery is 90%.

$$m = \frac{1}{0.9}\frac{10{,}000{,}000\ \text{gal}}{\text{d}} \times \frac{\text{d}}{24\ \text{h}} \times \frac{8.337\ \text{lb}}{\text{gal}} = 3{,}859{,}722\ \text{lb/h}$$

$$\Delta T_s = \frac{3332\ \text{kW}}{3{,}859{,}722\ \text{lb/h} \times \dfrac{1\ \text{Btu}}{\text{lb} \cdot {}^{\circ}\text{F}}} \times \frac{\text{kJ}}{\text{kW} \cdot \text{s}} \times \frac{\text{Btu}}{1.054\ \text{kJ}} \times \frac{3600\ \text{s}}{\text{h}} = 2.95^{\circ}\text{F}$$

Energy balance:

$$Q_d = m_d C_{pd} \Delta T_d = m_{1f} C_{pf} \Delta T_f$$

$$Q_b = m_b C_{pb} \Delta T_b = m_{2f} C_{pf} \Delta T_f$$

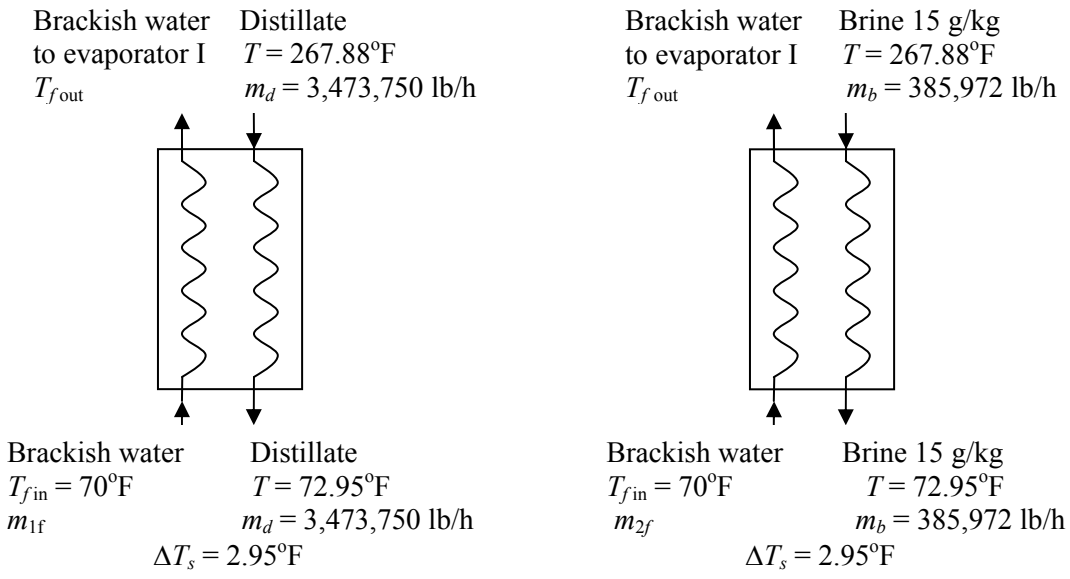

Figure C-2. Flow temperatures of the sensible heat exchangers for first evaporator stage.

Therefore, the rate of heat required in the distillate/brine sensible heat exchanger is

$$Q_d = 3{,}473{,}750\,\frac{\text{lb}}{\text{h}} \cdot 1.002\,\frac{\text{Btu}}{\text{lb}\cdot^\circ\text{F}}\left(267.88 - 72.95\right)^\circ\text{F} = m_{1f} \cdot 0.984\,\frac{\text{Btu}}{\text{lb}\cdot^\circ\text{F}}\left(T_{f\,\text{out}} - 70\right)^\circ\text{F}$$

$$Q_b = 385{,}972\,\frac{\text{lb}}{\text{h}} \cdot 0.984\,\frac{\text{Btu}}{\text{lb}\cdot^\circ\text{F}}(267.88 - 72.95)^\circ\text{F} = (3{,}859{,}722 - m_{1f}) \cdot 0.984\,\frac{\text{Btu}}{\text{lb}\cdot^\circ\text{F}}(T_{f\,\text{out}} - 70)^\circ\text{F}$$

The brackish water rate and temperature are calculated with the above equations.

m_{1f} = 3,480,215 lb/h

m_{2f} = 379,507 lb/h

$T_{f\,out}$ = 265.197°F

Sample Calculation of Reynold's Number

Equivalent diameter (D) = 4 r_H

$$r_H = \frac{\text{cross sectional area}}{\text{cross perimeter}} = \frac{tw}{2t + 2w} \approx \frac{tw}{2w} = \frac{t}{2}$$

$$D = 4\left(\frac{t}{2}\right) = 2t$$

$$\mathrm{Re} = \frac{Dv\rho}{\mu}$$

Water density (ρ) = 973.7 kg/m^3

Viscosity (μ) = 0.00037 kg/(m·s) at 170.4^{o}F (350.1 K)

e/D = 0 (smooth wall)

$$\mathrm{Re} = \frac{(2\times t)(v)\left(973.7\ \mathrm{kg/m^3}\right)}{0.00037\ \mathrm{kg/(m\cdot s)}} = 5.3\times 10^6\, tv$$

Heat Transfer Coefficient

Dittus-Boelter Equation (for Re > 6000)

$$\mathrm{Nu} = 0.023\mathrm{Re}^{0.8}\mathrm{Pr}^{0.333} = \frac{hD}{k}$$

$$h = \frac{k}{D}0.023\mathrm{Re}^{0.8}\ \mathrm{Pr}^{0.333} = \frac{k}{2t}0.023\,\mathrm{Re}^{0.8}\ \mathrm{Pr}^{0.333}$$

Pr = Prandtl Number = 2.34 for water at 170.4^{o}F (350.1 K)

k = water thermal conductivity = 0.664 J/(s·m·K)

h = heat transfer coefficient (J/(s·m^2·K)

$$h_{water} = \frac{0.664\ \mathrm{J/(s\cdot m\cdot K)}}{2t}0.023(\mathrm{Re})^{0.8}\,2.34^{0.333}$$

$$h_{water} = 0.0101\frac{\mathrm{Re}^{0.8}}{t}$$

Pressure Drop

$$A = \left[-2.457 \ln\left(\left(\frac{7}{\mathrm{Re}} \right)^{0.9} + 0.27 \frac{e}{D} \right) \right]^{16}$$

$$B = \left(\frac{37{,}350}{\mathrm{Re}} \right)^{16}$$

Churchill Equation for Fanning friction factor (for all Re and *e/D*)

$$f = 2\left[\left(\frac{8}{\mathrm{Re}} \right)^{12} + \frac{1}{(A+B)^{3/2}} \right]^{1/12}$$

$$f = \left(\frac{1}{2} \frac{D}{\rho v^2} \right) \frac{\Delta P}{\Delta L}$$

$$\frac{\Delta P}{\Delta L} = 2\frac{\rho v^2}{D} f = 2\frac{\rho v^2}{2t} f = \frac{\rho v^2}{t} f$$

$$\frac{\Delta P}{\Delta L} = 2\frac{\rho v^2}{t}\left[\left(\frac{8}{\mathrm{Re}} \right)^{12} + \frac{1}{\left(\left[-2.457 \ln\left(\left(\frac{7}{\mathrm{Re}} \right)^{0.9} + 0.27 \frac{e}{D} \right) \right]^{16} + \left(\frac{37{,}350}{\mathrm{Re}} \right)^{16} \right)^{3/2}} \right]^{1/12}$$

Figure C-3 shows curves describing trade-off between pressure drop ($\Delta P/\Delta L$) and one-side heat transfer coefficient. Assume that a pressure drop below 25 psi/ft is acceptable.

If t = 1.5 mm = 0.0015 m

Velocity (v) = 14 m/s

$$\mathrm{Re} = \frac{(2 \times 0.0015\ \mathrm{m})(14\ \mathrm{m/s})(973.7\ \mathrm{kg/m^3})}{0.00037\ \mathrm{kg/(m \cdot s)}} = 110{,}462$$

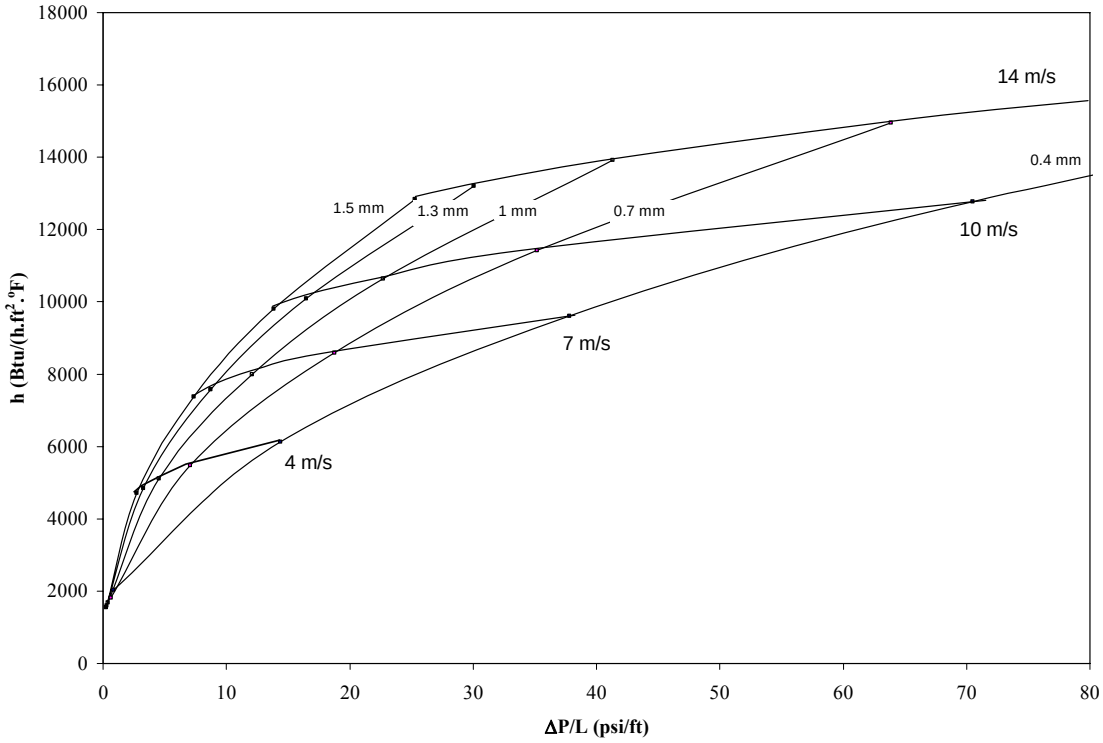

Figure C-3. One-side heat transfer coefficient for water at 170.4°F as a function of pressure drop, fluid velocity *v*, and channel thickness *t*.

$$h_{water} = 0.0101\frac{(110{,}462)^{0.8}}{0.0015} = 73{,}130\frac{\text{J}}{\text{s}\cdot\text{m}^2\cdot\text{K}}$$

$$h_{water} = 73{,}130\frac{\text{J}}{\text{s}\cdot\text{m}^2\cdot\text{K}}\times\frac{\text{Btu}}{1054\,\text{J}}\times\frac{3600\,\text{s}}{\text{h}}\times\left(\frac{\text{m}}{3.281\,\text{ft}}\right)^2\times\frac{\text{K}}{1.8^{\circ}\,\text{F}} = 12{,}898\frac{\text{Btu}}{\text{h}\cdot\text{ft}^2\cdot^{\circ}\,\text{F}}$$

Similarly, $h_{brine} = 12{,}878\ \dfrac{\text{Btu}}{\text{h}\cdot\text{ft}^2\cdot^{\circ}\,\text{F}}$

In this design, both surfaces of a naval brass sensible heat exchanger are clad with titanium. The overall heat transfer coefficient follows:

$$U = \frac{1}{\dfrac{1}{h_{water}} + \dfrac{1}{h_{brine}} + \left(\dfrac{x_{nb}}{k_{nb}}\right) + 2\left(\dfrac{x_{tit}}{k_{tit}}\right)}$$

k_{nb} = 67 Btu/(h·ft·°F) at 170.4°F (350.1 K)

x_{nb} = 0.000504 m = 0.00165 ft = 0.0138 in

k_{tit} = 12 Btu/(h·ft·°F) at 350.3 K

x_{tit} = 0.000498 m = 0.00163 ft = 0.0136 in

$$U = \frac{1}{\frac{1}{12{,}898}\frac{\text{h}\cdot\text{ft}^2\cdot^\text{o}\text{F}}{\text{Btu}} + \frac{1}{12{,}878}\frac{\text{h}\cdot\text{ft}^2\cdot^\text{o}\text{F}}{\text{Btu}} + \left(\frac{0.00165\,\text{ft}}{67\,\frac{\text{Btu}}{\text{h}\cdot\text{ft}\cdot^\text{o}\text{F}}}\right) + 2\left(\frac{0.00163\,\text{ft}}{12\,\frac{\text{Btu}}{\text{h}\cdot\text{ft}\cdot^\text{o}\text{F}}}\right)}$$

$$U = 2{,}212\,\frac{\text{Btu}}{\text{h}\cdot\text{ft}\cdot^\text{o}\text{F}}$$

$$A = \left[-2.457\ln\left(\left(\frac{7}{110{,}462}\right)^{0.9} + 0.27(0)\right)\right]^{16}$$

$$A = 1.9\times10^{21}$$

$$B = \left(\frac{37{,}350}{\text{Re}}\right)^{16} = \left(\frac{37{,}350}{110{,}462}\right)^{16} = 2.92\times10^{-8}$$

$$f = 2\left[\left(\frac{8}{\text{Re}}\right)^{12} + \frac{1}{(A+B)^{3/2}}\right]^{1/12}$$

$$f = 2\left[\left(\frac{8}{110{,}462}\right)^{12} + \frac{1}{\left(1.9\times10^{21} + 2.92\times10^{-8}\right)^{3/2}}\right]^{1/12} = 0.00438$$

$$f = \left(\frac{1}{2}\frac{D}{\rho v^2}\right)\frac{\Delta P}{\Delta L}$$

$$\frac{\Delta P}{\Delta L} = 2\frac{\rho v^2}{D}f = 2\frac{\rho v^2}{2t}f = \frac{\rho v^2}{t}f$$

$$\frac{\Delta P}{\Delta L} = \frac{\left(973.7\,\frac{\text{kg}}{\text{m}^3}\right)\left(\frac{14\,\text{m}}{\text{s}}\right)^2}{0.0015\,\text{m}}(0.00438) = 556{,}894\,\frac{\text{kg}}{\text{s}^2\cdot\text{m}^2} = 556{,}894\,\frac{\text{Pa}}{\text{m}}$$

$$= 556{,}894\,\frac{\text{Pa}}{\text{m}}\times\frac{14.696\,\text{psi}}{101{,}325\,\text{Pa}}\times\frac{\text{m}}{3.281\,\text{ft}} = 24.6\,\frac{\text{psi}}{\text{ft}}$$

Microchannel Heat Exchanger I

$$Q = 3{,}859{,}722\ \text{lb/h} \times \frac{1\ \text{Btu}}{\text{lb} \cdot {}^{\circ}\text{F}} \times (265.16 - 70)^{\circ}\text{F} = 753{,}251{,}810\ \text{Btu/h}$$

$$A = \frac{Q}{U\Delta T} = \frac{753{,}251{,}810\ \text{Btu/h}}{2{,}212 \dfrac{\text{Btu}}{\text{h} \cdot \text{ft}^2 \cdot {}^{\circ}\text{F}} (1.79^{\circ}\text{F})} = 115{,}510\ \text{ft}^2 = 10{,}731\ \text{m}^2$$

Microchannel heat exchanger price is $20.55/ft^2 (see Appendix D).

The cost is calculated for microchannel heat exchanger I because it is considered as the main equipment.

Cost = 10,731 ft^2 × $20.55/ft^2 = $2,373,735

Pump

The distillate flow rate produced in the desalination plant is 10,000,000 gal/d.

$$\text{Feed flow rate} = \frac{1}{0.9} \times 10{,}000{,}000\ \text{gal/d} \times \frac{\text{d}}{24\ \text{h}} \times \frac{\text{h}}{60\ \text{min}} = 7{,}716\ \text{gal/min}$$

The latent heat exchanger pressure is 104.7 psia.

Let sensible heat exchanger pressure drop is 60 psi (assume 2.43 ft of heat exchanger length). Therefore,

Pressure = (104.7 + 60) psi = 164.7 psi

$$\text{Power} = \frac{1}{0.8} \times 7{,}716\ \text{gal/min} \times 3.78\ \text{l/gal} \times \frac{\text{m}^3}{1000\ \text{l}} \times \frac{\text{min}}{60\ \text{s}} \times 164.7\ \text{psi} \times \frac{101{,}325\ \text{Pa}}{14.7\ \text{psi}} = 689{,}824\ \text{W}$$

$$\text{Energy} = 689.824\ \text{kW} \times \frac{\text{d}}{10{,}000\ \text{kgal}} \times \frac{24\ \text{h}}{\text{d}} = 1.656\ \text{kWh/kgal}$$

Cost = $48,367 (with motor)

Degassing Unit

The degassing unit chosen is a vacuum stripper with 90% recovery; the distillate flow rate is 10,000,000 gal/day. The solubility of air in water (294.26 K or 70°F) is 0.000024 g/g at 1 atm air pressure, then

$$m_{air} = \frac{1}{0.9} \times \frac{10{,}000{,}000\ \text{gal}}{\text{d}} \times \frac{\text{d}}{24\ \text{h}} \times \frac{8.337\ \text{lb}}{\text{gal}} \times 0.000024 \frac{\text{lb}_{\text{air}}}{\text{lb}_{\text{water}}} = 92.63 \frac{\text{lb}}{\text{h}}$$

Assume the air is removed at water temperature 294.26 K (70°F). The water vapor pressure is 2.5 kPa (0.36 psia).

$$V_{air} = 92.63 \frac{\text{lb}}{\text{h}} \times \frac{\text{lbmol}}{29\ \text{lb}} \times 10.73 \frac{\text{psia} \cdot \text{ft}^3}{\text{lbmol} \cdot \text{R}} \times (70 + 460)\text{R} \times \frac{1}{0.36\ \text{psia}} \times \frac{\text{h}}{60\ \text{min}} = 841 \frac{\text{ft}^3}{\text{min}}$$

Assume that the air can be stripped 100%, then

$$\text{Power} = \frac{1}{\eta} \frac{\gamma}{\gamma - 1} PV \left[\left(\frac{P_2}{P_1} \right)^{\left(\frac{\gamma - 1}{\gamma} \right)} - 1 \right]$$

$$= \frac{1}{0.8} \frac{1.35}{1.35 - 1} \left(0.36 \frac{\text{lb}_\text{f}}{\text{in}^2} \times \frac{144\ \text{in}^2}{\text{ft}^2} \right) \left(841 \frac{\text{ft}^3}{\text{min}} \times \frac{\text{min}}{60\ \text{s}} \right) \left(\frac{\text{hp} \cdot \text{s}}{550\ \text{ft} \cdot \text{lb}_\text{f}} \right) \left(\frac{0.746\ \text{kW}}{\text{hp}} \right) \left[\left(\frac{14.7}{0.36} \right)^{\left(\frac{1.35 - 1}{1.35} \right)} - 1 \right]$$

$$= 7.68\ \text{kW}$$

This power requirement can be reduced by spraying liquid water into the compressor to keep it cool.

$$\text{Energy} = 7.68\ \text{kW} \times \frac{\text{d}}{10{,}000\ \text{kgal}} \times \frac{24\ \text{h}}{\text{d}} = 0.018\ \text{kWh/kgal}$$

Compressor Cost = $4,300 [52]

The mass flow of water in the exiting vapor follows:

$$m_{water} = 92.63 \text{ lb water/h} \times \frac{\text{lbmol air}}{29 \text{ lb air}} \times \frac{1 \text{ lbmol water}}{\text{lbmol air}} \times \frac{18 \text{ lb water}}{\text{lbmol water}} = 57.5 \text{ lbwater/h}$$

Q = 57.5 lb water/h × 1,054.3 Btu/lb = 60,617 Btu/h

The evaporated water vapor from the feed liquid causes the temperature drop as follows.

$$\Delta T = \frac{60{,}617 \text{ Btu/h}}{(3{,}859{,}722 \text{ lb/h})\left(1 \frac{\text{Btu}}{\text{lb} \cdot {}^{\circ}\text{F}}\right)} = 0.016^{\circ}\text{F}$$

Clearly, the required steam to help strip the air can come from the feed itself.

The diameter of the stripper column is determined by calculating the vapor velocity needed to flood the packing:

$$V_{flood} = K_v \left(\frac{\rho_L - \rho_V}{\rho_V} \right)^{0.5}$$

where

V_{flood} = vapor velocity (ft/s)

K_v = Souder and Brown factor at flood conditions

= 0.08

ρ_L = liquid density = 62.299 lb/ft^3

ρ_V = vapor density = 0.00115 lb/ft^3

$$V_{flood} = 0.08 \left(\frac{62.299 - 0.00115}{0.00115} \right)^{0.5} = 18.6 \text{ ft/s}$$

Vapor velocity used is 70% of the velocity in order to be safe.

V_{flood} = 0.7 × 18.6 ft/s = 13.03 ft/s

Column cross-sectional area and column diameter are calculated as follows.

$$A = \frac{841\ \text{ft}^3/\text{min}}{13.03\ \text{ft/s} \times \dfrac{60\ \text{s}}{\text{min}}} = 1.08\ \text{ft}^2$$

$$d = \sqrt{\frac{4}{\pi}A} = \sqrt{\frac{4}{\pi}1.08\ \text{ft}^2} = 1.17\ \text{ft}$$

Assume column is 10 ft high and packing height is 8 ft, then

Column Cost = \$10,830 [54]

Packing Cost = 1.08 ft^2 × 8 ft × \$8/ft^3 = \$73 [54]

The packed column can be located 34 ft in the air, which requires a support structure, to eliminate the need for a pump. The support cost is estimated as same as the column cost, then

Total Capital Cost = \$4,300 + \$10,830 + \$73 + \$10,830 = \$26,033

Brine Injection Well

The capacity of brine injection well is 500,000 gal/day.

Capital cost = \$2 million [49]

Assume it is financed with 5% 30-yr mortgage.

$$R = P_o \frac{i}{1-(1-i)^{-n}} = \$2{,}000{,}000 \frac{0.05}{1-(1+0.05)^{-30}} = \$130{,}103/\text{yr} = \$356/\text{day}$$

Operating cost = \$10,000 per month = \$333/day (includes all expenses, such as electricity and maintenance) [49]

$$\text{Cost} = \frac{(\$356 + 333)/\text{day}}{500\ \text{thous gal/day}} = \$1.38/\text{thous gal brine}$$

$$\text{Cost} = \$1.38/\text{thous gal brine} \times \frac{0.1\ \text{brine/feed}}{0.9\ \text{distillate/feed}} = \$0.153/\text{thous distillate} = \$0.04/\text{m}^3$$

Table C-3. Electricity requirements for brackish water feed and $\Delta T = 2^{o}$F

Equipment	Electricity requirements (kWh/kgal)
Compressor electric motor	8.33
Pumps	1.656
Degassing unit	0.018
Total	10.00

Table C-3 shows the electricity requirements for the above case at 10,000,000 gal/d production capacity and $\Delta T = 2^{o}$F. Total energy requirement is 10.00 kWh/thousand gallons (2.64 kWh/m^3). Tables C-4 summarizes the capital costs needed in the advanced vapor-compression desalination plant using brackish water at 10,000,000 gal/d production. Fixed capital investment (FCI) is gained from multiplying the total equipment cost to Lang factor for installed skid-mounted fluid processing.

Table C-4. Capital costs for brackish water feed at $\Delta T = 2^{o}$F in latent heat exchanger

Equipment	Description	Purchase cost ($)
Latent heat exchanger	7,063.9 Btu/(h·ft^2·^{o}F), 436,140 ft^2	3,326,852
Compressor	14,599 ft^3/min, 2022 kW, compression ratio = 4.28	1,043,000
Electric motor	3,470 kW (electricity)	179,857
Sensible heat exchanger	2,212 Btu/(h·ft^2·^{o}F), 155,242 ft^2	2,940,522
Pump with motor	7716 gal/min, 164.7 psi	48,367
Degassing unit	Stripper column with compressor	26,033
	Total Equipment Cost	7,564,630
	Lang Factor	3.68
	Fixed Capital Investment (FCI)	27,837,839

Let R represents the periodic payment made during 30 years in an ordinary annuity. If interest rate is 5%, then

$$R = P_o \frac{i}{1-(1+i)^{-n}} = \$27{,}837{,}839 \frac{0.05}{1-(1+0.05)^{-30}} = \$1{,}810{,}891/\text{yr}$$

From these values, the water cost for 10,000,000 gal/day flow rate and 5% interest was calculated (Table 4-3). Table C-5 summarizes the results of a calculation performed to find cost of water at $\Delta T = 2^{o}$F, 104.7 psia, and various energy costs.

Table C-5. Calculated cost of water for brackish water feed at $\Delta T = 2^{o}$F

Energy cost	Cost of water for brackish water feed at $\Delta T = 1^{o}$F ($/kgal)			
	5% interest	10% Interest	15% interest	20% interest
$0.05/kWh	1.54	1.91	2.32	2.75
$0.10/kWh	1.97	2.33	2.74	3.17
$0.15/kWh	2.39	2.75	3.16	3.59

Similar calculation is also done for seawater feed at $\Delta T = 0.7^{o}$F, 104.7 psia, and the trends resulted are also similar (Tables C-6 to C-8). The calculation shows that 20-stage design is optimum condition for the system. Ion exchange unit is used for seawater pretreatment to reduce Ca^{2+} or SO_4^{2-} concentrations using cationic or anionic resins. The cost of the pretreatment includes capital cost and operating cost [45].

Ion Exchange Unit

The capacity of ion exchange unit is 1,000,000 gal/day.

Capital cost = $314,700 [45]

Assume it is financed with 5% 30-yr mortgage.

$$R = P_o \frac{i}{1-(1-i)^{-n}} = \$314{,}700 \frac{0.05}{1-(1+0.05)^{-30}} = \$20{,}472/\text{yr} = \$68/\text{day}$$

$$\text{Capital cost} = \frac{\$68/\text{day}}{1{,}000\ \text{kgal/day}} = \$0.068/\text{kgal}$$

Operating cost = \$0.14/kgal produced water (includes resin replacement, acid treatment, and labor) [45]

Total pretreatment cost = \$0.068/kgal + \$0.14/kgal = \$0.208/kgal = \$0.055/m^3

Electricity consumption = 0.1 kWh/m^3 [45]

Electricity cost = 0.1 kWh/m^3 × 3.78 m^3/kgal = 0.378 kWh/kgal ≈ 0.38 kWh/kgal

Table C-6. Electricity requirements for seawater feed and $\Delta T = 0.7^oF$

Equipment	Electricity requirements (kWh/kgal)
Compressor electric motor	11.32
Pumps	2.98
Degassing unit	0.03
Ion exchange unit	0.38
Total	14.71

Table C-7. Capital costs for seawater feed at $\Delta T = 0.7^oF$ and 20 evaporator stages

Equipment	Description	Purchase cost ($)
Latent heat exchanger	9,504 Btu/(h·ft^2·^{o}F), 463,073 ft^2	3,968,534
Compressor	34,007 ft^3/min, 4529 kW compression ratio = 2.07	1,297,000
Electric motor	4,718 kW (electricity)	304,305
Sensible heat exchanger	2,190 Btu/(h·ft^2·^{o}F), 267,859 ft^2	5,504,496
Pump with motor	13,889 gal/min, 164.7 psi	59,960
Degassing unit	Stripper column with compressor	27,562
	Total Equipment Cost	11,161,857
	Lang Factor	3.68
	Fixed Capital Investment (FCI)	41,075,635

The optimum costs of water for seawater feed are calculated at 5% interest rate (Table 4-4). The cost of water in seawater MVC system is the result of contribution from the following components: electricity, labor, bond, maintenance, insurance, and ion exchange unit. With 20-stage design resulted from similar calculation to brackish water feed, the cost of water is calculated to be \$2.31/kgal (\$0.61/m^3) at energy cost \$0.05/kWh. The costs of water for seawater feed at ΔT = 0.7°F (0.389 K), various interest rates and energy costs are noted in Table C-8. The table shows that the higher the interest rate and energy cost, the more expensive the cost of water.

Table C-8. Calculated cost of water for seawater feed at ΔT = 0.7°F and 20 stages

Energy cost	Cost of water for seawater feed at ΔT = 0.7°F (\$/kgal)			
	5% interest	10% Interest	15% Interest	20% interest
\$0.05/kWh	2.31	2.82	3.39	3.99
\$0.10/kWh	3.05	3.55	4.12	4.73
\$0.15/kWh	3.79	4.29	4.86	5.46

Tables C-9 to C-11 shows calculated cost of water for brackish water and seawater feeds as comparison at various interest rates and pressures in the latent heat exchanger. The tables show that the higher the temperature difference in latent heat exchanger, the less the number of stages needed. The 10,000,000 gallons/day plant can produce fresh water at the lowest unit cost when brackish water used. The lowest cost of \$1.54/kgal is below the target price of \$2/kgal (\$0.53/m^3) set by a public water authority in Southern California to compete with surface water [33].

Table C-9. Calculated cost of water at 104.7 psia and various interest rates

Energy cost ($/kWh)	Feed	Temperature difference (°F)	Optimum number of stages	Cost of water ($/kgal)			
				5%	10%	15%	20%
0.05	Brackish water	0.34	54	2.08	2.65	3.29	3.96
		0.70	50	1.65	2.10	2.61	3.15
		1.00	40	1.63	2.09	2.60	3.13
		2.00	25	**1.54**	**1.91**	2.32	2.75
		3.00	20	1.62	1.95	**2.31**	**2.70**
		3.98	15	1.74	2.06	2.41	2.78
	Seawater	0.34	20	2.40	2.95	3.58	4.23
		0.70	20	**2.31**	2.82	3.39	3.99
		1.00	15	2.32	2.81	3.37	3.95
		2.00	15	2.33	**2.75**	**3.24**	**3.74**
		3.00	15	2.43	2.84	3.29	3.77
		3.98	10	2.75	3.21	3.74	4.28
0.10	Brackish water	0.34	54	2.31	2.88	3.52	4.19
		0.70	50	1.94	2.39	2.90	3.43
		1.00	40	**1.88**	2.34	2.86	3.39
		2.00	25	1.97	**2.33**	**2.74**	**3.17**
		3.00	20	2.20	2.53	2.90	3.29
		3.98	15	2.49	2.80	3.16	3.53
	Seawater	0.34	20	3.07	3.63	4.25	4.91
		0.70	20	**3.05**	**3.55**	**4.12**	4.73
		1.00	15	3.10	3.60	4.15	4.72
		2.00	15	3.28	3.71	4.19	**4.69**
		3.00	15	3.55	3.95	4.41	4.89
		3.98	10	4.03	4.49	5.01	5.56
0.15	Brackish water	0.34	54	2.54	3.10	3.74	4.41
		0.70	50	2.23	2.68	3.19	3.72
		1.00	40	**2.14**	**2.59**	**3.10**	3.66
		2.00	25	2.39	2.75	3.16	**3.59**
		3.00	20	2.79	3.12	3.48	3.87
		3.98	15	3.24	3.55	4.90	4.27
	Seawater	0.34	20	**3.75**	4.31	4.93	5.59
		0.70	20	3.79	**4.29**	**4.86**	**5.46**
		1.00	15	3.88	4.38	4.94	5.50
		2.00	15	4.23	4.66	5.14	5.64
		3.00	15	4.66	5.07	5.52	6.00
		3.98	10	5.30	5.76	6.29	6.83

Table C-10. Calculated cost of water at 76.7 psia and various interest rates

Energy cost ($/kWh)	Feed	Temperature difference (°F)	Optimum number of stages	Cost of water ($/kgal)			
				5%	10%	15%	20%
0.05	Brackish water	0.34	54	2.38	3.06	3.83	4.64
		0.70	50	2.07	2.68	3.37	4.10
		1.00	40	1.93	2.49	3.13	3.80
		2.00	25	**1.78**	**2.23**	2.74	3.27
		3.00	20	1.85	2.26	**2.72**	**3.21**
		3.98	15	1.98	2.38	2.82	3.29
	Seawater	0.34	20	2.70	3.37	4.13	4.93
		0.70	20	2.58	3.18	3.87	4.59
		1.00	15	2.57	3.15	3.81	4.51
		2.00	15	**2.54**	**3.05**	**3.63**	**4.24**
		3.00	15	2.65	3.14	3.69	4.27
		3.98	10	2.77	3.24	3.77	4.33
0.10	Brackish water	0.34	54	2.60	3.28	4.05	4.85
		0.70	50	2.35	2.96	3.65	4.37
		1.00	40	**2.17**	2.74	3.38	4.05
		2.00	25	2.21	**2.65**	**3.15**	3.69
		3.00	20	2.45	2.86	3.32	3.81
		3.98	15	2.75	3.14	3.59	4.06
	Seawater	0.34	20	3.35	4.02	4.79	5.64
		0.70	20	**3.28**	**3.89**	4.58	5.59
		1.00	15	3.33	3.92	4.58	5.30
		2.00	15	3.48	4.00	**4.57**	5.27
		3.00	15	3.76	4.25	4.80	**5.18**
		3.98	10	4.06	4.53	5.06	5.61
0.15	Brackish water	0.34	54	2.81	3.49	4.26	5.07
		0.70	50	2.63	3.24	3.93	4.65
		1.00	40	**2.42**	**2.99**	3.63	4.26
		2.00	25	2.63	3.08	**3.58**	4.30
		3.00	20	3.05	3.46	3.92	**4.11**
		3.98	15	3.51	4.91	4.36	4.82
	Seawater	0.34	20	**3.99**	4.68	5.44	6.24
		0.70	20	4.00	**4.61**	**5.29**	**6.01**
		1.00	15	4.10	4.69	5.35	6.04
		2.00	15	4.42	4.94	5.51	6.12
		3.00	15	4.87	5.36	5.91	6.49
		3.98	10	5.34	5.81	6.34	6.89

Table C-11. Calculated cost of water at 59.2 psia and various interest rates

Energy cost ($/kWh)	Feed	Temperature difference (^oF)	Optimum number of stages	Cost of water ($/kgal)			
				5%	10%	15%	20%
0.05	Brackish water	0.34	54	2.89	3.77	4.76	5.80
		0.70	50	2.49	3.28	4.18	5.13
		1.00	40	2.21	2.77	3.46	4.20
		2.00	25	**1.99**	**2.54**	3.12	3.72
		3.00	20	2.04	2.57	**3.09**	3.65
		3.98	15	2.14	2.60	3.10	**3.62**
	Seawater	0.34	20	3.23	4.11	5.10	6.14
		0.70	20	2.94	3.69	4.53	5.42
		1.00	15	2.87	3.58	4.37	5.20
		2.00	15	**2.74**	**3.33**	4.00	4.70
		3.00	15	2.83	3.38	**4.00**	**4.65**
		3.98	10	3.16	3.77	4.46	5.18
0.10	Brackish water	0.34	54	3.10	3.98	4.97	6.01
		0.70	50	2.67	3.47	4.37	5.31
		1.00	40	2.46	3.09	3.79	4.69
		2.00	25	**2.42**	**3.05**	**3.62**	4.23
		3.00	20	2.65	3.25	3.78	**4.21**
		3.98	15	3.15	3.64	4.19	4.77
	Seawater	0.34	20	3.86	4.74	5.73	6.77
		0.70	20	3.64	4.39	5.23	6.12
		1.00	15	**3.62**	4.33	5.12	5.96
		2.00	15	3.68	**4.27**	**4.93**	**5.63**
		3.00	15	3.94	4.49	5.12	5.77
		3.98	10	4.45	5.06	5.75	6.47
0.15	Brackish water	0.34	54	3.31	4.19	5.18	6.22
		0.70	50	2.86	3.66	4.56	5.50
		1.00	40	**2.71**	**3.42**	**4.12**	4.94
		2.00	25	2.86	3.56	4.13	**4.73**
		3.00	20	3.26	3.94	4.47	4.83
		3.98	15	3.71	4.20	4.70	5.19
	Seawater	0.34	20	4.49	5.38	6.37	7.41
		0.70	20	**4.33**	5.09	5.93	6.82
		1.00	15	4.38	**5.08**	**5.88**	6.70
		2.00	15	4.61	5.20	5.86	**6.56**
		3.00	15	5.05	5.61	6.23	6.88
		3.98	10	5.74	6.35	7.04	7.77

APPENDIX D

COST OF LATENT AND SENSIBLE HEAT EXCHANGER CALCULATION

Cost of Latent Heat Exchanger

The cost of latent heat exchanger consists of the following.

a. Unitary cost of naval brass sheet
b. Manufacturing cost
c. Cost of vessel
d. Cost of coating

Unitary cost of naval brass sheet

The cost per pound obtained on December 27, 2008 was \$11.95/lb (rolled) [55]

Sheet volume = (8 ft) (8 ft) (0.007 in) (ft/12 in) = 0.0373 ft^3 = 1,057 cm^3

Sheet weight = (8.41 g/cm^3) (1,057 cm^3) = 8,891 g = 19.60 lb

Cost per sheet = (19.60 lb) (\$11.95/lb) = \$234.26

Cost per square foot = \$234.26/64 ft^2 = \$3.66/ft^2

Manufacturing cost

Unitary cost of manufacturing is \$0.15/ft^2 [6]

Other (assembly, gaskets, vessel modification) cost is \$4.14/ft^2 [6]

Amortized cost of die is negligible because the manufacturing is considered in a large production run.

Cost of vessel

Area per plate = 64 ft^2

Separation between plates = 0.25 in = 0.02083 ft

Plate thickness = 0.007 in = 0.00058 ft

Unitary space per plate = plate thickness + separation

= 0.02083 + 0.00058 = 0.02141 ft

Vessel diameter = $\sqrt{8^2 + 8^2} = \sqrt{64} = 11.31 \text{ ft} \approx 4 \text{ m}$

From Figure D-1 [48], consider a vessel 20 m = 65.6 ft long

Cost of purchase = $60,000

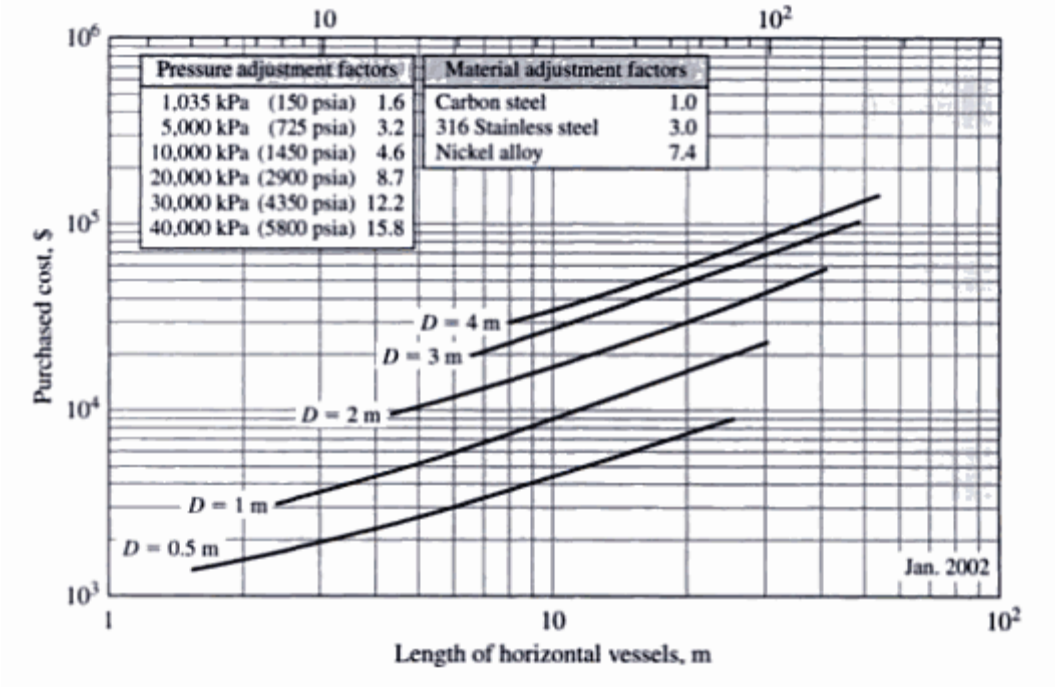

Figure D-1. Purchased cost for horizontal vessels [48]

The *Engineering News-Record Construction Cost Index* for 2002 is 6354 [54]

The *Engineering News-Record Construction Cost Index* for 2008 is 6750 [54]

$$\text{Cost of purchase in 2008} = \$60{,}000\,\frac{6750}{6354} = \$63{,}739$$

Pressure adjustment factor = 1.6 for 104.7 psia

Number of plates = (65.6 ft) (plate/0.02141 ft) = 3,064 plates

$$\text{Cost} = \left(\frac{1.6 \times \$63{,}739}{3{,}064\ \text{plates}}\right)\left(\frac{\text{plates}}{64\ \text{ft}^2}\right) = \frac{\$0.52}{\text{ft}^2}$$

Cost of coating

Cost of paint naval brass = $147.47/gal [56]

Assume film thickness = 1 mils

Transfer efficiency for brush application = 0.95 [57]

$$\text{Coating cost} = \text{Cost of paint solids per gallon} \times \text{film thickness in mils} \times 0.0006233\ [58]$$

$$\text{Coating cost} = \frac{\$147.47}{\text{gallon of naval brass}} \times 1\ \text{mils finished film thickness} \times \frac{1}{0.95} \times 0.0006233$$

$$\text{Coating cost} = \$0.1/\text{ft}^2$$

Table D-1 summarizes the cost of the latent heat exchanger components.

Table D-1. Latent heat exchanger unitary cost

Latent heat exchanger components	Cost ($/ft^2)
Naval brass sheet (0.007 in)	3.66
Sheet manufacture	0.15
Other (assembly, gaskets, vessel modification)	4.14
Vessel	0.52
Coating cost	0.10
Total unitary cost	8.57

Cost of Sensible Heat Exchanger

Unitary cost of naval brass

Cost per pound: \$11.95/lb [55]

Plate volume = (2.4 ft) (2.4 ft) (0.0198 in) (ft/12 in) = 0.0095 ft^3 = 269 cm^3

Plate weight = (8.41 g/cm^3) (269 cm^3) = 2,263 g = 4.99 lb

Cost per plate = (4.99 lb) (\$11.95/lb) = \$59.64

Cost per square foot = \$59.64/5.76 ft^2 = \$10.35/ft^2

Similarly, for titanium grade 2:

Cost per pound: \$66.95/lb [55]

Plate volume = (2.4 ft) (2.4 ft) (0.0196 in) (ft/12 in) = 0.0094 ft^3 = 266 cm^3

Plate weight = (4.5 g/cm^3) (266 cm^3) = 1,198 g = 2.64 lb

Cost per plate = (2.64 lb) (\$66.95/lb) = \$20.84

Cost per square foot = \$20.84/5.76 ft^2 = \$3.62/ft^2

Manufacturing cost

Information on microchannel heat exchanger cost was the estimates of the original equipment manufacturer cost developed by Modine [59].

Original equipment manufacturer cost = \$150 [59]

Area of microchannel heat exchanger = 22.8 ft^2 [59]

Unitary cost of manufacturing is \$150/22.8ft^2 = \$6.58/ft^2

A preliminary estimate total unitary cost is \$(10.35 + 3.62 + 6.58)/ft^2 = \$20.55/ft^2.

VITA

Name: Mirna Rahmah Lubis

Address: C/o Dr. Mark T. Holtzapple, Artie McFerin Department of Chemical Engineering, TAMU, College Station, Texas, 77843-3122

Education: English Language Institute, Texas A&M University, 2006
Diploma, Teaching Training and Education, Open University, 2004
B.E., Chemical Engineering, Syiah Kuala University, Indonesia, 2000

Profession: Teaching Staff. 2003 – present. Syiah Kuala University, Indonesia.
Teaching Staff. 2000 – 2004. Industrial Technology High School.
Quality Controller and Computerizer. 2000-2002. Indonesia.

Publication:
1. M. R. Lubis, Production of Adhesive from Durian Kernel, Publication in Journal Reaksi Polytechnic, Indonesia, 2004.
2. M. R. Lubis, Grindability of Clinker with Difference of SO_3 Content. Paper presented at Seminar for Development of Cement Andalas Indonesia Company's Employees, Indonesia, 2002.

Experience:
1. Article: Aceh Student Retreat in Historical Note, AFA News, 2009.
2. Workshop of Networking – Learning by Doing, Arkansas, 2008.
3. Conference of Tsunami Fulbright Leadership, Texas, 2007.
4. Workshop of Community Development, Arkansas, 2007.
5. Seminar of Fulbright Science and Technology, San Jose, 2007.
6. Article: When the Workshop is Over..., Fulbright Newsletter, 2007
7. Article: Horas, Fulbright Newsletter, Texas A&M, 2007.
8. Article: Open Our Mind before Our Mouth, Fulbright Newsletter.
9. Outstanding Achievement, English Language Institute, 2006.
10. Student Progress Award, English Language Institute, TAMU, 2006.